

***Single-channel Speech Separation Based on
Instantaneous Frequency***

Lingyun Gu

CMU-LTI-10-004

Language Technologies Institute
School of Computer Science
Carnegie Mellon University
5000 Forbes Ave, Pittsburgh, PA 15213
www.lti.cs.cmu.edu

Thesis Committee:

Richard Stern, Chair
Bhiksha Raj
Alex Rudnicky
Dan Ellis (Columbia University)

*Submitted in partial fulfillment of the requirements
for the degree of Doctor of Philosophy
In Language and Information Technologies*

Copyright © 2010 Lingyun Gu

SINGLE-CHANNEL SPEECH SEPARATION BASED ON INSTANTANEOUS
FREQUENCY

By

LINGYUN GU

Thesis Committee:

Richard M. Stern, Chair (Carnegie Mellon University)

Bhiksha Raj (Carnegie Mellon University)

Alex Rudnicky (Carnegie Mellon University)

Dan Ellis (Columbia University)

A DISSERTATION PRESENTED TO THE GRADUATE SCHOOL
OF CARNEGIE MELLON UNIVERSITY IN PARTIAL FULFILLMENT
OF THE REQUIREMENTS FOR THE DEGREE OF
DOCTOR OF PHILOSOPHY

CARNEGIE MELLON UNIVERSITY

2010

© 2010 Lingyun Gu

To my beloved wife, Jing

To my parents

To my baby girl, Yiya

To all Bodhisattvas who have been blessing and shining my family

ACKNOWLEDGMENTS

My dissertation comes from two parts. One is necessary. But the other is essential. The former is my diligent though nature-decide-limited effort. The latter is a tremendous and unbounded amount of love and help I have been receiving from many people whom I want to thank here.

No doubt I want to bring my advisor Richard Stern to the first place to thank him for his immense support, guidance, help and fruitful discussions over the past six years. He brought me to Carnegie Mellon to help me fulfill my dream to get professional training not only at a top school, but also in one of the world-class labs in the speech recognition area. What he says and does sets up a perfect model for me to follow, not only in the area of research, but also extended to many other fields. There is an old Chinese saying, "One day your advisor, forever your father". I want to borrow this adage and give my endless gratitude to him, for everything he does for me.

I also want to take this opportunity to thank my thesis committee members, Professors Bhiksha Raj, Alex Rudnicky and Dan Ellis, for their valuable suggestions, comments and great ideas. Special thanks also goes to Bhiksha, for his role not only being my committee member, but also a truly helpful elder academic brother.

Members of the almighty robust speech recognition group also have played a very important role in both my research and dissertation writing. Many thanks to previous members Alex Acero, Evandro Gouêa, Pedro Moreno, Xiang Li and current members Rita Singh, Kshitiz Kumar, Ziad Al Bawab, Chanwoo Kim and Yuhsiang Chiu, for their abundant discussions. My best friends cross the country also deserve an equal amount of my gratitude. Jun Qian, Rui Yan, Wei Ye, Wei Luo, Jingdong Deng, Hailing Wang, Gao Yao, Qi Xiangli, Zhipan Guo, Jinge Zhong, Shuguang Tan, Henry Lin, Grace Yang, Kamin Chang, Jin Xie, Rong Zhang, Ying Zhang, Rong Yan, Yan Liu, Wen Wu, Yanjun Qi, Le Zhao, Ni Lao, Luo Si, Hua Yu, Chun Jin, Jian Zhang, Yue Cui, Pradipta Ray, Andrew Schlaikjer, Hideki Shima, Oznur

Tastan, Andres Zollmann, Matthew Bilotti, Meryem Donmez, Yiqing Wang, Hang Yu and Justin Betteridge, thank all of you for your endless support.

I am truly grateful to my parents. I couldn't have achieved anything without their enormous time, energy, love since the first moment I came to this world. Even though they are living thousands miles away from me in China, their love breezes me everyday and will continue forever.

The last, but never ever the least indebtedness, goes to my beloved wife Jing. Without her years of years continuous support, my dissertation could not possibly have been completed. Neither Shakespeare nor Dickens can come up with the best words I can ever use to tell her how fortunate I am to share happiness and shred tears with her together. She is the fifth element in my life.

TABLE OF CONTENTS

	<u>page</u>
ACKNOWLEDGMENTS	i
LIST OF TABLES	vi
LIST OF FIGURES	vii
ABSTRACT	x
CHAPTER	
1 INTRODUCTION	1
1.1 Motivation	1
1.1.1 Speech Separation Systems	2
1.1.2 Why is Single-Channel Speech Recognition Important?	3
1.1.3 Why is Single-Channel Speech Recognition Challenging?	4
1.2 Overview of the Speech Separation System base on Instantaneous Frequency	4
1.3 Dissertation Outline	5
2 REVIEW OF ALGORITHMS FOR SINGLE-CHANNEL SPEECH SEPARATION	7
2.1 CASA Introduction	7
2.1.1 Motivation for Exploiting CASA	8
2.1.2 Examples of CASA Systems and Applications	10
2.1.3 CASA Mask Generation and Evaluation	11
2.2 Amplitude-Modulation Spectral Analysis	12
2.2.1 Amplitude Modulation based Algorithms	13
2.2.2 Differences between Amplitude and Frequency Modulation Schemes	15
2.3 Multi-Pitch Tracking based Speech Separation	16
3 ESTIMATION OF INSTANTANEOUS FREQUENCY AND ITS APPLICATION TO SOURCE SEPARATION	19
3.1 Modulation Frequency and Its application to Speech Separation	19
3.2 Instantaneous Frequency and Its Calculation	22
3.2.1 Instantaneous Frequency Calculation	22
3.2.2 Two Alternative ways to Calculate Instantaneous Frequency	28
3.3 Instantaneous Frequency Estimation for Frequency-modulated Complex Tone	31
3.3.1 Frequency-modulated Complex Tones	32
3.3.2 Extracting Instantaneous Frequency from Frequency-modulated Complex Tones	33
3.4 Factors Affecting Instantaneous Frequency Estimation	35

4	CROSS-CHANNEL CORRELATION AND OTHER MASK-CLUSTERING METHODS	38
4.1	Cross-channel Correlation	38
4.1.1	Patterns of Separated Speech Components Obtained by Cross-channel Correlation	39
4.1.2	Mean Square Difference Mask Generation	44
4.2	One-Dimensional Projection Solution	47
4.3	Graph-Cut Solution	50
5	GROUPING SCHEMES AND EXPERIMENTAL DESIGN	57
5.1	Grouping Schemes	57
5.1.1	Pitch Detection for Dominant Speakers for the Different-Gender Case	58
5.1.2	Speaker Identification for the Same-Gender Case	59
5.2	Mask Generation	61
5.3	Experimental Procedures and Databases	63
5.3.1	Sphinx-III Recognition Platform	63
5.3.2	The Resource Management and Grid Corpora	63
5.4	Experimental Results and Discussion	66
5.5	A Sieve Function for Selecting Relevant Frequency Components from Partial Harmonic Structure	71
5.5.1	Harmonic Pattern Recognition	71
5.5.2	The Harmonic Sieve	73
5.5.3	Objective Function	74
6	INSTANTANEOUS-AMPLITUDE-BASED SEGREGATION FOR UNVOICED SEGMENTS	77
6.1	Feature Extraction Based on Instantaneous Amplitude	78
6.2	Detection of Boundaries Between Voiced and Unvoiced Segments	80
6.2.1	The Teager Energy Operator	82
6.2.2	Autocorrelation	82
6.2.3	Energy Detection	83
6.2.4	Zero Crossing Rate (ZCR)	83
6.2.5	Ratio of Energy in High and Low Frequency Bands	85
6.3	Experimental Results using Instantaneous Amplitude-based Segregation	86
6.3.1	Evaluation of V/UV Decisions	86
6.3.2	Evaluation of WER Using Amplitude-Based Features	87
7	SUMMARY AND CONCLUSIONS	89
7.1	Major Findings and Contributions	89
7.2	Directions of Possible Future Research	90
7.2.1	Combine long term and short term cross-channel correlation	90
7.2.2	Combine instantaneous frequency and amplitude	90
7.2.3	Introduce image processing algorithms for mask generation	90

7.3 Summary and Conclusions	91
REFERENCES	92
BIOGRAPHICAL SKETCH	96

LIST OF TABLES

Table	page
3-1 Correlation comparison among harmonic members and between harmonic and non-harmonic members.	36
4-1 Correlation using the cross-channel correlation method.	46
4-2 Instantaneous frequency distance using the mean square difference method.	47
4-3 Confusion matrix of performance of selected harmonic frequencies for the clean case using the 1-D projection method.	49
4-4 Confusion matrix of performance of selected harmonic frequencies at 15 dB using the 1-D projection method.	49
4-5 Confusion matrix of performance of selected harmonic frequencies at 10 dB using the 1-D projection method.	50
4-6 Confusion matrix of performance of selected harmonic frequencies at 5 dB using the 1-D projection method.	50
4-7 Confusion matrix of performance of selected harmonic frequencies at 0 dB using the 1-D projection method.	50
4-8 Confusion matrix of performance of selected harmonic frequencies for the clean case by using the graph-cut method.	53
4-9 Confusion matrix of performance of selected harmonic frequencies at 15 dB by using the graph-cut method.	53
4-10 Confusion matrix of performance of selected harmonic frequencies at 10 dB by using the graph-cut method.	54
4-11 Confusion matrix of performance of selected harmonic frequencies at 5 dB by using graph-cut method.	54
4-12 Confusion matrix of performance of selected harmonic frequencies at 0 dB by using graph-cut method.	54
5-1 Structure of the sentences in the Grid database.	65
6-1 Confusion matrix of voiced and unvoiced detection using pitch detection developed by de Cheveigné.	86
6-2 Confusion matrix of voiced and unvoiced detection using features developed in this thesis.	88

LIST OF FIGURES

<u>Figure</u>	<u>page</u>
2-1 A simplified end-to-end CASA speech separation system, where the most three important parts are domain transformation, speech-component segregation, and speech-component regrouping.	9
2-2 In CASA, speech can be first projected into time-frequency cells in a 2-D representation. Based on how close each time-frequency region is relative to the others, the regions can be grouped and reconstructed into streams from different sources. How to classify each region and use various cues to group them into streams provides great flexibility to reconstruct target speech from interfering sources.	10
2-3 The speech signal is first decomposed into a time-frequency representation by STFT. Then within each frequency channel, a second FFT is calculated to transfer to time-frequency representation to a frequency-frequency representation, where one frequency axis represents physical frequency and the other frequency axis represents modulation frequency.	14
2-4 In this figure, panel (a) shows a pure tone with period T . The corresponding spectra peak is also shown on the right. Panels (b), (c), (d) and (e) share the same period T of the signal in panel (a) with different waveforms. However, by looking at the spectral response on the right, it is truly difficult to determine the fundamental frequency simply by locating the position of the global spectra peak.	17
2-5 A mixture of speech and interference is processed in four main stages after the cochlear filtering. First, a normalized correlogram is obtained within each channel. Channel/peak selection is performed to select a subset of relatively clean frequency channels. In this third stage, the periodicity information is integrated across neighborhood channels. Finally, an HMM is utilized to form continuous pitch tracks.	18
3-1 Spectrogram of a chirp signal whose frequency increases linearly with time.	20
3-2 A simple example compares the concepts of modulation frequency, deviation frequency, and instantaneous frequency. In the figure, the modulation frequency is 5 Hz, the deviation frequency is 20 Hz. The modulation period is 200 ms, the reciprocal of the modulation frequency of 5 Hz.	21
3-3 A block diagram that describes how instantaneous frequency is calculated by the method discussed in Equation 3.6.	25
3-4 A block diagram that describes how instantaneous frequency is calculated by using the method discussed in Equation 3.15.	26
3-5 The upper panel is the estimated phase before phase unwrapping and the lower panel is the corresponding estimate after phase unwrapping.	28

3-6	The instantaneous frequency estimate of a multi-sinusoid signal using Equations 3.6 or 3.15.	29
3-7	A general diagram of how instantaneous frequency is calculated by using the differentiated window method discussed in Equation 3.29.	32
3-8	The instantaneous frequency estimation from a multi-sinusoid signal using continuous window derivative methods.	33
3-9	Spectrogram of the sum of three frequency-modulated complex tones.	34
3-10	Instantaneous frequencies estimated from corresponding frequency channels from a frequency-modulated complex tones at SNR 0 dB, where the upper and middle signal are from the same harmonic structure and the lower signal is from another irrelevant channel.	35
4-1	Instantaneous frequency estimates from corresponding frequency channels where a multi-sinusoid target signal and the single-sinusoid interfering signal have most of their energy.	41
4-2	Spectrogram of the signal described in Equation 4.3.	42
4-3	Cross-channel correlation of four frequency channels where a multi-sinusoid target signal and single-sinusoid interfering signal have most of their energy.	43
4-4	Cross-channel correlation of a typical frequency-modulated complex tone at the fundamental frequency of 150 Hz.	44
4-5	Cross-channel correlation over all frequency bins for a short voiced segment with fundamental frequency 135.5 Hz. The red and yellow regions represent high correlation, while blue and green regions represent low correlation.	45
4-6	One-dimensional projection for the same signal used in Figure 4-2.	48
4-7	An undirected graph G , which has 9 vertices and should be divided into two partitions.	52
4-8	Graph-cut method to extract classification information from correlation matrix.	55
4-9	1-D projection method to extract classification information from correlation matrix.	56
5-1	Block diagram of a system that uses pitch detection to determine the dominant speaker.	60
5-2	Block diagram of a speech separation system that uses speaker identification to determine the dominant speaker.	62
5-3	A block diagram of the Sphinx-III speech recognition system.	64

5-4	Experimental results using the RM database that compare the performance of the graph-cut and 1-D projection methods. The two speakers in these experiments were of different genders and presented at an SNR of +6 dB.	67
5-5	Performance comparison among instantaneous frequency, baseline MFCC, pitch tracking algorithm and instantaneous-amplitude-based algorithm obtained from the RM database.	69
5-6	Comparison of performance of the instantaneous frequency, baseline MFCC, pitch tracking, and instantaneous-amplitude-based algorithm using data from the Grid database.	70
5-7	Comparison of WER obtained using a reconstruction of masked speech using all components of the dominant speaker (“clean mask”) with a similar reconstruction using only those components that are identified as undistorted by the instantaneous-frequency-based method (“real mask”).	72
5-8	Comparison of WER obtained before and after applying the sieve function. . . .	76
6-1	Block diagram of system that combines instantaneous frequency and instantaneous amplitude to separate simultaneously-presented speech.	79
6-2	Block diagram of the system that detects boundaries between voiced and unvoiced segments.	81
6-3	A comparison between Teager energy and conventional energy operator. In this case, the frequency is 200 Hz for the 1 s and changes to 1000 hz in the duration from 1 s to 2s, while the amplitude keeps the same.	83
6-4	Autocorrelation comparison between voiced and unvoiced segments.	84
6-5	ZCR histogram comparison between unvoiced and voiced segments	85
6-6	A comparison of histograms of high frequency energy feature from both unvoiced and voiced segments	87
6-7	Recognition accuracy comparison between methods using voiced and unvoiced detection and without it on Grid database.	88

Abstract of Dissertation Presented to the Graduate School
of Carnegie Mellon University in Partial Fulfillment of the
Requirements for the Degree of Doctor of Philosophy

SINGLE-CHANNEL SPEECH SEPARATION BASED ON INSTANTANEOUS
FREQUENCY

By

Lingyun Gu

May 2010

Chair: Richard M. Stern

Major: Language Technologies Institute

While automatic speech recognition has become useful and convenient in daily life as well as an important enabler for other modern technologies, speech recognition accuracy is far from sufficient to guarantee a stable performance. It can be severely degraded when speech is subjected to additive noises. Though speech may encounter various types of noises, the work described in this dissertation concerns one of the most difficult problems in robust speech recognition: corruption by an interfering speech signal with only a single channel of information. This problem is especially difficult because the acoustical characteristics of the desired speech signal are easily confused with those of the interfering masking signal, and because useful information pertaining to the location of the sound sources is not available with only a single channel.

The goal of this dissertation is to recover the target component of speech mixed with interfering speech, and to improve the recognition accuracy that is obtained using the recovered speech signal. While we will accomplish this by combining several types of temporal features, the major novel approach will be to exploit instantaneous frequency to reveal the underlying harmonic structures of a complex auditory scene. The proposed algorithm extracts instantaneous frequency from each narrow-band frequency channel using short-time Fourier analysis. Pair-wise cross-channel correlations based on instantaneous frequency are obtained for each time frame, and clusters of frequency components that are believed to belong to a common source are initially identified on the basis of their

mutual cross-correlation. In the dissertation, several methods are discussed in order to obtain better estimates of instantaneous frequency. Conventional and graph-cut algorithms are demonstrated to collect efficiently the pattern used to identify the underlying harmonic structures. As a complementary means to boost the final performance, a computationally efficient test for voicing is proposed. Speaker identification and pitch detection are also presented to refine further the final performance.

An estimate of the target signal is ultimately obtained by reconstruction using inverse short-time Fourier analysis based on selected components of the combined signals. The recognition accuracy obtained in situations of speech-on-speech masking is assessed and compared to the corresponding performance of speech recognition systems using previous approaches.

CHAPTER 1 INTRODUCTION

1.1 Motivation

Speech recognition has been the object of extensive research for many decades. While recognition accuracy in clean environments improved substantially after Hidden Markov Models (HMMs) were introduced [36], recognition in noisy environments still suffers due to many reasons such as the mismatch between clean training and noisy testing conditions. Among many different types of interference (including but not limited to white noise, colored noise, background music, and speech babble), competing speech has been considered to be among the most challenging type of interference. The high correlation of temporal structures between the speech from target and masking speakers is one major reason for poor recognition accuracy.

Nevertheless, in daily communication among humans, competing speech is among one of the most commonly-encountered noises. For example, speech by news anchors is sometimes overshadowed by background speakers and multiple speakers talk simultaneously in teleconferences. In both examples mentioned above, the target speech is more or less corrupted by interfering speech. While machines still do a very poor job of recognizing combined speech correctly, human beings are impressive in their ability to either extract the target speech, suppress interfering speech sources or both to achieve reasonably good recognition accuracy in communicating with each other. While the detailed mechanism of exactly how humans separate signals is still not truly clear, one popular computational model, auditory scene analysis (ASA) proposed by Bregman in the early 1990s [9, 50] suggests that the one-dimensional speech signal is projected onto a two-dimensional time-frequency space for further processing. After this projection, some capabilities that humans use in image detection (*e.g.* edge detection) can also be used to separate speech sources from one another. The computational implementation of this theory is called computational auditory scene analysis (CASA). The major processing in CASA can be divided into two main steps, segmenting and regrouping. The goal of

segmenting is that of placing similar units into different regions of the higher dimensional space, and regrouping concerns the reorganization of those regions according to the sources that they are assumed to represent. Detailed discussions about CASA will be presented in the following chapters.

1.1.1 Speech Separation Systems

Researchers have developed various types of systems to address the problem of minimizing the negative effects from competing speech, which can be characterized in a number of different ways. For example, systems with inputs from multiple microphones have the advantage of being able to take advantage of exploiting spatial information such as interaural time difference (ITD) and interaural intensity difference (IID). Nevertheless, multiple microphones are not always available, so there will always be a role for single-channel systems, which have only the intrinsic information carried by speech itself, in the absence of spatial cues. Systems can be also characterized as being knowledge-based versus statistically-based. This is actually a continuum that depends on the extent to which the structure of the system is developed manually through background knowledge about speech versus statistical learning from a large database. Knowledge-based systems have the advantage of requiring fewer constraints and in principle are more easily adapted to unknown speakers. However, due to the lack of precise fundamental knowledge of how human perceptual processing really works, imperfect modeling makes this type of system tend not to be able to achieve the same level of word error rate (WER) that statistically-based systems enjoy. In contrast, statistically-based systems frequently require significant computational resources as well as a pool of speakers for training and testing. In many cases, the WER from speech recognition systems becomes worse due to changes in the testing environment. Speech separation systems can also be characterized as being directed toward speech enhancement (which refers to improving the quality of speech for human listeners) versus recognition-based systems, which are designed to improve automatic speech recognition accuracy.

In the context of the above discussion of various types of systems, the system developed in this dissertation can be classified as a single-channel, knowledge-based system that will be evaluated in terms of the WER obtained from speech recognition experiments based on the outputs of the system.

1.1.2 Why is Single-Channel Speech Recognition Important?

In the real world, speech activity is collected by a single microphone or by multiple microphones and sent to computers for further processing. During the collection procedure, if conditions permit, multiple microphones are naturally preferred. In this case, spatial information can be preserved and used as additional cues to separate combined speech. However, in cocktail-party environments with multiple sound sources, if the target speaker is not predetermined, microphone arrays may not be used to good advantage. Even worse, an environment that facilitates multiple microphones is not always available. In many scenarios using one microphone is the only choice.

One good example of single-channel speech processing is automatic speech recognition of radio broadcasts. In this case, speech activity is transmitted and collected from radio channels, and there is no spatial information available. In many speech segments, the news anchor's voice is corrupted by background speakers. Directly sending this simultaneous speech into a speech recognizer results in poor accuracy. Another example is speech recognition in teleconferences. The presence of more than one interfering speaker presents a very difficult task for any state-of-the-art recognizer.

The examples above are frequently the first step of some very complex systems. Usually, these systems apply further processing to the output of the recognition system, such as news summarization, categorization, question answering, dialogue systems and text-to-speech systems. All these applications require a good single-channel speech system to achieve reasonably good speech recognition accuracy, as poor speech recognition accuracy may lead to a serious accumulation of errors. For these reasons solutions to the problem of single-channel speech recognition in interfering noise are very important.

1.1.3 Why is Single-Channel Speech Recognition Challenging?

It is widely believed that single-channel speech separation (SCSS) is a very challenging task. Unlike multi-channel speech separation (MCSS), spatial information can not be utilized. Only those intrinsic acoustic features, such as pitch, harmonic structure, local time or frequency proximity can be exploited to separate speech.

Due to highly correlated temporal structures, it is very difficult to extract many good inherent acoustic features accurately from combined speech. Pitch information has been widely considered to be a good way to extract harmonic structure. But it is very difficult to estimate accurately pitch contours from target speech while interfering speech is present. Since competing speech contains many similar human speech characteristics, unlike the case of other noise types such as white/colored noise or mechanical noise, the usage of time/frequency proximity, amplitude modulation and other features provides only limited improvement.

The major goal of this dissertation is to address the speech-on-speech problem by developing a system that separates speech sources based on instantaneous frequencies within a CASA framework, when only one microphone is available.

1.2 Overview of the Speech Separation System base on Instantaneous Frequency

In this dissertation an instantaneous frequency-based single-channel speech separation system will be discussed in detail. A brief description is given here to provide an overview of the end-to-end system.

Target speech is corrupted by interfering speech at various global SNRs ranging from 0 dB to 15 dB. After the combined speech is generated, the simultaneously-presented speech is decomposed into a time-frequency representation using the short-time Fourier transform (STFT). Within each frequency channel, continuous phase information is obtained through a transformation from the discrete representation (details may be found in Chapter 3). A first derivative of the estimated phase is obtained, which produces the main feature used

in the dissertation, instantaneous frequency. Once instantaneous frequency is obtained, pair-wise cross-channel correlation and mean square difference are both calculated as a way to identify those frequency channels that are believed to be dominated by the same source. A voiced/unvoiced segment detection is applied to identify the rough boundaries between voiced and unvoiced segments. While instantaneous frequency-based features are applied in voiced segments, amplitude-based features are used in unvoiced segments to group frequency components from the same source. Speaker identification is applied to each processed time frame to group the separated clusters according to speaker, so that after processing is complete ideally only frequency channels dominated by the target speaker are extracted, while other frequency channels believed to be from the interfering speaker are suppressed. Finally, the reconstructed speech is sent to a speech recognizer for the final recognition task.

1.3 Dissertation Outline

This section gives a brief review of the organization of this dissertation.

In Chapter 2, some relevant previous research results in single-channel speech separation area are briefly discussed. Because we exploit the fact that speech components from the same source tends to vary together in terms of amplitude modulation, instantaneous amplitude and modulation spectrogram-based methods are discussed first. Another natural way to think about the source separation problem is that of trying to detect pitch contours from each individual source. Multi-pitch tracking algorithms are introduced subsequently.

Chapter 3 first discusses a few ways to calculate instantaneous frequency, which is the most important feature used in this dissertation to group speech components from the same source. We discuss the calculation of instantaneous frequency in the context of some real examples based on multiple sine tones, frequency-modulated complex tones, and real speech.

After calculating instantaneous frequency, the development of methods to identify correlated frequency channels is the next step. In Chapter 4, cross-correlation-based and mean-square-error-based methods are discussed with the goal of correlating frequency channels from the same source.

At the end of this chapter, one dimensional projection and graph-cut methods are proposed as methods to extract the correlation information.

In chapter 5, two regrouping methods, pitch-based regrouping and regrouping based on speaker identification, are introduced. Some general principles about mask generation are discussed here as well. Finally, experimental results are presented and discussed.

While instantaneous frequency is a useful feature for voiced segments, unvoiced segments from the same source become a little less reliable to group same source frequency components together. In Chapter 6, both voiced/unvoiced segment detection and threshold-based time-frequency cell suppression are discussed in detail.

Finally, Chapter 7 summarizes our work and its major conclusions. Potential future work is also discussed.

CHAPTER 2 REVIEW OF ALGORITHMS FOR SINGLE-CHANNEL SPEECH SEPARATION

This chapter will review several speech separation algorithms which can be used for single-channel speech separation in the CASA framework. A general discussion of CASA and the motivation of using CASA will be given first. Following the CASA discussion, speech separation based on instantaneous amplitude and multi-pitch tracking will be discussed in detail in terms of their ability to separate speech.

2.1 CASA Introduction

Computational Auditory Scene Analysis (CASA) has broad application to source separation. Generally speaking, CASA is a wide collection of various computational implementations of auditory scene analysis (ASA). Before a more advanced discussion of CASA is provided, it is necessary to briefly introduce ASA and its major application. Many scientists believe that audition shares many similarities with vision [24, 33]. The human auditory system transforms speech into a neural representation which is then presumed to be processed in a fashion that is similar to image processing. The entire ASA procedure can be separated into two stages: segregation and regrouping. In the first stage, speech is decomposed into a higher-dimensional space (such as a spectro-temporal two-dimensional representation) where similar units (*e.g.*, time-frequency cells in the previous 2D representation example) are collected together into different regions. In the second stage, these regions are grouped together into different streams based on the values of various acoustic cues or other information. Finally, the target speech or interfering speech or both can be reconstructed for different purposes. These functions will be discussed below in detail.

In general, CASA uses computational methods to generate a machine perception system which may have similar functionality to that of humans. We consider primarily either one or two microphones (the two ears of human audition). In this scenario, Wang and Brown [50] define CASA as “the field of computational study that aims to achieve human performance in ASA by using one or two microphone recordings of the acoustic scene.”

Figure 2-1 below shows a simplified diagram of a typical CASA system, where input speech is first going through a domain transformation function. Most of the time, this function transforms the one-dimensional speech signal into the very popular two-dimensional time-frequency representation, either by standard short time Fourier transformation (STFT) or a Gammatone filter bank. Following the domain transformation, the next procedure is speech component segregation. In this part, all time-frequency cells are segmented into different regions. All cells sitting in the same region are believed to be from the same speech source. Various feature extraction algorithms are proposed in this stage in order to optimize the segmentation results. The next step in the figure is described as speech component regrouping. This stage is processed in an utterance-based format to extract all the segments believed to be from the same speech source while suppressing all others. The most popular such method is speaker identification. Finally, all extracted time-frequency cells are used to reconstruct the resynthesized speech.

2.1.1 Motivation for Exploiting CASA

Speech is challenging because of its high dynamic range in both the time and frequency domains. When competing speech is presented, the combined speech presents an even more complicated structures that must be recognized or separated. CASA provides a good angle to look at this problem by projecting one dimensional speech into higher dimensions. In the following sections, discussion will be limited to the two dimensional time-frequency representation. Due to energy sparsity, it is frequently the case that corrupted signals in the time domain may be separable after transformation into a time-frequency representation. To further clarify the concept of “energy sparsity”, by looking at any spectrogram of a given speech, it is easy to discover that not every time-frequency cell plays an equally important role in representing the information carried by the speech. A large percent of cells carrying very low energy are much less important compared to a few percent of high-energy cells. The transformation makes the target speech look less “ambiguous” than it was before. As a

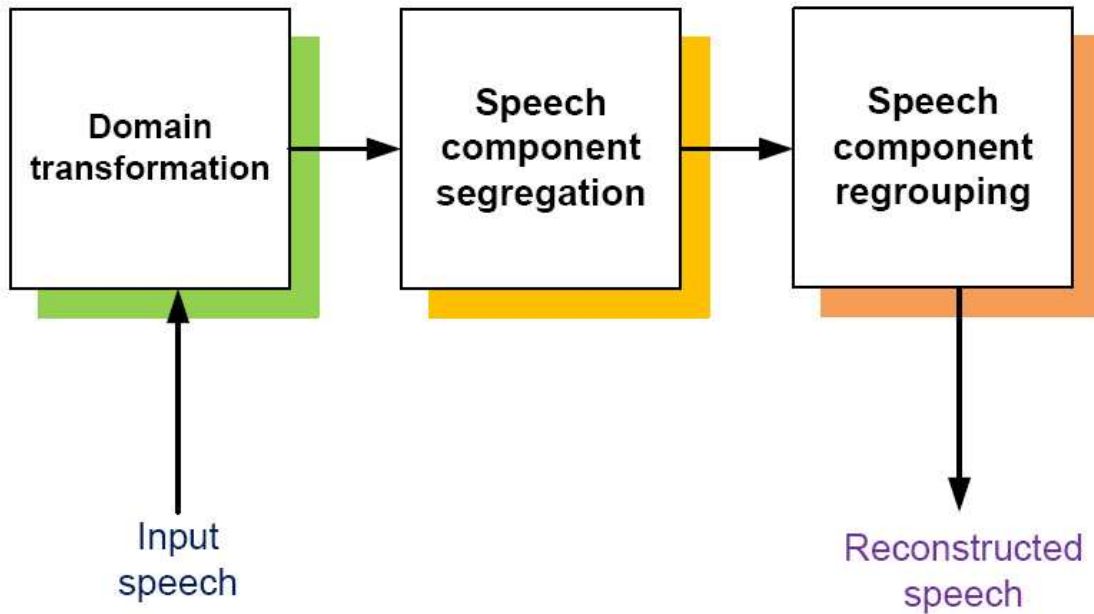


Figure 2-1. A simplified end-to-end CASA speech separation system, where the most three important parts are domain transformation, speech-component segregation, and speech-component regrouping.

result, those time-frequency cells, which are less corrupted by the interfering speech, can be used as the basis for reconstructing the target speech.

In addition to this useful 2-dimensional projection, the two-stage theory of ASA discussed in Section 2.1 also provides helpful insights into the source separation problem. Figure 2-2 [50] shows a simple way to demonstrate the theory. In Figure 2-2, the upper panel shows time-frequency cells/regions could be grouped into one single stream if they are close enough, while the lower panel illustrates the case of two streams of speech that are grouped separately if the time-frequency cells/regions are sufficiently far from each other.

A third issue is the CASA system’s ability to handle both bottom-up and top-down processing. These two approaches are also called primitive and schema-based processing [6, 9, 18, 32, 50]. Primitive processing is usually closely related to feature-based procedures,

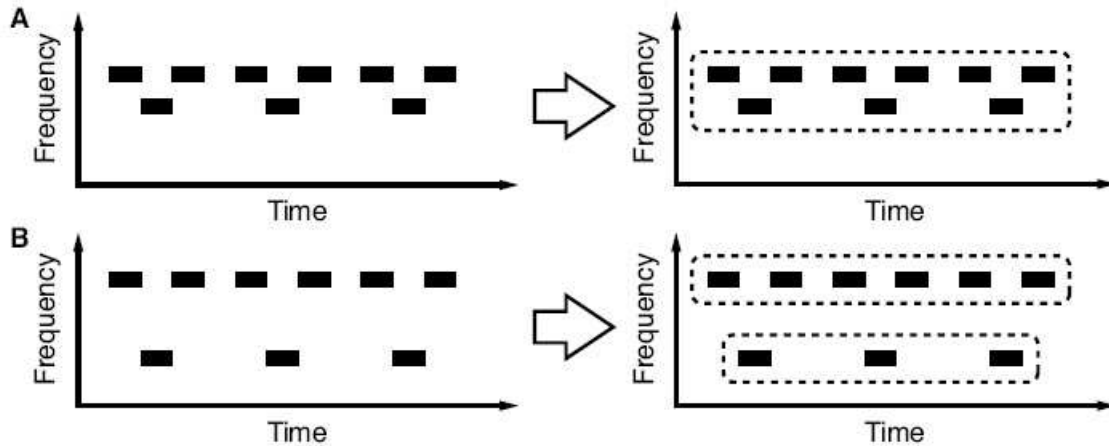


Figure 2-2. In CASA, speech can be first projected into time-frequency cells in a 2-D representation. Based on how close each time-frequency region is relative to the others, the regions can be grouped and reconstructed into streams from different sources. How to classify each region and use various cues to group them into streams provides great flexibility to reconstruct target speech from interfering sources.

such as time and frequency proximity, onset/offset detection, smoothness of pitch or formant trajectory, periodicity, etc. Human beings have the ability of accumulating knowledge gradually after they are first born. The learning procedure generates many patterns, or prior knowledge. Those stored patterns help to interpret corrupt patterns in many different scenarios. In source separation, when certain parts of speech in the 2-D representation become discontinuous due to the presence of competing speech, human beings tend to use *a priori* knowledge to fill the gaps in the representation and recover the speech to its maximum intelligibility.

2.1.2 Examples of CASA Systems and Applications

CASA systems have been widely used in many different applications. Below is a limited collection of several examples [50].

- Robust automatic speech and speaker recognition
- Hearing prostheses
- Automatic music transcription
- Audio information retrieval

- Auditory scene reconstruction

In this dissertation, the discussion of CASA systems will be limited to the application of monaural speech separation.

Projecting time-domain speech into the time-frequency domain is generally considered to be the first step towards solving the problem. The short-time Fourier Transform (STFT) and Gammatone filterbank are both considered to be proper vehicles to implement the transform. In STFT, the center frequencies of each frequency channel are separated by the same difference in frequency. For each fixed time frame, the frequency response is the Fourier transform of that given time frame. While each frequency channel is fixed, the output of each channel can be considered as a filter output of a specific bandpass filter. In the application of Gammatone filtering, the spacing of the center frequency of each channel varies with frequency. This provides better frequency resolution for low frequencies at the expense of worse spectral resolution for high frequencies.

After the transformation is done, an attempt is made to determine which time-frequency cells are believed to have similar characteristics. This step is usually done by applying different intrinsic acoustic cues. The next step is that of regrouping different time-frequency regions into different streams to reconstruct either target speech, interfering speech or both. In this stage, the most popular method used is speaker identification based on the training data, from which each speaker’s acoustic characteristics are learned by the system. In the reconstruction procedure, the *a posteriori* probability of each speaker in the training pool is calculated for each time frame to get the best match. Based on speaker identification results, further extraction or suppression is performed to generate different speech streams.

2.1.3 CASA Mask Generation and Evaluation

A key part of both the segmentation and regrouping stages of CASA systems is mask generation. The term mask generation generally refers to the judgement of each individual time-frequency cell or region whether they are reliable or not. “Reliable” here generally means the time-frequency cell belongs to the target speaker. A “binary masks” is made about

whether each time-frequency cell is reliable or unreliable, while the cells of “continuous” masks are assigned a probability of reliability. The final construction of either target or competing speech is performed based on these values.

There are various ways of evaluating the CASA systems. In this section, several popular assessments are briefly listed.

Word Error Rate (WER): In this method, the reconstructed speech is fed into a speech recognizer for automatic speech recognition. WER can be used as an objective assessment to value different separation algorithms, where the best approaches yield the lowest WER value.

Spectrogram Distance: Another way to assess separation algorithm is spectrogram distance. In the method, the spectrogram of reconstructed speech is compared with the original clean speech. The smaller the distance between these spectrograms, the better the separation algorithm is.

Mean Opinion Score (MOS): The Mean Opinion Score (MOS) is a very popular subjective evaluation scheme using human subjects. In this method, professional personnel are asked to score to each reconstructed speech utterance on a scale of 1 to 5, from the worst to the best.

We will use WER exclusively as the standard of evaluation of the success of the various separation algorithms considered.

2.2 Amplitude-Modulation Spectral Analysis

In many analyses [1, 4, 7, 8, 39, 41] it is useful to separate speech and music signals into two parts, a low-frequency modulating signal and a higher-frequency modulated carrier [39, 41]. Equations 2.1 and 2.2 describe a single-component modulation and a multi-component modulated signal, respectively.

$$x(t) = m(t)c(t) \tag{2.1}$$

$$x(t) = \sum_{n=1}^N s_n(t) = \sum_{n=1}^N m_n(t)c_n(t) \quad (2.2)$$

where $x(t)$ is the single-component or multi-component signal, $m(t)$ or $m_n(t)$ are the low-frequency modulating signals and $c(t)$ or $c_n(t)$ are the high-frequency carriers.

Many researchers believe that the modulator of a speech signal is more important than its own carrier signal in terms of speech perception. When a real modulator signal is replaced by a constant envelope, speech becomes unintelligible. On the contrary, if the carrier is replaced by white noise but the modulator signal is untouched, the speech remains very intelligible. This observation has led many researchers to apply amplitude modulation to monaural source separation with the hope of making amplitude modulation an important intrinsic acoustic feature.

A popular implementation of this idea is the decomposition of the original signal into many narrowband frequency subbands. Within each subband, the signal is further decomposed into a modulator and a carrier. Then various feature-extraction methods based on this implementation are used to further group components from the same source together.

2.2.1 Amplitude Modulation based Algorithms

The use of long-term temporal features to improve speech recognition accuracy has been shown to be successful by a number of research groups (*e.g.* [25]). For example, Atlas and his colleagues (among others) have proposed the use of modulation spectral analysis as a tool to separate mixed speech in higher-dimensional spaces [40] [2]. The time-domain signal is first transformed into a time-frequency representation by applying Short-time Fourier Transform (STFT). Then, the instantaneous amplitude is calculated for each narrow-band frequency bin. Conventional coherent demodulation is accomplished through the use of the Hilbert transform approach. An improved “coherent demodulation” [28], which removes the carrier frequency (*i.e.* the center frequency of each bandpass filter) to a high degree, has been shown to provide better performance in term of extracting the envelope. A second FFT for the new estimated envelope is calculated within each frequency bin. If the envelope is indeed

modulated at a certain frequency, the FFT operation will produce a spike at that frequency,

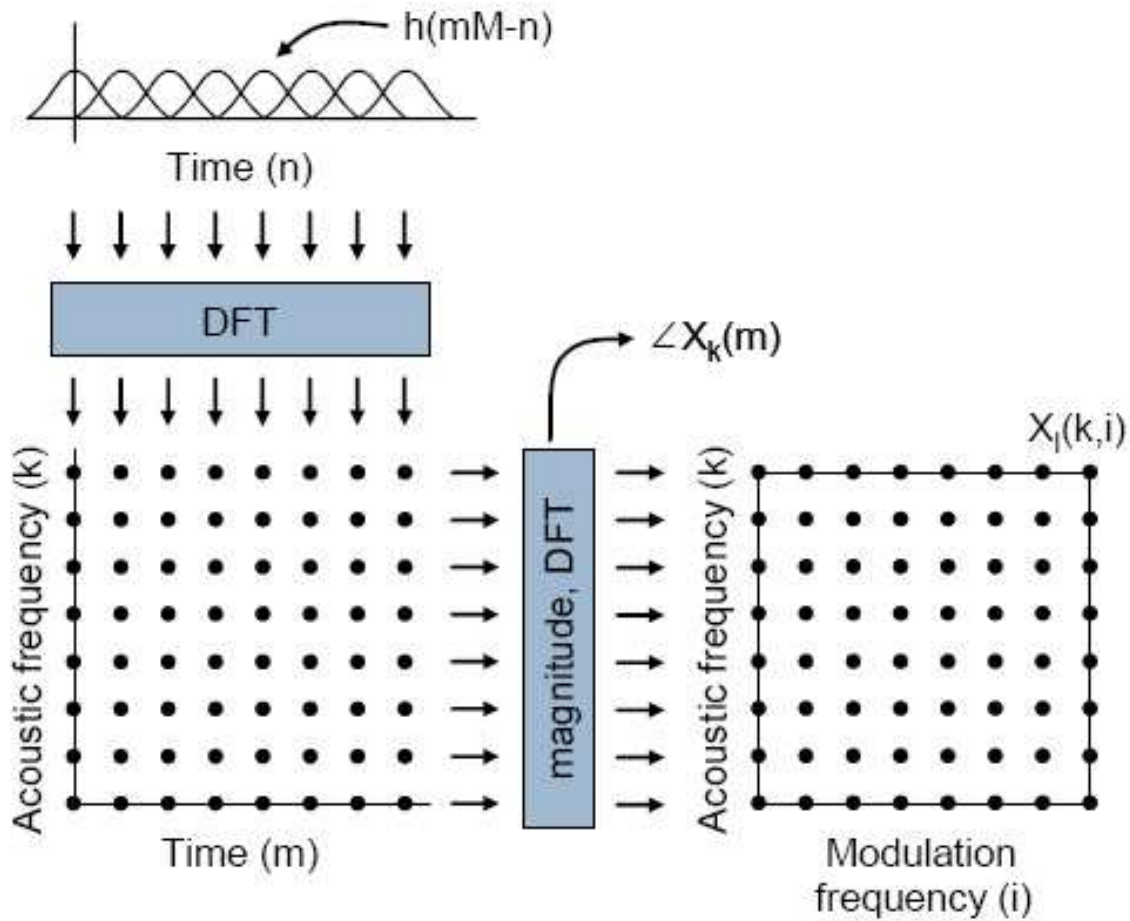


Figure 2-3. The speech signal is first decomposed into a time-frequency representation by STFT. Then within each frequency channel, a second FFT is calculated to transfer to time-frequency representation to a frequency-frequency representation, where one frequency axis represents physical frequency and the other frequency axis represents modulation frequency.

Modulation-spectral theory assumes that natural speech is modulated at a rate from 2 to 20 Hz. While mixed speech may have a great deal of overlap in the time domain, modulation frequency analysis provides an additional dimension that can provide a greater degree of separation among sources. In other words, the original time-frequency representation obtained from analyses such as STFT can be augmented to a third dimension representing modulation frequency. Components of signals from a common source are more likely to exhibit the

same modulation frequency. By selecting non-overlapped elements according to modulation frequency and regrouping them together, the target speech can in principle be reconstructed and used either for speech enhancement or speech recognition.

Nevertheless, this approach has its own issues. Since modulation frequency usually is low (again on the order of 5 to 20 Hz), a long time window is needed to estimate frequency components reliably. (For example, a 5-Hz signal typically requires an analysis frame of more than 200 ms in duration to capture the frequency components of this slowly-varying signal.) This is a problem because it is well known that instantaneous frequency changes are important for the final recognition result, and that long temporal windows will cause these frequency changes to be averaged out. This problem is similar to the tradeoff between time and frequency resolution in conventional STFT. In addition, the “coherent demodulation” method described by [28] requires an estimate of the concentrated frequency energy for each predefined frequency block. An incorrect estimation will lead to the wrong carrier frequency and will adversely affect the quality of the envelope that is estimated.

2.2.2 Differences between Amplitude and Frequency Modulation Schemes

Although amplitude and frequency modulation schemes are different, it is worthwhile to compare their mathematical details and make a few comparisons. Equation 2.3 describes a signal that could have both amplitude and frequency modulation.

$$y(t) = m_1(t) \cos(\theta(t)) = m_1(t) \cos(\omega_0 t + \int_0^t m_2(\tau) d\tau + \theta_0) \quad (2.3)$$

In Equation 2.3, $m_1(t)$ represents the amplitude modulation, where $m_2(t)$ represents the frequency modulation. When $m_2(t)$ is equal to zero, the signal is completely modulated by amplitude modulation. While $m_1(t)$ is equal to zero, the signal is only modulated by frequency modulation.

In practice, coherent amplitude modulation is not very easy to obtain. Errors incurred in the process of amplitude estimation will contribute severe negative effects to the next step regardless of whether the modulation spectrogram or adjacent correlation patterns are used.

While it is not possible to get a perfect estimate of instantaneous frequency, the results in the following chapters will show that instantaneous frequency can be used directly without very strict accuracy requirements to obtain better WER than can be obtained from instantaneous amplitude estimation.

2.3 Multi-Pitch Tracking based Speech Separation

It is very natural to imagine that speech separation can be accomplished by detecting the pitch of the mixed speech. Generally speaking, pitch estimation can be done using either temporal, spectral or spectro-temporal methods [3, 10, 20]. Unfortunately, it is very difficult to obtain perfect pitch estimation due to mutual interference from the harmonic structure of each speaker, and a reliable algorithm that can detect each of several simultaneously-presented pitches is critical in this approach. Figure 2-4 [50] shows that determining F_0 by looking at global or local maxima from spectra from pure or complex tones may not be very promising without further complicated modification. If we could identify the pitch contours of each of several simultaneous speakers, comb filtering or other techniques could be used to select the frequency components of the target speaker and suppress other components from competing speakers.

Because of its straightforward physical meaning and overall appeal, a great deal of effort has been put into algorithms that accomplish multi-pitch detection (*e.g.* [51], [21], [15], [30] and [5]). Weintraub's system [30] was among the first algorithm in this field that was applied to speech recognition. Weintraub computed the autocorrelation function of cochlear outputs, and used dynamic programming (DP) to estimate the dominant pitch from these results. After removing the components from the dominant speaker, this process was repeated to retrieve the pitch values from the weaker speaker. This method is simple and easy to implement, but it does not generally lead to a satisfactory reduction in word error rate. In addition, a Markov model is used to estimate whether zero, one, or two speakers are speaking simultaneously, and this classifier must be trained from data from the same

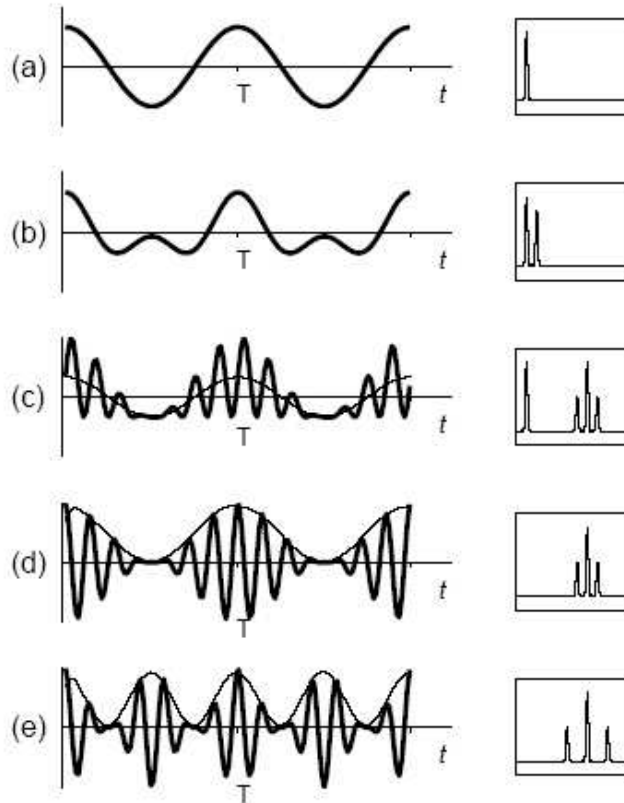


Figure 2-4. In this figure, panel (a) shows a pure tone with period T . The corresponding spectra peak is also shown on the right. Panels (b), (c), (d) and (e) share the same period T of the signal in panel (a) with different waveforms. However, by looking at the spectral response on the right, it is truly difficult to determine the fundamental frequency simply by locating the position of the global spectra peak.

speakers, which may not always be available. Other researchers [15] [14] have proposed similar recursive cancellation algorithms in which the dominant pitch value is first estimated, and then removed so that a second pitch value can be calculated. All of these algorithms are critically dependent on the performance of the first estimation stage, and errors in the first pass usually lead to errors in all subsequent passes.

Hu and Wang (*e.g.* [21]) have used a different approach to estimate pitch from simultaneously-presented speech, and their algorithm has the additional advantage of performing voiced/unvoiced decisions at the same time. A block diagram of this procedure is shown in Figure 2-5. They begin by calculating correlograms of the outputs of a model of peripheral auditory

processing, and they separate speech into low and high frequency segments. Based on the correlogram values, a decision is made concerning whether a given narrow-band frequency bin is sufficiently clean to be likely to represent only one speaker. A Hidden Markov Model (HMM) was used to estimate a pitch value from each frequency bin and to further integrate the information from all frequency channels, obtaining final pitch contours for the target and interfering speakers. However, the success of these estimate depends critically on the accuracy with which the parameters of the underlying statistical models, and this approach may not generalize well to new speakers, new pitch patterns, and/or new environments.

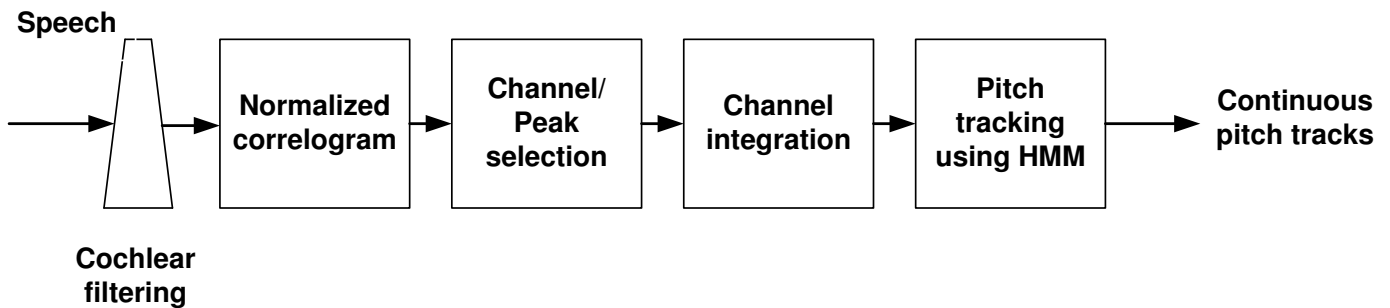


Figure 2-5. A mixture of speech and interference is processed in four main stages after the cochlear filtering. First, a normalized correlogram is obtained within each channel. Channel/peak selection is performed to select a subset of relatively clean frequency channels. In this third stage, the periodicity information is integrated across neighborhood channels. Finally, an HMM is utilized to form continuous pitch tracks.

CHAPTER 3

ESTIMATION OF INSTANTANEOUS FREQUENCY AND ITS APPLICATION TO SOURCE SEPARATION

This chapter introduces a new temporal feature based on instantaneous frequency that is intended to address some of the drawbacks to the approaches that were discussed in the previous chapter. In the early days of research, the ways in which the human auditory system interprets basic stimuli have been carefully studied by many researchers [47–49, 52–54]. As in the case of many other signal processing concepts, instantaneous frequency was originally considered in the context of frequency modulation (FM) theory that has been used in many types of communications systems. One of the most important concepts is the observation that the spectral characteristics of many real signals are not constant over time [7, 8]. Signal containing these characteristics are considered to be non-stationary. A simple example is the chirp signal, where the instantaneous frequency is a linear function of time as in Figure 3-1.

For speech signals, instantaneous frequency is also an important characteristic. It is a time-varying parameter which defines the location of the signal’s spectral peak as it varies with time. Theoretically speaking, it can be interpreted as the frequency of the best fit to the signal under analysis [7, 8]. This analysis assumes that the signal contains only a single frequency in the analysis band. Multi-component signals must first be decomposed into many narrow-band ranges for further processing.

Many research results [9] have shown that the frequency components of human speech tend to be modulated in the frequency range of 2 Hz to 20 Hz. The carrier frequencies of voiced speech segments are usually harmonically related, and modulated by a modulation frequency in the range discussed above. This implies that the frequency deviation, which refers to the amplitude of the instantaneous frequency, is proportional to the harmonic number.

3.1 Modulation Frequency and Its application to Speech Separation

There are many different types of inherent information contained in speech, such as pitch, onset/offset, time/frequency continuity, etc, as noted in Chapter 2. Among all the

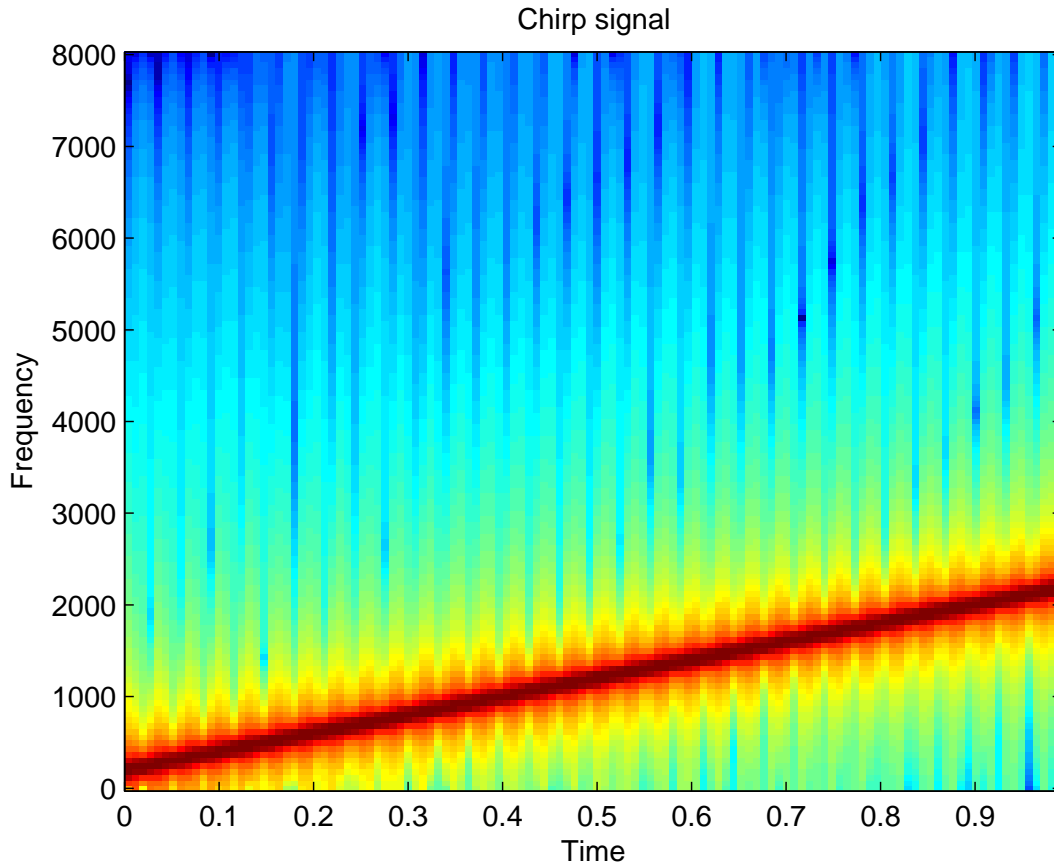


Figure 3-1. Spectrogram of a chirp signal whose frequency increases linearly with time.

various features, long-term temporal features are worthy of great attention. Among these long-term temporal features, in addition to instantaneous frequency, the similar concept of modulation frequency has also been the subject of much attention and have been used to detect pitch, separate speech, and modify speech. While instantaneous frequency and modulation frequency are related, they are not exactly the same. Modulation frequency is independent of both frequency modulation or amplitude modulation, and simply refers to the reciprocal of an entire period of a slow time-varying modulating signal. Figure 3-2 demonstrates the concepts of modulation frequency and instantaneous frequency. As discussed above, the instantaneous frequency is the entire waveform shown in Figure 3-2, while the reciprocal of the period of a given instantaneous frequency is the modulation frequency.

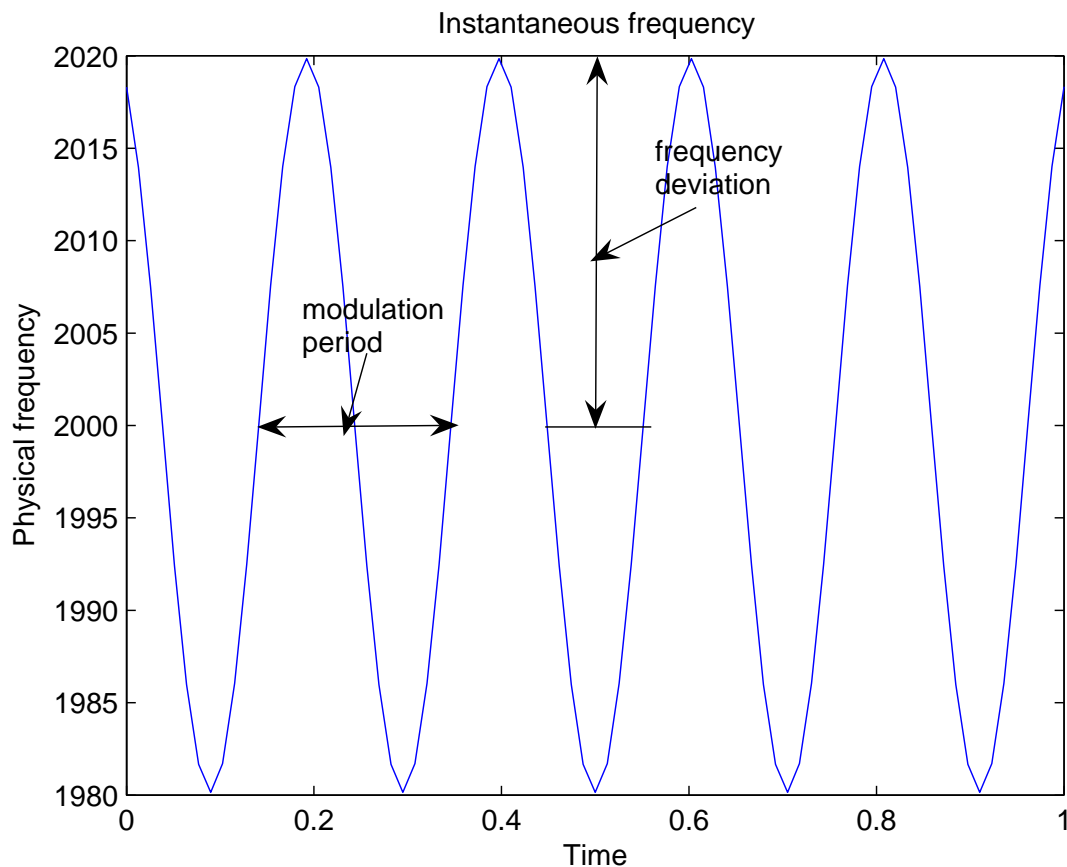


Figure 3-2. A simple example compares the concepts of modulation frequency, deviation frequency, and instantaneous frequency. In the figure, the modulation frequency is 5 Hz, the deviation frequency is 20 Hz. The modulation period is 200 ms, the reciprocal of the modulation frequency of 5 Hz.

Many studies have focused on modulation frequency in the fields of psychoacoustics and speech production, and it is now beginning to be exploited for speech processing and recognition. For example, the impact of modulation frequency on speech recognition was discussed in [46]. Filter design based on modulation frequency has also been proposed for preprocessing to mitigate the effects of reverberation [26]. Modulation frequency can also be combined with nonnegative matrix factorization to estimate pitch explicitly [42].

The potential exploitation of modulation frequency can contribute greatly to improved source separation. Traditional signal processing techniques such as short-time Fourier transform (STFT) separate signals according to time and frequency. If modulation frequency can be

consistently extracted, it provides a potential third orthogonal dimension along which signal components can be separated and clustered. The target speech signal can potentially be reconstructed by selecting those localized time-frequency regions that exhibit a particular common modulation frequency [40]. Nevertheless, accurate estimation of modulation frequency can be quite difficult for natural signals as discussed in Chapter 2.

In this chapter instantaneous frequency will be the main focus of discussion.

3.2 Instantaneous Frequency and Its Calculation

A narrowband signal can be represented by a higher-frequency carrier modulated in amplitude and phase at lower frequencies. While there are many different ways to calculate the instantaneous frequency, the primary way is to take the first derivative of the phase information. In this section, several different methods of calculating instantaneous frequency will be discussed.

3.2.1 Instantaneous Frequency Calculation

Consider, for example, the continuous-time representation of a sinusoid with time-varying amplitude $A(t)$ and phase $\theta(t)$, where the phase $\theta(t)$ is given by Equation 3.2.

$$y(t) = A(t) \cos(\theta(t)) = A(t) \cos(\omega_0 t + \int_0^t m(\tau) d\tau + \theta_0) \quad (3.1)$$

where

$$\theta(t) = \omega_0 t + \int_0^t m(\tau) d\tau + \theta_0 \quad (3.2)$$

The instantaneous frequency $\omega_i(t)$ is the derivative of the instantaneous phase $\theta(t)$ with respect to time:

$$\omega_i(t) = \frac{d\theta(t)}{dt} = \omega_0 + m(t) \quad (3.3)$$

where ω_0 is the carrier frequency and $\omega_i(t)$ is the instantaneous frequency which represents deviations about the nominal frequency value ω_0 . $m(t)$ is an arbitrary signal that can be added to the carrier frequency. If a signal is a complex tone with multiple harmonics, the n^{th} harmonic of the fundamental would exhibit the same instantaneous frequency of fundamental

frequency multiplied by n :

$$\omega_n(t) = n\omega_0 + nm(t) \quad (3.4)$$

Because instantaneous frequency is a concept that is meaningful only for narrowband signals as discussed above, an incoming speech signal must be passed through a bank of bandpass filters to provide parallel narrowband components from which instantaneous frequency may be estimated. In addition, this processing normally must take place in discrete time. The short-time Fourier transform (STFT) provides a convenient way to obtain this bandpass filtering implicitly [16, 19, 34, 37]. The combined speech $x[n]$ is decomposed into the two-dimensional time-frequency representation $X[n, k]$ where n is the time frame index and k is the index of frequency bins. Each frequency bin can be considered to be the output obtained by passing the original input through a narrow bandpass filter. The instantaneous amplitude and phase of the filter outputs for each frequency bin will be slowly time varying. The phase information $\theta[n, k]$ is obtained easily from the inverse tangent of the quotient of the imaginary and real parts of the filter output $X[n, k]$:

$$\theta[n, k] = \arctan\left(\frac{\Im(X[n, k])}{\Re(X[n, k])}\right) \quad (3.5)$$

The instantaneous frequency $\omega[n, k]$ is estimated by taking the first difference of the instantaneous phase, with care taken to deal appropriately with the effects of phase wrapping.

$$\omega[n, k] = \theta[n, k] - \theta[n - 1, k] \quad (3.6)$$

In [19, 37], an alternative calculation was proposed as follows. Suppose $X(\omega_n, t)$ is the time frequency representation of a given signal $x(n)$ obtained by applying Short-Time Fourier Transform (STFT). $X(\omega_n, t)$ can then be represented in Equation 3.7, where a and b are the corresponding real and imaginary parts of the complex spectrum.

$$X(\omega_n, t) = a(\omega_n, t) - jb(\omega_n, t) \quad (3.7)$$

where

$$a(\omega_n, t) = \int_{-\infty}^t x(\tau)h(t - \tau) \cos(\omega_n \tau) d\tau \quad (3.8)$$

and

$$b(\omega_n, t) = \int_{-\infty}^t x(\tau)h(t - \tau) \sin(\omega_n \tau) d\tau \quad (3.9)$$

From these equations the instantaneous frequency can be calculated as follows:

$$\frac{d(\theta(\omega_n, t))}{dt} = \frac{(da/dt)b - (db/dt)a}{a^2 + b^2} \quad (3.10)$$

In the actual calculation of instantaneous frequency, all the work must be done in the discrete domain. Equation 3.8 and 3.9 can be represented in their discrete form as in Equation 3.11 and 3.12

$$a[\omega_n, m] = \sum_{l=0}^m x[l] \cos[\omega_n l] h[m - l] \quad (3.11)$$

$$b[\omega_n, m] = \sum_{l=0}^m x[l] \sin[\omega_n l] h[m - l] \quad (3.12)$$

Again, m is the frame index along the time axis. Simply by taking the first-order difference of Equation 3.11 and 3.12, Δa and Δb can be calculated:

$$\Delta a = a[\omega_n, (m + 1)] - a[\omega_n, m] \quad (3.13)$$

$$\Delta b = b[\omega_n, (m + 1)] - b[\omega_n, m] \quad (3.14)$$

Finally, the discrete form of instantaneous frequency can be calculated in Equation 3.15:

$$\frac{\Delta \varphi}{T} [\omega_n, mT] = \frac{1}{T} \frac{b\Delta a - a\Delta b}{a^2 + b^2} \quad (3.15)$$

where T is the sampling period to collect the signal. Before other alternative ways to calculate instantaneous frequency introduced in the following section, Figure 3-3 is a block diagram

that describes how to obtain instantaneous frequency in the original way as discussed above.

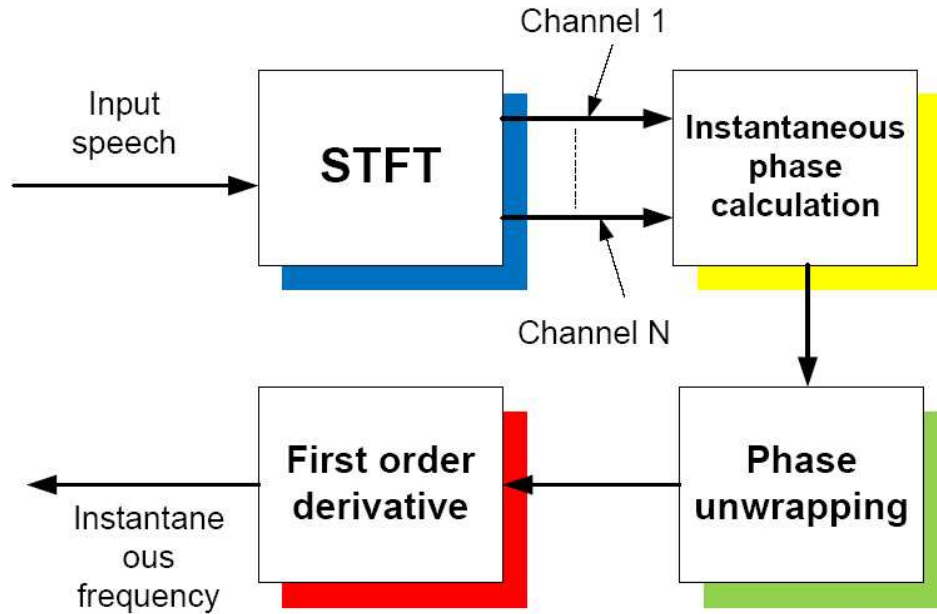


Figure 3-3. A block diagram that describes how instantaneous frequency is calculated by the method discussed in Equation 3.6.

Although the schemes shown in Figures 3-3 and 3-4 are perfect for continuous signals, some practical issues arise when discrete signals are involved. Equation 3.16 shows a discrete Short-Time Fourier Transform:

$$X[n, k] = \sum_{m=-\infty}^{\infty} x[m]w[n - m]e^{-\frac{j2\pi mk}{N}} \quad (3.16)$$

where n is the frame index and k is the frequency index. Therefore, the phase information and thus the corresponding instantaneous frequency calculated from Equation 3.6 and 3.15 are all functions of n and k . Every instantaneous phase calculated here is the difference between an average version of all samples included in the current frame and its neighbor. More specifically, the instantaneous phase calculated in the discrete case is dependent on

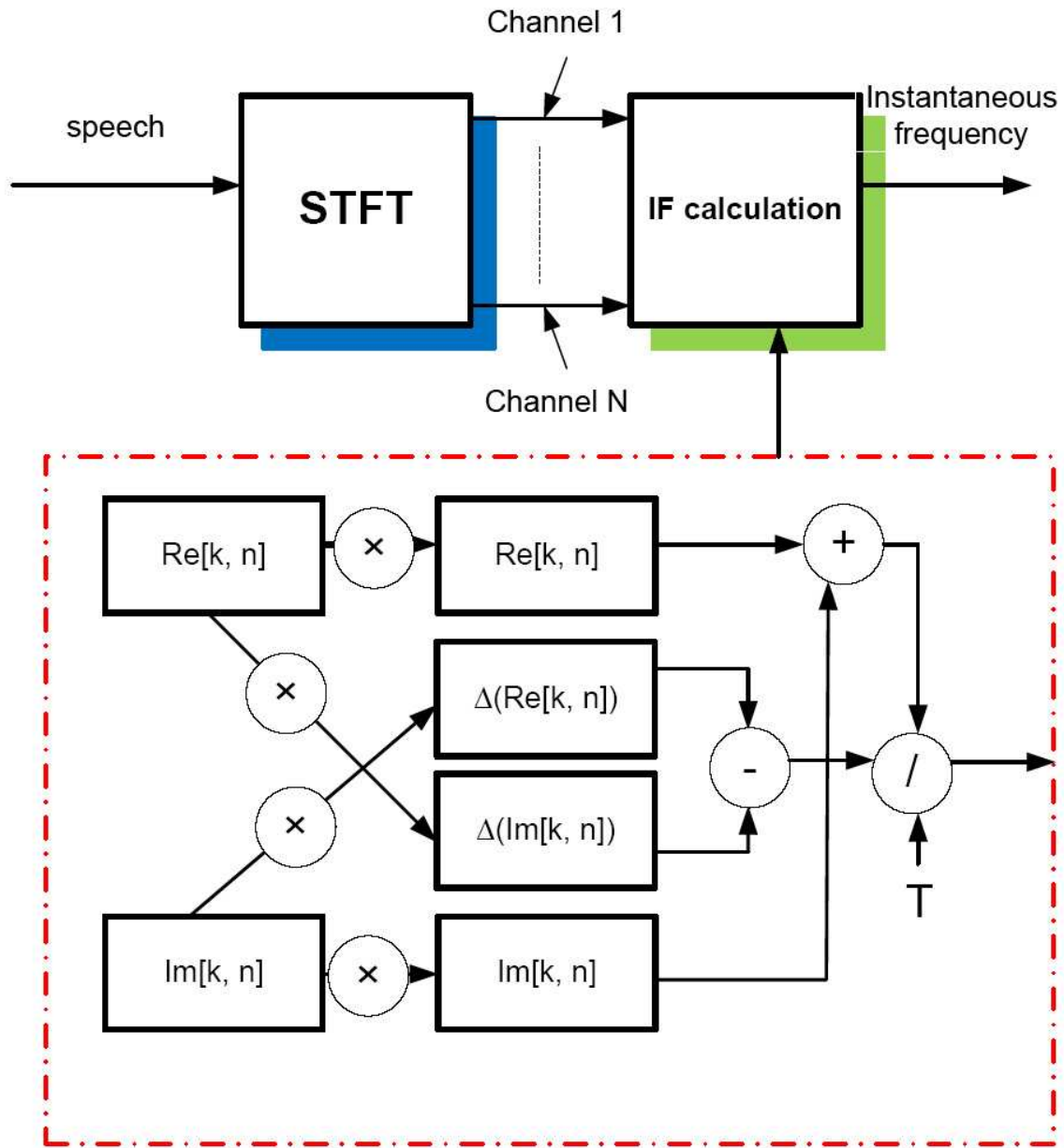


Figure 3-4. A block diagram that describes how instantaneous frequency is calculated by using the method discussed in Equation 3.15.

three factors. The first is the length of the analysis window. The second is the shape of the analysis window. And the third is the overlap between adjacent windows. The last factor gives us a hint that the calculated instantaneous phase may result in an unnecessary phase discontinuity. In other words, the adjacent phase difference can jump out of the range of π . In this case, phase unwrapping is often done by adding multiples of $\pm 2\pi$ to limit the change of phase over successive frames. Figure 3.2.1 demonstrates how phase unwrapping works. [FIX FIG REF]

However, phase unwrapping only partially solves the problem. The following example shows that the calculations based on both Equations 3.6 and 3.15 give the wrong phase of the estimated instantaneous frequency.

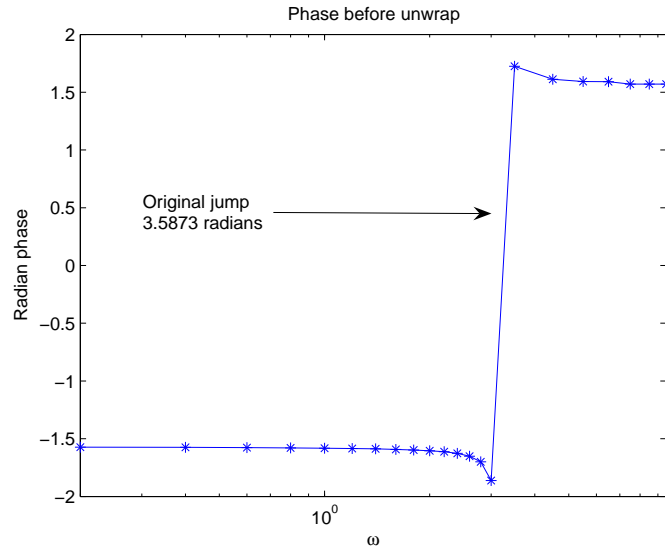
$$x(t) = A\cos(\theta(t)) \quad (3.17)$$

$$\theta(t) = 2\pi f_c t + \frac{20}{f_m} \sin(2\pi f_m t) \quad (3.18)$$

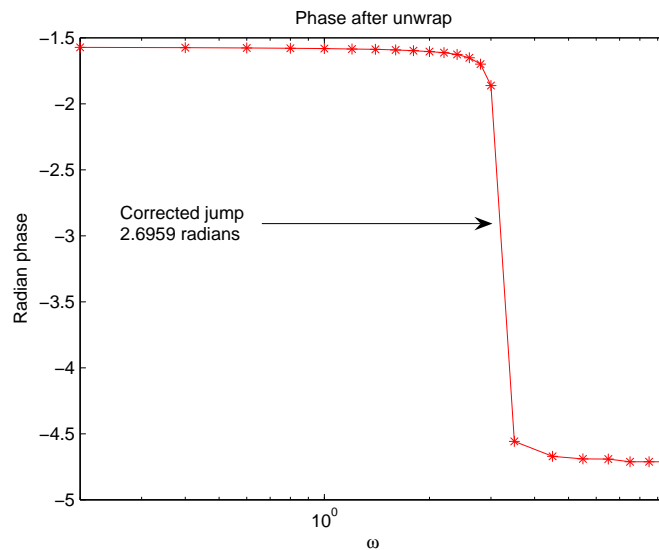
$$\omega(t) = 2\pi f_c + 2\pi 20 \cos(2\pi f_m t) \quad (3.19)$$

Equation 3.18 and 3.17 illustrate an expression of a testing signal, in which the instantaneous frequency is given in Equation 3.19. However, Figure 3-6 shows that the instantaneous frequency from all three channels in the harmonic structure contains instantaneous frequency in the form of a sine wave rather than a cosine, even though the frequency deviation and modulation frequency value are correct in this example.

In the following section, two “continuous” forms of instantaneous frequency calculation will be presented in order to solve this problem, where “continuous” refers to avoiding using the phase difference between adjacent windows in the discrete case.



A Before phase unwrapping, a wide phase jump exists



B After phase unwrapping, the wide phase jump is removed

Figure 3-5. The upper panel is the estimated phase before phase unwrapping and the lower panel is the corresponding estimate after phase unwrapping.

3.2.2 Two Alternative ways to Calculate Instantaneous Frequency

As discussed in the previous section, assume $X(\omega, t)$ is the time frequency representation of a given signal $x(n)$ in the time domain. An alternate representation of $X(\omega, t)$ is in the form of Equation 3.20 below:

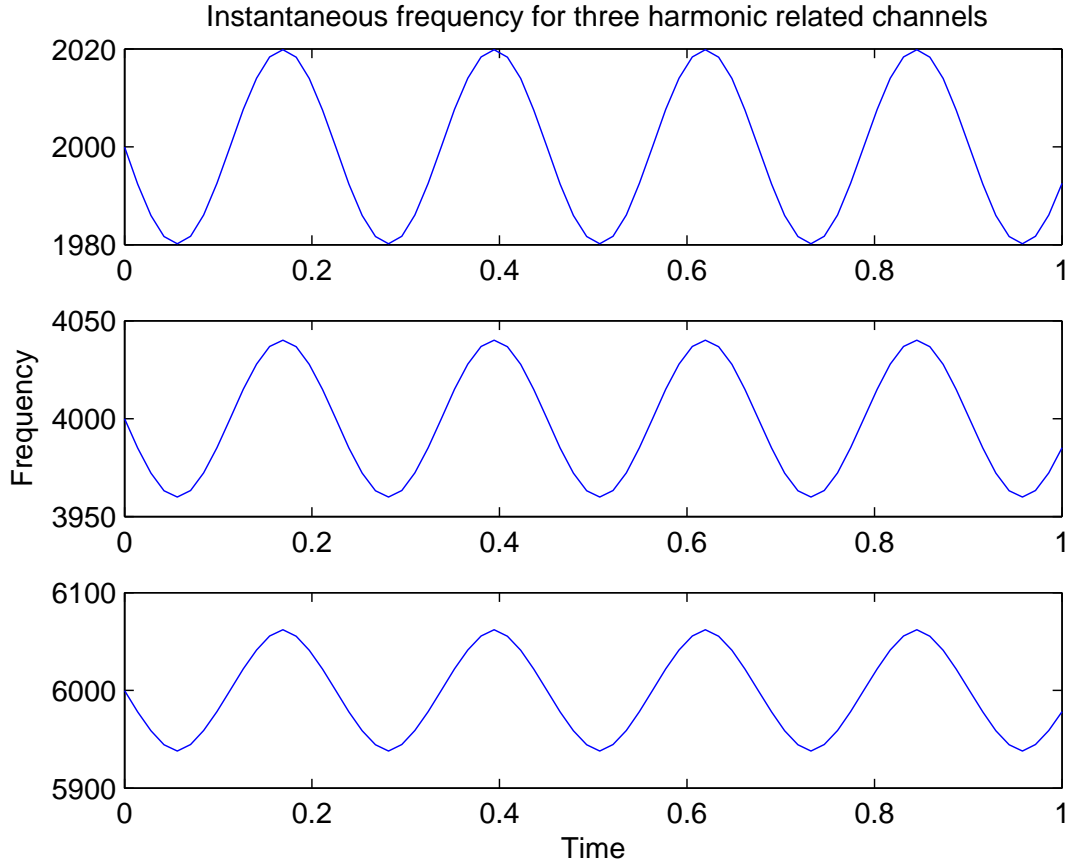


Figure 3-6. The instantaneous frequency estimate of a multi-sinusoid signal using Equations 3.6 or 3.15.

$$X(\omega, t) = A(\omega, t)e^{j\theta(\omega, t)} \quad (3.20)$$

where $A(\omega, t)$ is the instantaneous amplitude and $\theta(\omega, t)$ is the instantaneous phase information. Since instantaneous frequency is related only to its instantaneous phase, the phase can be calculated as in Equation 3.22 [27]:

$$\theta(\omega, t) = \angle X(\omega, t) = \Im \log[X(\omega, t)] \quad (3.21)$$

where $\angle x$ and $\Im x$ denote the angle and the imaginary part of the complex number x , respectively.

$$\begin{aligned}
\frac{\partial \theta(\omega, t)}{\partial t} &= \frac{\partial \Im(\log[X(\omega, t)])}{\partial t} \\
&= \Im\left(\frac{\partial \log[X(\omega, t)]}{\partial t}\right) \\
&= \Im\left(\frac{\partial X(\omega, t)/\partial t}{X(\omega, t)}\right) \\
&= \Im\left(\frac{\frac{\partial}{\partial t} \int_{-\infty}^{\infty} x(\tau)w(\tau - t)e^{-j\omega\tau} d\tau}{X(\omega, t)}\right) \\
&= \Im\left(\frac{\int_{-\infty}^{\infty} x(\tau) \frac{\partial w(\tau - t)}{\partial t} e^{-j\omega\tau} d\tau}{X(\omega, t)}\right) \\
&= \Im\left(\frac{X_1(\omega, t)}{X(\omega, t)}\right) \tag{3.22}
\end{aligned}$$

where $X(\omega, t)$ is the Short-Time Fourier Transform (STFT) of the time domain signal $x(n)$ and $X_1(\omega, t)$ is the STFT of the same signal $x(n)$ but using the derivative of the original window $w(t)$ as the new window signal. Equation 3.23 and 3.24 show details below:

$$X(\omega, t) = \int_{-\infty}^{\infty} x(\tau)w(\tau - t)e^{-j\omega\tau} d\tau \tag{3.23}$$

$$X_1(\omega, t) = \int_{-\infty}^{\infty} x(\tau) \frac{\partial w(\tau - t)}{\partial t} e^{-j\omega\tau} d\tau \tag{3.24}$$

Equation 3.22 does not calculate instantaneous frequency through each windowed frame. Instead, it takes the derivative of the window signal itself and calculates instantaneous frequency in a “continuous” way while remaining in discrete form. By using this method, there is no first-order discrete difference operation needed to calculate instantaneous frequency. All calculations are based on the same operation of the STFT with a different type of window signal.

Given the time-frequency representation of signal $x(n)$ in Equation 3.23, the filter bank can be expressed in Equation 3.25:

$$F(\omega, t) = e^{j\omega t} X(\omega, t) \tag{3.25}$$

As a result, the instantaneous frequency can be represented by Equation 3.26 :

$$\frac{\partial\theta(\omega, t)}{\partial t} = \frac{\partial}{\partial t} \arg[F(\omega, t)] \quad (3.26)$$

If $F(\omega, t)$ is also represented as:

$$F(\omega, t) = a - jb \quad (3.27)$$

Inspired by Equation 3.10,

$$\frac{\partial\theta(\omega, t)}{\partial t} = \frac{(\partial a/\partial t)b - (\partial b/\partial t)a}{a^2 + b^2} \quad (3.28)$$

To solve $\partial a/\partial t$ and $\partial b/\partial t$ in a “continuous” way, we perform the operation

$$\begin{aligned} \frac{\partial}{\partial t} F(\omega, t) &= \frac{\partial a}{\partial t} - j \frac{\partial b}{\partial t} \\ &= \int_{-\infty}^{\infty} \left(-\frac{\partial w(\tau - t)}{\partial t} + j\omega w(\tau - t) \right) e^{-jw(\tau - t)} x(\tau) d\tau \end{aligned} \quad (3.29)$$

In Equation 3.29, it is easy to see the equation is nothing but a STFT of the same signal $x(n)$. Again, the only difference is the window signal $w(\tau - t)$ is replaced by a new window $-\frac{\partial w(\tau - t)}{\partial t} + j\omega w(\tau - t)$. By doing this transformation, all parameters in Equation 3.28 can be calculated in “continuous” form and thus achieve the best possible results. Figure 3-8 illustrates the estimate of instantaneous frequency obtained by using the instantaneous phase represented by Equation 3.18. By contrasting it to Figure 3-6, it is easy to see that this estimate has the correct cosine form with the correct deviation and modulation frequencies.

3.3 Instantaneous Frequency Estimation for Frequency-modulated Complex Tone

In the previous sections we discussed methods for estimating instantaneous frequency in both continuous and discrete form. We now discuss some actual examples using a multi-sinusoidal signal, along with the estimation of instantaneous frequency for frequency-modulated complex tones.

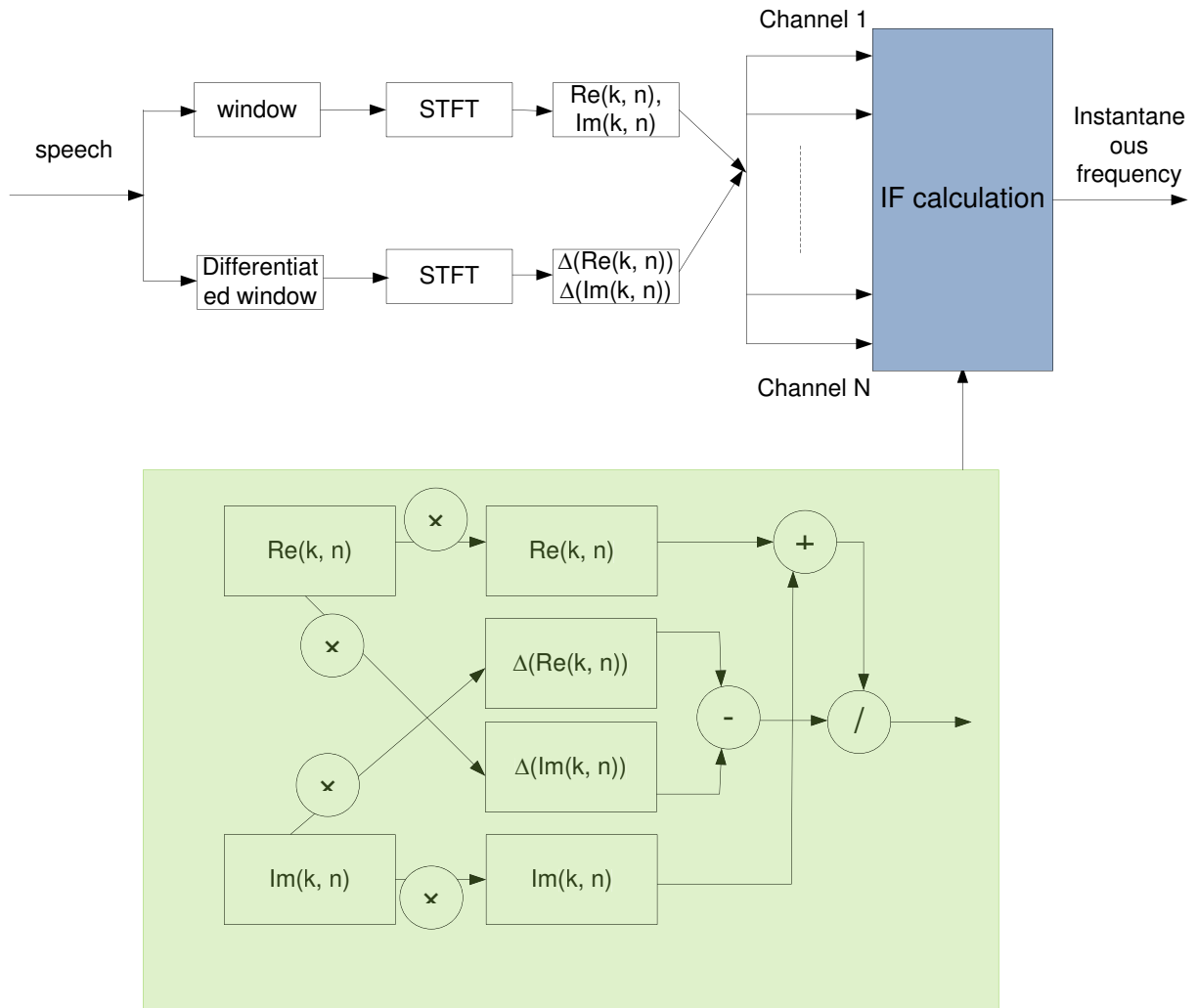


Figure 3-7. A general diagram of how instantaneous frequency is calculated by using the differentiated window method discussed in Equation 3.29.

3.3.1 Frequency-modulated Complex Tones

John Chowning is a pioneer in electronic music who is perhaps best known as the father of FM synthesis. Around 1982, Chowning demonstrated the importance of micro-modulation in perceptual grouping of complex tones. Figure 3-9 shows the waveform we refer to as the sum of three frequency-modulated complex tones, where each tone has its own fundamental frequency with its own corresponding instantaneous frequency. In the figure, from left to right, the number of complex tones increased gradually from one to three, and the fundamental frequencies of each of the three complex tones undergo separate micro-modulations

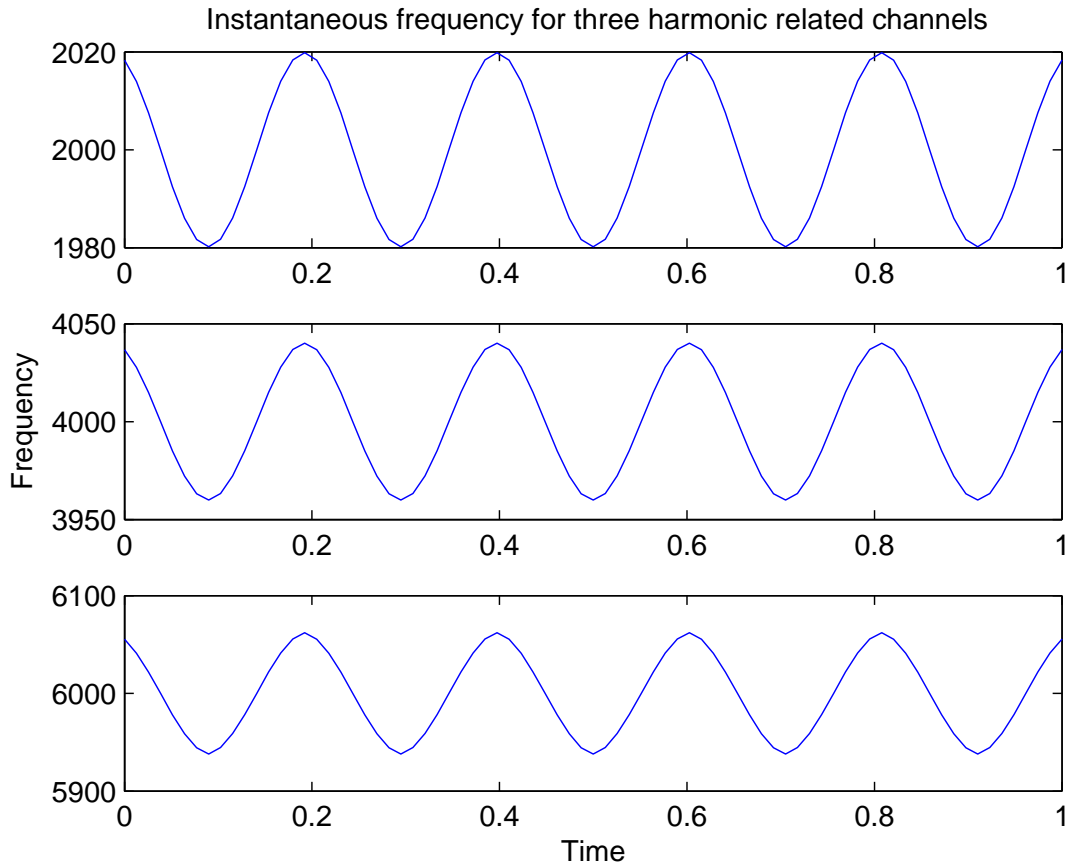


Figure 3-8. The instantaneous frequency estimation from a multi-sinusoid signal using continuous window derivative methods.

in frequency.

3.3.2 Extracting Instantaneous Frequency from Frequency-modulated Complex Tones

Figure 3-10 illustrates a simple example of the estimation of instantaneous frequency from a frequency-modulated complex tone. In this example, the signal consists of two complex tones at 0 dB, where the target tone has a fundamental frequency at 300 Hz with 5-Hz modulation frequency and 10-Hz frequency deviation, while the interfering tone has a fundamental frequency at 400 Hz with 3-Hz modulation frequency and 15-Hz frequency deviation. The figure shows the instantaneous frequency estimated from frequency channels corresponding to the first and second harmonics and a third irrelevant channel, respectively.

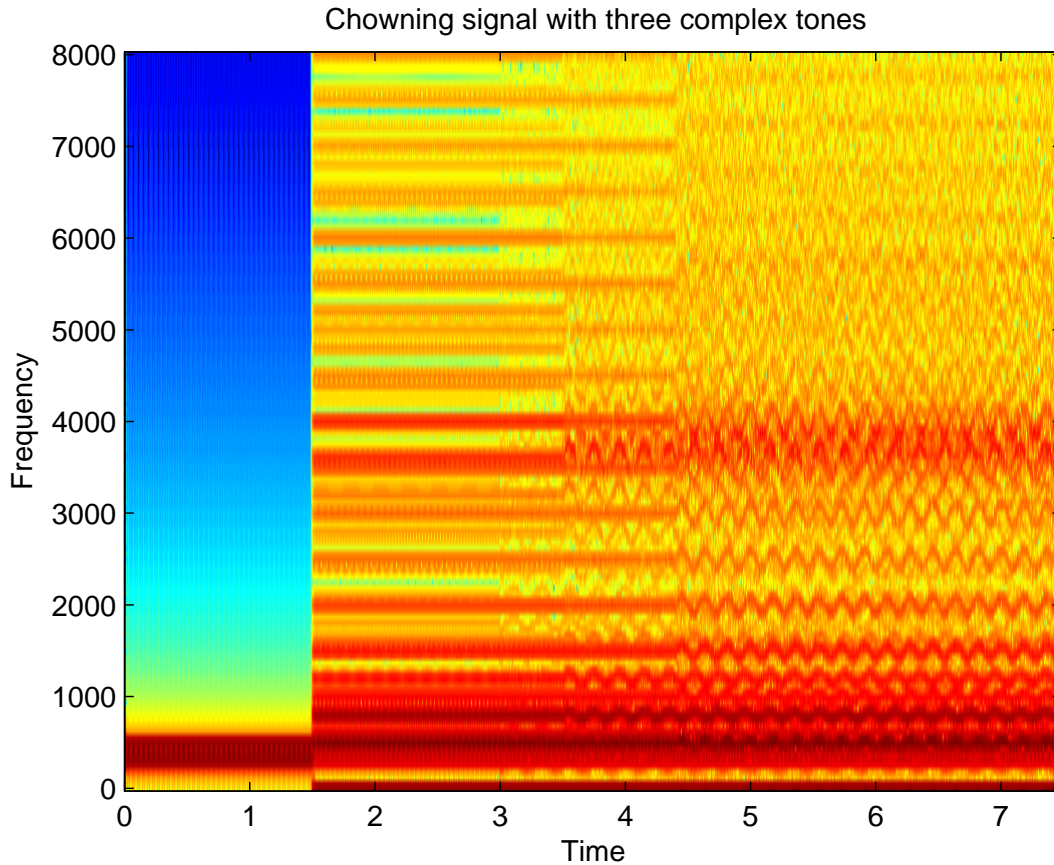


Figure 3-9. Spectrogram of the sum of three frequency-modulated complex tones.

It is clear that the instantaneous frequencies from these correlated channels behave in a similar fashion, while harmonic members' behavior are quite different from non-harmonic member's. While the estimation is not perfect compared with ground truth (which would be a perfect sinusoid), the correlation of those related channels would still be identified using traditional cross-channel correlation methods, as discussed in the following chapters. Without too much discussion on the cross-channel correlation methods itself, Table 3-1 shows the experimental results of comparisons among harmonic members as well as the ones between harmonic members and non-harmonic member. In this experiment, instantaneous frequencies are estimated from three channels at various SNRs. Two of these three channels correspond to harmonic members, while the other is from the pool of non-harmonic channels. The second column in the table shows the correlation value among the two harmonic members.

Similarly, the third column shows the correlation between harmonic and non-harmonic members. This table clearly shows that harmonic members show strong correlation even in the very challenging 0-dB environment. At the same time, non-harmonic members are easy to rule out after calculating their correlation values.

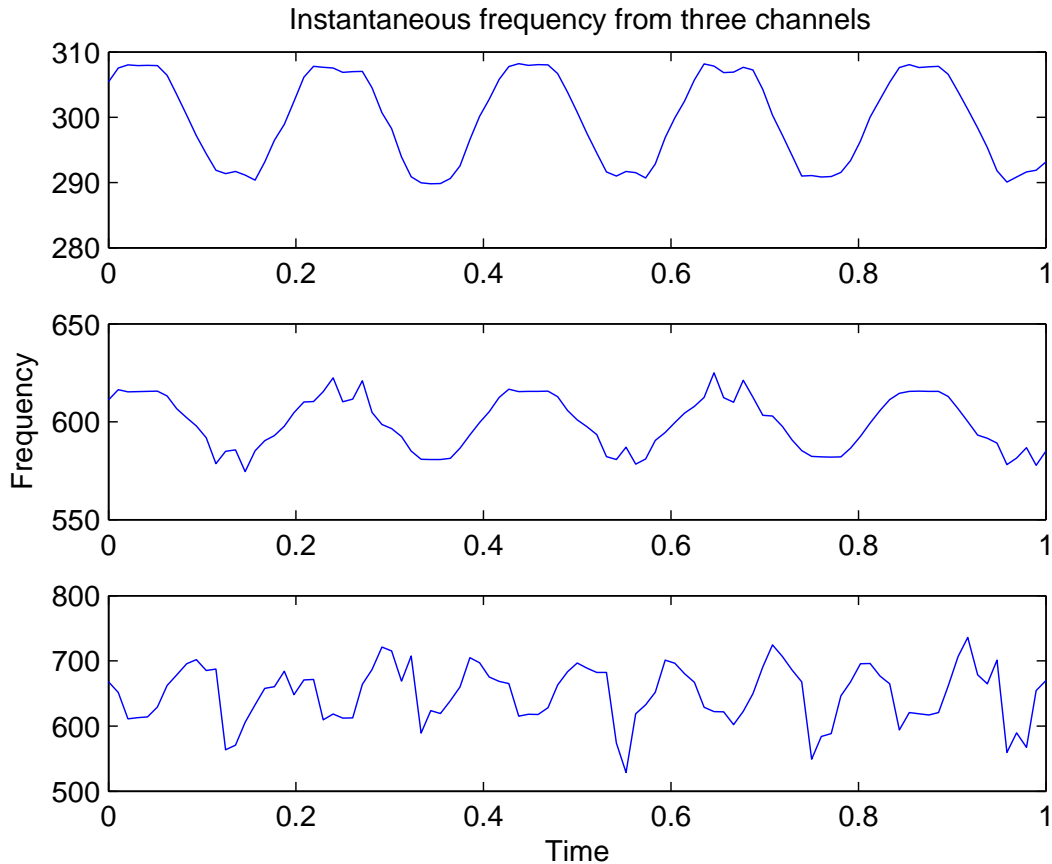


Figure 3-10. Instantaneous frequencies estimated from corresponding frequency channels from a frequency-modulated complex tones at SNR 0 dB, where the upper and middle signal are from the same harmonic structure and the lower signal is from another irrelevant channel.

3.4 Factors Affecting Instantaneous Frequency Estimation

In this chapter, multiple methods to estimate instantaneous frequency have been discussed. There are several factors that affect estimation accuracy.

SNR	correlation between harmonics	correlation with non-harmonic
Clean	0.9999	0.1011
20 dB	0.9996	0.0994
15 dB	0.9991	0.0981
10 dB	0.9976	0.0954
5 dB	0.9928	0.0904
0 dB	0.9776	0.0823

Table 3-1. Correlation comparison among harmonic members and between harmonic and non-harmonic members.

The STFT is a popular method to project the one-dimensional time signal into a two-dimensional time-frequency representation. In this representation, the center of each frequency channel is linearly spaced across the whole frequency range with bandwidth overlapping depending on how many frequency channels are used in the application. Several issues may cause inaccuracy of estimating the final instantaneous frequency. As discussed above, as the order of harmonics increases, the corresponding frequency deviation also increases proportionally. This is not an issue when harmonics are in the low frequency range. Unfortunately, this becomes a serious problem when frequency becomes greater. Since the bandwidth of each frequency channel is only determined by the number of samples contained in each frame used to do the Fourier transform, bandwidth is not a function of the order of harmonics. Therefore, when the frequency deviation becomes larger than the bandwidth of the frequency channel in the high-frequency range, the estimation of instantaneous frequency is no longer as accurate as in the low frequency range. Fortunately, the experiments shown in the following chapters will demonstrate that it is possible to obtain reasonable results by dealing only with frequency components up to 4000 Hz.

The second issue of estimation comes from corruption by frequency components from other sources. When more than one source is involved in the same mixed signal, instantaneous frequency estimation cannot be perfect due to either noisy components sitting in the same frequency channel or due to smearing from adjacent frequency channels. Nevertheless, Table 3-1 indicates that imperfect estimation of instantaneous frequency can still yield reasonably good classification results.

In general, our proposed method is valid when the target signal does not fall below 0 dB compared to interfering speech, when the fundamental frequencies of the target and interfering speakers are not too close to one another, limiting processing to frequencies below 4000 Hz. Fortunately, in practice, all these conditions are not too difficult to meet.

CHAPTER 4 CROSS-CHANNEL CORRELATION AND OTHER MASK-CLUSTERING METHODS

In Chapter 3, multiple ways to estimate instantaneous frequency have been discussed. This is the first step to extract similar temporal features shared among harmonic structures from simultaneous speech. In this chapter, cross-channel correlation and other mask-clustering methods are proposed in order to identify which frequency channels are from the same harmonic structures.

4.1 Cross-channel Correlation

The term “cross-channel correlation” used in this dissertation is defined to be the pair-wise correlation between every pair of frequency channels cross the entire designed frequency regions. It is proposed to extract to the greatest extent possible those frequency channels that are believed to come from the same speech source. The key idea of using cross-channel correlation is to identify the common frequency trajectory movement within each frequency channel. In this chapter, the major trajectory we try to track is instantaneous frequency. As discussed in the previous chapter, with the presence of other competing speech or any other type of noises, perfect estimation of instantaneous frequency is not possible. By using this method, a certain degree of instantaneous frequency estimation inaccuracy can be tolerated. As long as the direction of movement of instantaneous frequencies from the same source remains intact, cross-channel correlation is able to pick up the common tendency even though the estimation of instantaneous frequency is not perfect. Other complementary methods will also be discussed in this chapter to prune out further certain frequency channels that are extracted in error using this algorithm.

If this can be done, frequency components from different speakers should be categorized into different groups. There is one important assumption in using this method, which is that the fundamental frequencies of the two speakers do not overlap too much. If this is the case, most, if not all, of the harmonic structures of the two speakers will overlap with each other, which makes the separation task almost impossible.

As briefly mentioned before, one way to determine these intrinsic relationships among frequency components is to calculate pair-wise cross-channel correlations across the entire frequency axis. Once the instantaneous frequency is obtained based on Equation 3.6 for each time-frequency element, a pair-wise short-time cross-channel correlation of instantaneous frequency can be computed based on Equation 4.1 below. Let $R(k_0, k_1)$ represent the cross-channel correlation evaluated for two frequency channels represented by the indices k_0 and k_1 . Specifically, $R(k_0, k_1)$ is expressed as

$$R(k_0, k_1) = \frac{C(k_0, k_1)}{\sqrt{C(k_0, k_0)C(k_1, k_1)}} \quad (4.1)$$

where $C(k_0, k_1)$ is the covariance of the instantaneous frequency for indices k_0 and k_1 :

$$C(k_0, k_1) = E[(\omega[n, k_0] - \overline{\omega[n, k_0]})(\omega[n, k_1] - \overline{\omega[n, k_1]})] \quad (4.2)$$

4.1.1 Patterns of Separated Speech Components Obtained by Cross-channel Correlation

Since the motivation for using cross-channel correlation is to identify common changes of instantaneous frequency trajectory, the expected result is that the more common movement shared by two frequency channels, the higher the correlation value should be.

To demonstrate this idea, we first construct a multi-sinusoid signal. Equation 4.3 shows the combined signal, where Equation 4.5 shows the phase representation of the target signal at its fundamental frequency f_c , with the modulation frequency f_m and deviation frequency at 20 Hz, where $f_c = 2000$, $f_m = 5$. Equation 4.4 shows the phase representation of the interfering signal with fundamental frequency f_{c1} equal to 5000 and all other parameters the same. The other difference is the phase has $\pi/2$ shift.

$$x(t) = \cos(\theta(t)) + \cos(2\theta(t)) + \cos(3\theta(t)) + \cos(\theta_1(t)) \quad (4.3)$$

$$\theta_1(t) = 2\pi f_{c1}t + \frac{20}{f_m} \sin(2\pi f_m t + \pi/2) \quad (4.4)$$

$$\theta(t) = 2\pi f_c t + \frac{20}{f_m} \sin(2\pi f_m t) \quad (4.5)$$

In the experiment based on the above equations, a complex signal with fundamental frequency 2000 Hz has two harmonics at 4000 Hz and 6000 Hz, respectively. The modulation frequency added to this harmonic structure is 5 Hz, while the deviation frequency is 20 Hz. Meanwhile, an interfering sinusoid signal is added with fundamental frequency 5000 Hz, with same modulation frequency but with $\pi/2$ phase difference. Figure 4-1 shows the instantaneous frequency output from the four corresponding frequency channels, where sub-figures 1, 2 and 4 show the harmonic structure from the desired multi-sinusoid signal at frequency 2000 Hz, 4000 Hz and 6000 Hz, respectively, while sub-figure 3 shows the interfering signal at frequency 5000 Hz. From the sub-figures corresponding to the desired signal, the instantaneous frequencies tend to change in a similar fashion as they share the same modulation frequency. Meanwhile, the deviation frequency is steadily increasing from 20 Hz for the fundamental frequency to 60 Hz for the third harmonic.

Figure 4-2 demonstrates the details of these frequency changes in its spectrogram. The red parts indicates high concentrations of energy while low energy is represented by blue. Again, the frequency channels at 2000, 4000, 5000 and 6000 Hz contain most of the energy of the signal. As the harmonic order increases, the deviation frequency or the change of frequency as a function of time, becomes greater and greater.

Figure 4-3 illustrates the two-dimensional cross-channel instantaneous frequency correlation representation, where each pair-wise correlation between frequency channels is calculated and illustrated in the figure. In this case, instantaneous frequencies from four different frequency channels are used to calculate the correlation. As shown above, the instantaneous frequencies from frequency channels centered at 2000, 4000 and 6000 Hz should be highly correlated, or in other words, should be represented as red boxes in the figure, while the channel centered at

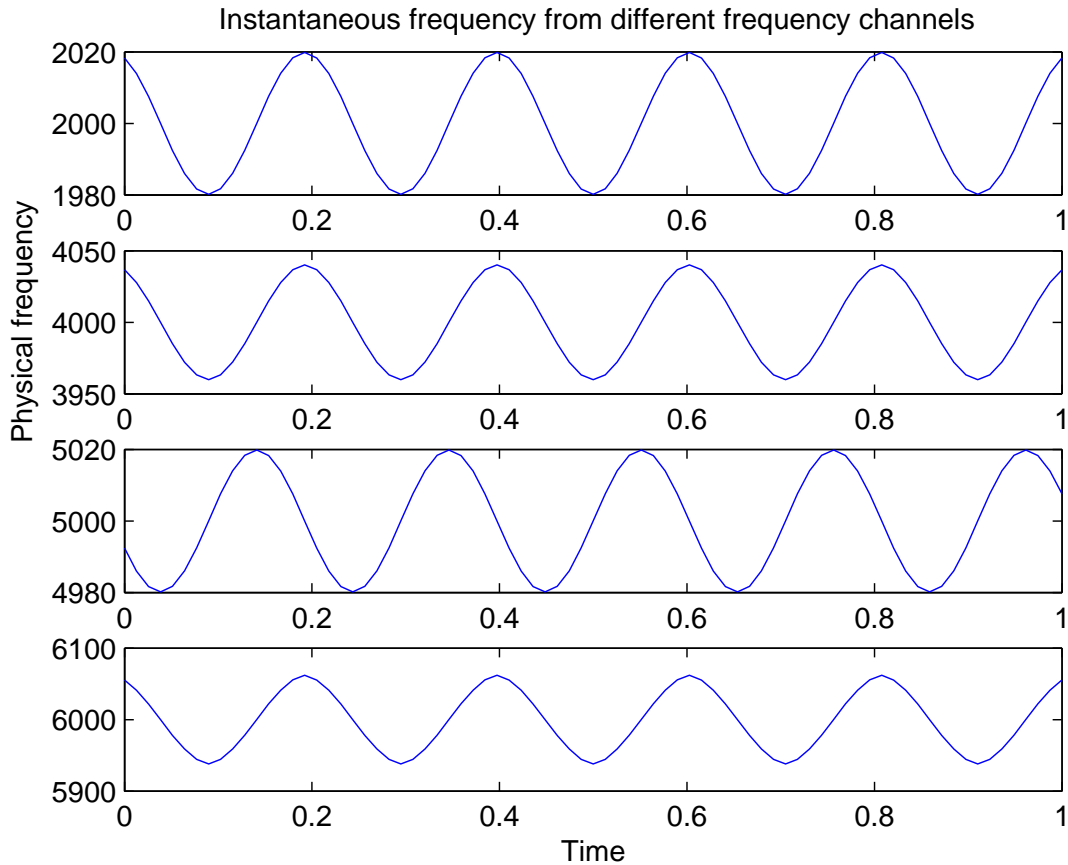


Figure 4-1. Instantaneous frequency estimates from corresponding frequency channels where a multi-sinusoid target signal and the single-sinusoid interfering signal have most of their energy.

5000 Hz should have low correlation with the other three frequency channels (*i.e.* represented by a blue box). Figure 4-3 accurately reflects this information. In the figure, Channel 3 (the frequency channel centered at 5000 Hz) is only highly correlated with itself but with no other channel.

Figure 4-4 provides an example of the cross-channel correlation of a typical frequency-modulated complex tone. Details of the type of signal were discussed in Chapter 3. In this figure, the signal has a fundamental frequency at 150 Hz with a modulation frequency at 5 Hz. Due to the overlap of frequency channels and the frequency smearing effects, several frequency channels around centers of harmonically-related frequencies show similar behavior. Each small red box in the figure represents high correlation among those frequency channels.

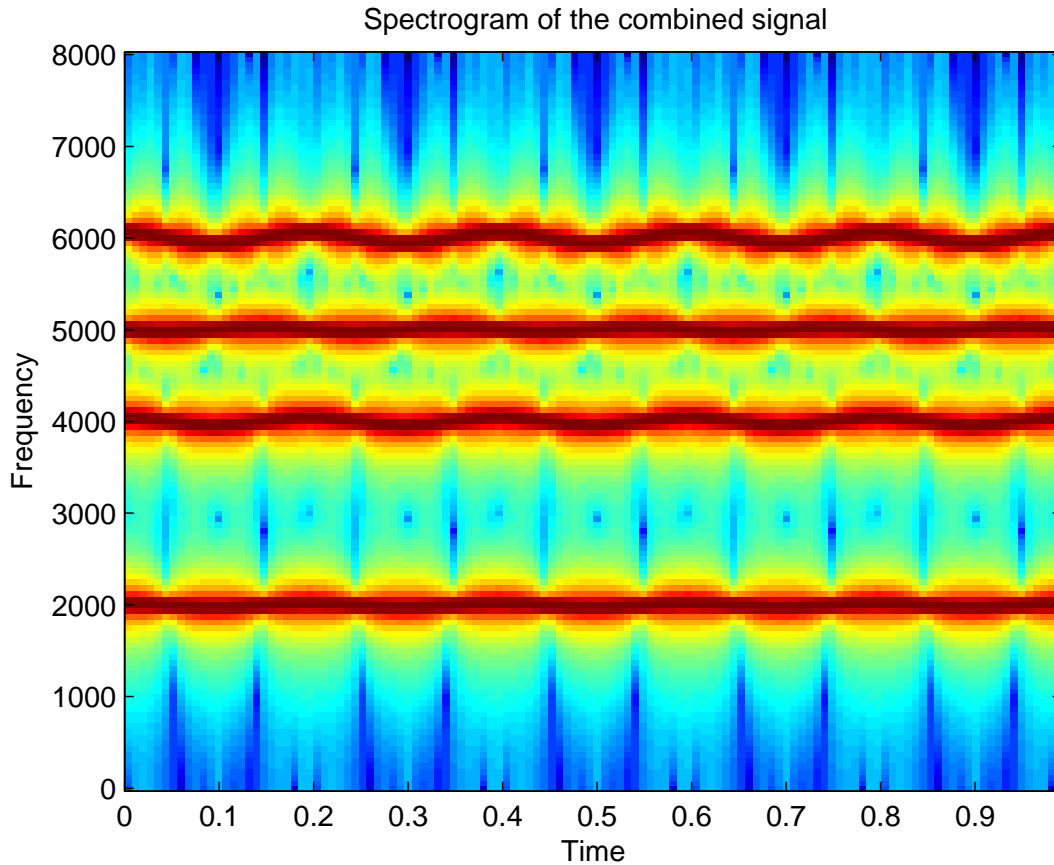


Figure 4-2. Spectrogram of the signal described in Equation 4.3.

Figure 4-4 clearly shows that all the red boxes (“pixels”) are concentrated at frequencies which are multiple integers of the fundamental frequency of 150 Hz. In the figure the first and second blue lines represent the first and second harmonics at 150 Hz and 300 Hz, respectively.

Figure 4-5 shows the two-dimensional symmetric correlation matrix R from a real speech segment where the dominant fundamental frequency is around 135.5 Hz. For any particular frequency index k in a given correlation matrix R , a row vector (or equivalently a column vector due to symmetry) represents every correlation values of this particular frequency bin K with respect to the other frequency bins. It is reasonable to assume that those frequency bins with harmonic structure should be highly correlated with each other, thus providing a

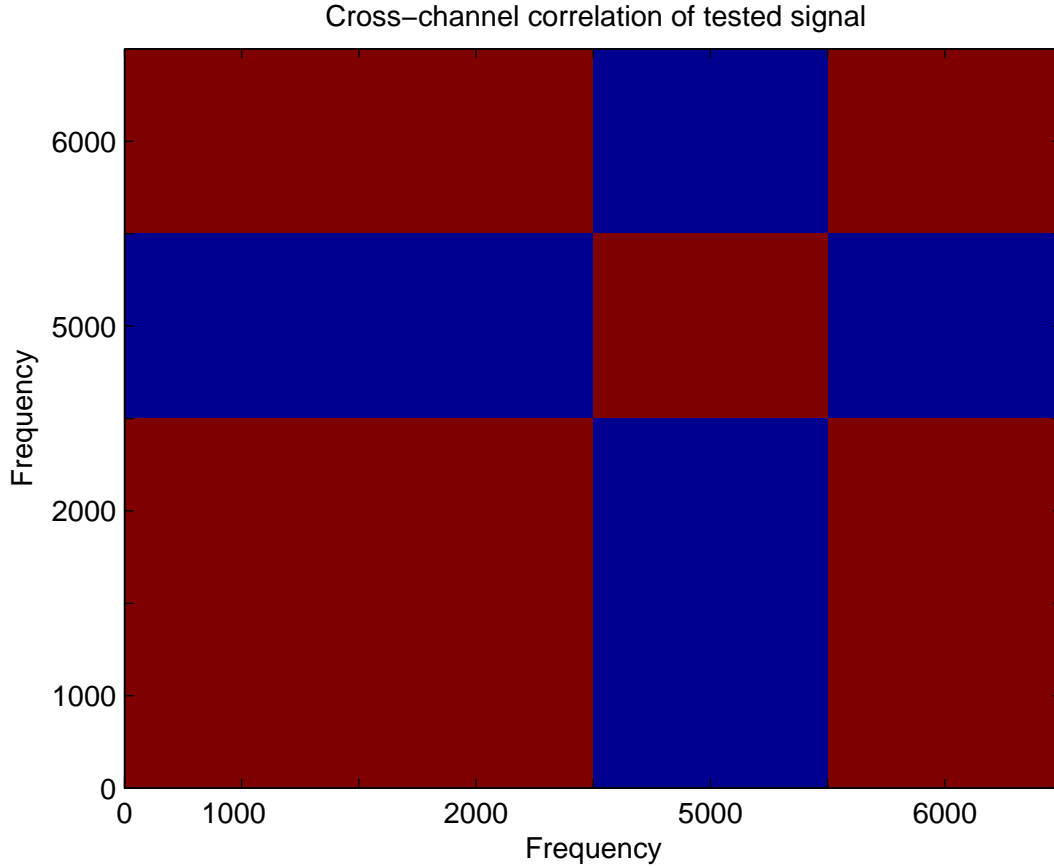


Figure 4-3. Cross-channel correlation of four frequency channels where a multi-sinusoid target signal and single-sinusoid interfering signal have most of their energy.

relatively high average value if all correlation values for a given k are averaged. Equation 4.6 below describes how to calculate the average correlation value for each frequency bin.

$$RM(k) = \frac{1}{K} \sum_{m=1}^K R(k, m) \quad (4.6)$$

where, k and m are frequency bin indices, K is the total number of frequency bins, which are typically the positive frequencies of the FFT that is evaluated in the STFT computation.

Once the average correlation is obtained, an empirically-derived threshold can be applied to determine which frequency bins have an average correlation value that exceeds the threshold and thus can be assumed to be correlated. We have observed empirically that a weak

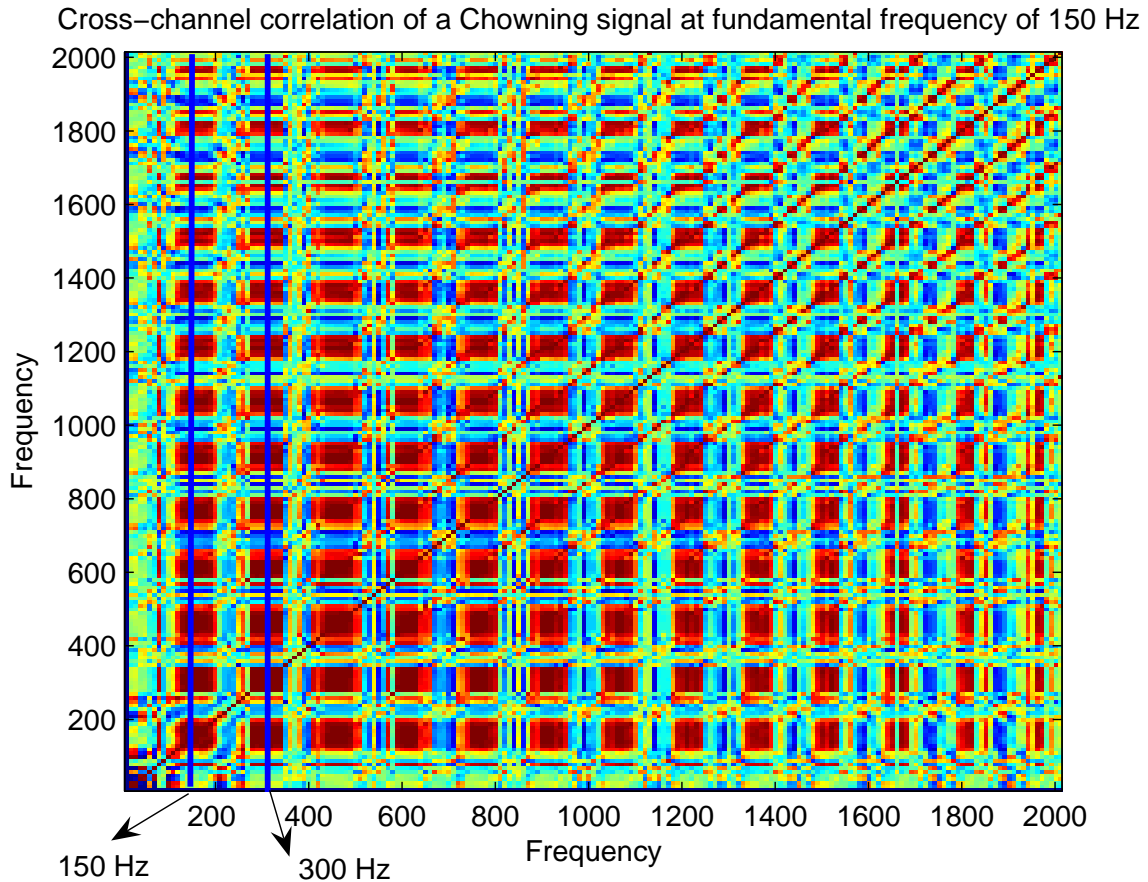


Figure 4-4. Cross-channel correlation of a typical frequency-modulated complex tone at the fundamental frequency of 150 Hz.

speaker's harmonic correlations do not have any impact as long as the local SNR is not too close to zero (which is usually satisfied).

4.1.2 Mean Square Difference Mask Generation

Cross-channel correlation has already been demonstrated to be able to identify correlated frequency components with common instantaneous frequency changes. Nevertheless, there is an issue which may cause possible errors in grouping the frequency components. From the theory discussed in Chapter 3, it is known that while the modulation frequency value itself remains the same within a given harmonic structure with the same fundamental frequency, the frequency deviation value is proportional to the order of the harmonics. In other words, with a larger harmonic number, a larger frequency deviation will be observed. If

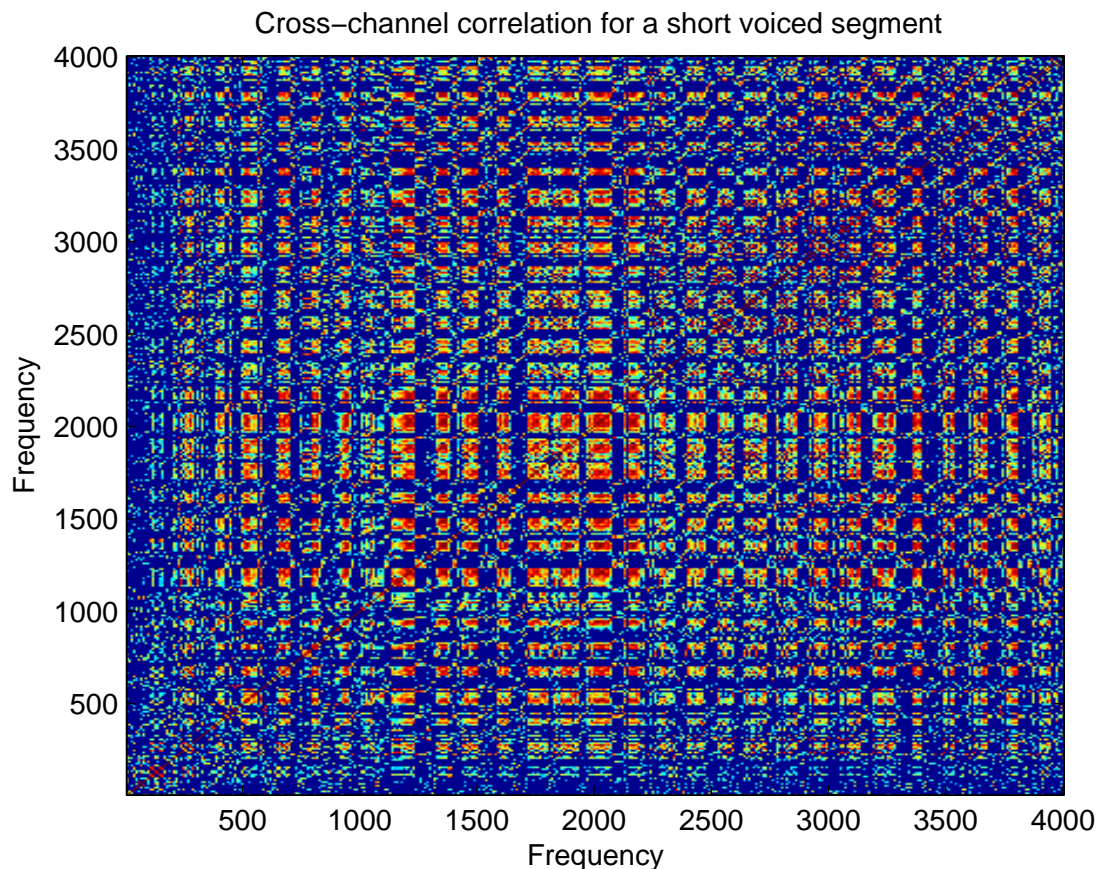


Figure 4-5. Cross-channel correlation over all frequency bins for a short voiced segment with fundamental frequency 135.5 Hz. The red and yellow regions represent high correlation, while blue and green regions represent low correlation.

different harmonics reflect the same modulation, then their actual frequency deviation will be proportional to their harmonic numbers, so they will correlate with one another, but not be equal. The problem with correlation is that it can lead to spurious matches between components whose changes are proportional, but not in the appropriate scale (*e.g.* a high frequency with a slightly positive trend in instantaneous frequency can correlate strongly with a lower frequency with a much larger instantaneous frequency trend that happens to be linear and positive as well).

In addition to applying correlation, other methods such as mean-squared difference (MSD) can be used to provide further pruning of those frequency channels which are picked up mistakenly. This combined method will be more reliable.

We make use of the signal described in Equations 4.5 and 4.3 to demonstrate this case, but with a different interfering signal. Specifically, the frequency deviation is changed to 10 Hz as in Equation 4.7 to test whether MSD can detect and further prune it out from the selection of cross-channel correlation.

$$\theta_1(t) = 2\pi f_{c1}t + \frac{10}{f_m} \sin(2\pi f_m t) \quad (4.7)$$

Table 4-1 shows the correlation values obtained using the cross-correlation method, where the ground truth is that frequency channel 3 should not be included in the final selection. As it is, frequency channel 3 demonstrates as a high correlation value in Table 4-1, as do all other frequency channels, which results in a failure to exclude Channel 3 from the frequency-component grouping. The reason is simply because the correlation calculation rules out consideration of a proportional increase of deviation frequency as discussed above.

	FREQ1	FREQ2	FREQ3	FREQ4
FREQ1	1	1	1	0.997
FREQ2	1	1	1	0.998
FREQ3	1	1	1	0.997
FREQ4	0.997	0.998	0.997	1

Table 4-1. Correlation using the cross-channel correlation method.

To solve this problem, Equation 4.8 is used to calculate the Mean Square Difference (MSD). Using this method, the distance between frequency channels from the same harmonic structures should have smaller values than those between the other channels.

$$MSD(k_0, k_1) = \frac{1}{M} \sum_{m=1}^M \left(\frac{\omega(m, k_0) - \overline{\omega(m, k_0)}}{\overline{\omega(m, k_0)}} - \frac{\omega(m, k_1) - \overline{\omega(m, k_1)}}{\overline{\omega(m, k_1)}} \right)^2 \quad (4.8)$$

where $\omega(m, k_0)$ and $\omega(m, k_1)$ represent the instantaneous frequencies from channel k_0 and k_1 at time index m and M is the total number of frames included in the calculation.

Table 4-2 illustrates results calculated using the MSD method and applied to the same signal, where the difference between channel 1 and channel 3 is abnormally high. Table 4-1 first provides a set of frequency channels that are believed to come from the same source.

Table 4-2 is used to further remove the spurious channels. Combining Table 4-2 with Table 4-1, the desired final result can be achieved.

	FREQ1	FREQ2	FREQ3	FREQ4
FREQ1	0	0	0.3103	0.0003
FREQ2	0	0	0.3120	0.0002
FREQ3	0.3103	0.3120	0	0.3154
FREQ4	0.0003	0.0002	0.3154	0

Table 4-2. Instantaneous frequency distance using the mean square difference method.

4.2 One-Dimensional Projection Solution

Both cross-channel correlation and mean square difference provide a two-dimensional representation of the relationships among all frequency channels. Nevertheless, the best way to project this two-dimensional information into one dimension and obtain the corresponding frequency index remains unclear. There are many ways to extract this information. One straightforward idea is to take the sum or average across each frequency index (*e.g.* across each row or column in Figure 4-3, 4-4). Since the correlation matrix is symmetric, the sum or average could be calculated across either the rows or columns.

Equation 4.6 shows how the one-dimensional projection is calculated. By averaging over the columns of $R(k, m)$ we obtain the average correlation for each row or column.

The frequency channels, which are members of the harmonic structure corresponding to the fundamental frequency, usually have high correlation values with other frequency channels also belong to the same harmonic structure. If one channel does not share a common modulation frequency with the others, it is rare to observe high correlation values with other frequency channels. Therefore, for the final one-dimensional average across the frequency index, it is reasonable to see that the members of the harmonic structure generally have high average correlation values, while other frequencies have relatively low values.

Figure 4-6 demonstrates the simplest case of the application of one-dimensional projection where the signal described in Equation 4.3 is used. In this case, it is already known from ground truth that the third frequency channel analyzed does not come from the same

harmonic structure as the other three channels, even though the modulation frequency is the same. In Figure 4-6, it is clear to see that the average correlation of the third frequency channel is much lower compared with the other three. A predetermined empirical threshold can be easily applied to exclude this channel from the final selection.

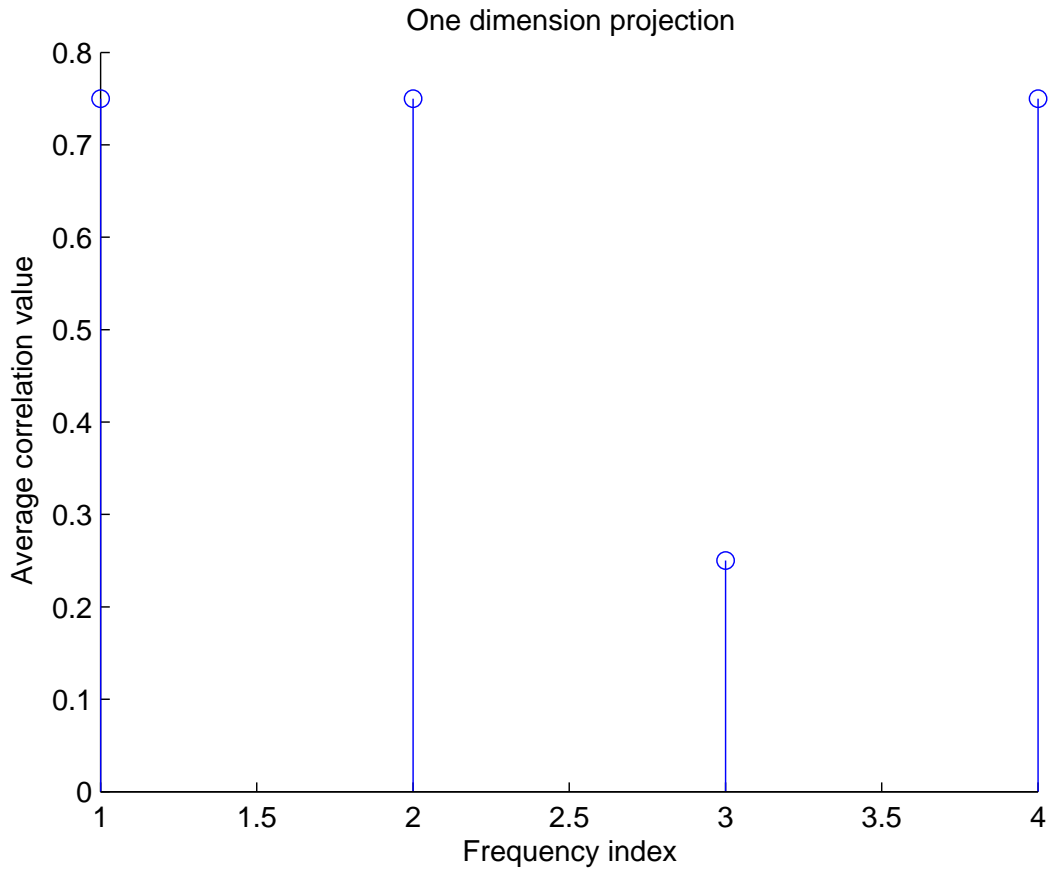


Figure 4-6. One-dimensional projection for the same signal used in Figure 4-2.

The average correlation values from a frequency-modulated complex tone is shown. When pair-wise correlation is calculated, attention should be paid only to those frequency channel pairs having relatively high correlation values. Frequency channel pairs having low correlation or even negative correlation are best filtered out before the averaging operation performed. Equation 4.9 presets all the correlation less or equal to 0.3 to zero while keeping the others intact, where 0.3 is an empirical value that may vary according to the database.

After the pre-filtering, Equation 4.6 is applied to calculate the one-dimensional average correlation values.

$$R_1(k, m) = \begin{cases} R(k, m), & \text{for } R(k, m) \geq 0.3, \\ 0, & \text{otherwise} \end{cases} \quad (4.9)$$

To show how the average correlation method can be used to successfully pick up harmonic members from all frequency channels, we designed an experiment using a frequency-modulated complex tone with two complex tones presented simultaneously at various SNRs involved. The two complex tones in each signal have different fundamental frequencies as well as modulation frequencies. In the experiment, we build up confusion matrices to illustrate the harmonic selection accuracy. Table 4-3 to Table 4-7 show the accuracies at different SNRs. In those tables, “Desired harmonics (H)” means the frequency channels that should be selected by the algorithm as harmonics, while “Undesired frequencies (H)” means those channels that should not be selected by the algorithm as harmonics. In contrast, “Desired harmonics (A)” and “Undesired frequencies (A)” represent the frequency channels that are actually identified as harmonics or not. These tables indicate that the accuracy of selecting the right harmonics decreases as SNR decreases, as would be expected. Meanwhile, the rate of missing the right harmonics increases as SNR decreases. This decreasing accuracy will eventually lead to a decrease in the final WER, which will be presented later.

	UNDESIREF FREQUENCIES(H)	DESIRED HARMONICS(H)
UNDESIREF FREQUENCIES(A)	94.55%	5.45%
DESIRED HARMONICS(A)	18.68%	81.32%

Table 4-3. Confusion matrix of performance of selected harmonic frequencies for the clean case using the 1-D projection method.

	UNDESIREF FREQUENCIES(H)	DESIRED HARMONICS(H)
UNDESIREF FREQUENCIES(A)	94.12%	5.88%
DESIRED HARMONICS(A)	24.62%	75.38%

Table 4-4. Confusion matrix of performance of selected harmonic frequencies at 15 dB using the 1-D projection method.

	UNDESIREF FREQUENCIES(H)	DESIRED HARMONICS(H)
UNDESIREF FREQUENCIES(A)	97.06%	2.94%
DESIRED HARMONICS(A)	26.15%	73.85%

Table 4-5. Confusion matrix of performance of selected harmonic frequencies at 10 dB using the 1-D projection method.

	UNDESIREF FREQUENCIES(H)	DESIRED HARMONICS(H)
UNDESIREF FREQUENCIES(A)	97.06%	2.94%
DESIRED HARMONICS(A)	38.46%	61.54%

Table 4-6. Confusion matrix of performance of selected harmonic frequencies at 5 dB using the 1-D projection method.

4.3 Graph-Cut Solution

Currently simple average correlation approach discussed in the previous section has been used to find highly-correlated frequency bins, by simple averaging along one dimension to reduce the two-dimensional correlation matrix to one dimension with modest computation. While this approach is attractive because of its low computation load, straightforward physical meaning, and relatively easy implementation, it does not exploit the structure of the correlation matrix itself. Image segmentation and grouping have provided many promising directions toward better solutions of this problem. The idea in image segmentation is to minimize the distance between members from the same group while maximizing the distance between members from different groups, which is quite similar to linear discriminant analysis (LDA) [17]. Among several graph-cut algorithms, Shi and Malik’s work [43] provides a good entry point to explore the correlation and improve the final performance.

Rather than focusing on local features and their consistencies in the two-dimensional correlation representation, the graph-cut approach aims at extracting the global impression of the 2D image. Image segmentation is treated as a graph partitioning problem. The

	UNDESIREF FREQUENCIES(H)	DESIRED HARMONICS(H)
UNDESIREF FREQUENCIES(A)	77.94%	22.06%
DESIRED HARMONICS(A)	33.85%	66.15%

Table 4-7. Confusion matrix of performance of selected harmonic frequencies at 0 dB using the 1-D projection method.

graph-cut criterion measures both the total dissimilarity between the different groups as well as the total similarity within the groups. In this way, the problem of how to efficiently extract the pattern contained in the 2D correlation matrix can be transferred into an eigenvalue and eigenvector problem, where the correlation can be the target matrix to be solved.

This approach is most related to the graph theoretic formulation of grouping. The set of points in an arbitrary feature space is represented as a weighted undirected graph $G = (V, E)$, where the nodes of the graph are the points in the feature space (a set V), and an edge is formed between every pair of nodes (a set E). The weight on each edge, $w(i, j)$, is a function of the similarity between nodes i and j .

In grouping, the goal is to seek to partition the set of vertices into disjoint sets $V_1; V_2; \dots ; V_m$, where by some measure the similarity among the vertices in a set V_i is high and, across different sets V_i, V_j is low.

Figure 4-7 shows an undirected graph G , which has 9 nodes. The index of each node is marked in red and the correlation between each node is represented in black. From the figure, it is easy to see that the entire graph can be divided into two sub-graphs, where Nodes 1, 2, 3 and 4 fall into one sub-graph and Nodes 5 to 9 belong to the other graph. All the nodes can be considered as an n -dimensional feature vector. The undirected graph is sitting in the same n -dimensional space. There are multiple ways to calculate the values between each node. Euclidean distance and other distance measures can be used, where the closer two nodes are, the smaller values are. In Figure 4-7, all values shown in the figure are correlation, where the closer two nodes are, the larger values are.

Equation 4.10 below is a matrix representation of the graph shown in Figure 4-7. The matrix is also called affinity matrix, which will be discussed in detail. Suppose there is a binary weight vector w (which is also called an indicator vector) with length equal to the number of nodes in the entire graph G , where each of its component is 1 when the corresponding node is sitting in a desired sub-graph C , as in Equation 4.11. Equation 4.12 can be used to calculate the average association between all nodes in the same sub-graph

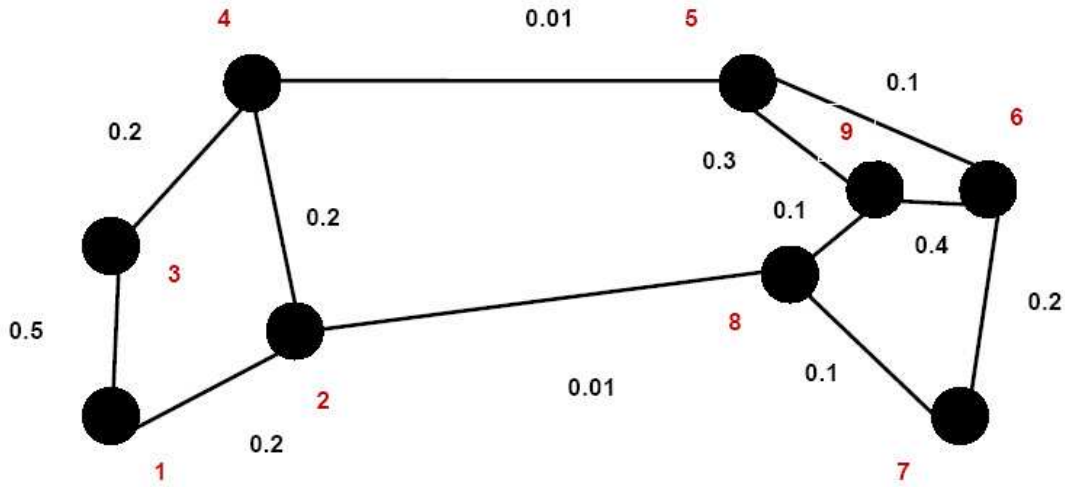


Figure 4-7. An undirected graph G , which has 9 vertices and should be divided into two partitions.

C . It is very reasonable to believe that the average association described in Equation 4.12 should have a large value if the choice of sub-graph C is a good cluster. If $\mathbf{w}^t\mathbf{w}$ is also used to normalize the calculated average association, the problem of identifying the optimal sub-graph transforms itself into the new problem of finding a proper vector w to maximize the average value of $\mathbf{w}^t\mathbf{M}\mathbf{w}$. If the requirement that vector w be binary is removed, it is expected that elements w_i in vector w would be large value compared to other elements if node i is a member of sub-graph C . This idea can be expressed in Equation 4.13. Based on Rayleigh's ratio theorem, for any symmetric affinity matrix M , the maximum value of d in Equation 4.13 can be obtained by picking up the eigenvector corresponding to the largest eigenvalue of M . For the affinity matrix M given in Equation 4.10, the largest eigenvalue λ_{max} is 1.6951, where the corresponding eigenvector is $[0.5739, 0.4326, 0.6249, 0.3044, 0.0101, 0.0085, 0.0036, 0.0083, 0.0105]$. It is easy to set up a threshold to make the decision that Nodes 5 to 9 are sitting in the

sub-graph C, which also automatically places Nodes 1 to 4 in the other sub-graph if the assumption is that there are only two sub-graphs.

$$R = \begin{bmatrix} 1 & 0.2 & 0.5 & 0 & 0 & 0 & 0 & 0 & 0 \\ 0.2 & 1 & 0.2 & 0.2 & 0 & 0 & 0 & 0.01 & 0 \\ 0.5 & 0.2 & 1 & 0.2 & 0 & 0 & 0 & 0 & 0 \\ 0 & 0.2 & 0.2 & 1 & 0.01 & 0 & 0 & 0 & 0 \\ 0 & 0 & 0 & 0.01 & 1 & 0.1 & 0 & 0 & 0.3 \\ 0 & 0 & 0 & 0 & 0.1 & 1 & 0.2 & 0 & 0.4 \\ 0 & 0 & 0 & 0 & 0 & 0.2 & 1 & 0.1 & 0 \\ 0 & 0.1 & 0 & 0 & 0 & 0 & 0.1 & 1 & 0.1 \\ 0 & 0 & 0 & 0 & 0.3 & 0.4 & 0 & 0.1 & 1 \end{bmatrix} \quad (4.10)$$

$$w_i = \begin{cases} 1, & \text{if } i \in C, \\ 0, & \text{otherwise} \end{cases} \quad (4.11)$$

$$\mathbf{w}^t \mathbf{R} \mathbf{w} = \sum_{i,j \in C} m_{ij} \quad (4.12)$$

$$d = \text{Max} \frac{\mathbf{w}^t \mathbf{R} \mathbf{w}}{\mathbf{w}^t \mathbf{w}} \quad (4.13)$$

	UNDESIRE D FREQUENCIES(H)	DESIRED HARMONICS(H)
UNDESIRE D FREQUENCIES(A)	95.28%	4.72%
DESIRED HARMONICS(A)	13.14%	87.86%

Table 4-8. Confusion matrix of performance of selected harmonic frequencies for the clean case by using the graph-cut method.

	UNDESIRE D FREQUENCIES(H)	DESIRED HARMONICS(H)
UNDESIRE D FREQUENCIES(A)	94.97%	5.03%
DESIRED HARMONICS(A)	19.77%	80.23%

Table 4-9. Confusion matrix of performance of selected harmonic frequencies at 15 dB by using the graph-cut method.

Though both one-dimensional projection and the graph-cut approach provide good ability to identify a correlation pattern from its 2-D representation in theory, the later demonstrates superior performance compared to the former. In Equation 4.13, the vector \mathbf{w} is able to iterate all possibilities of cutting the 2-D correlation into different sub-graphs by changing each individual element inside \mathbf{w} . The best existing vector \mathbf{w} is the eigenvector corresponding to the largest eigenvalue of the correlation matrix \mathbf{R} .

	UNDESIRED FREQUENCIES(H)	DESIRED HARMONICS(H)
UNDESIRED FREQUENCIES(A)	97.79%	2.21%
DESIRED HARMONICS(A)	20.28%	79.72%

Table 4-10. Confusion matrix of performance of selected harmonic frequencies at 10 dB by using the graph-cut method.

Figure 4-8 and Figure 4-9 illustrate the superiority of using the graph-cut method compared to one-dimensional projection by plotting the selection results using the two methods.

Table 4-8 to Table 4-12 show the performance with confusion matrices by applying the graph-cut method to the same signals described above. The results reconfirm that the graph-cut method is more reliable than one-dimension projection with a penalty of a greater computational load in calculating eigenvalues and eigenvectors for each correlation matrix. We will compare these two methods in terms of their impact on speech recognition accuracy in the following chapter.

	UNDESIRED FREQUENCIES(H)	DESIRED HARMONICS(H)
UNDESIRED FREQUENCIES(A)	96.36%	3.64%
DESIRED HARMONICS(A)	30.77%	69.23%

Table 4-11. Confusion matrix of performance of selected harmonic frequencies at 5 dB by using graph-cut method.

	UNDESIRED FREQUENCIES(H)	DESIRED HARMONICS(H)
UNDESIRED FREQUENCIES(A)	76.47%	23.53%
DESIRED HARMONICS(A)	32.31%	67.69%

Table 4-12. Confusion matrix of performance of selected harmonic frequencies at 0 dB by using graph-cut method.

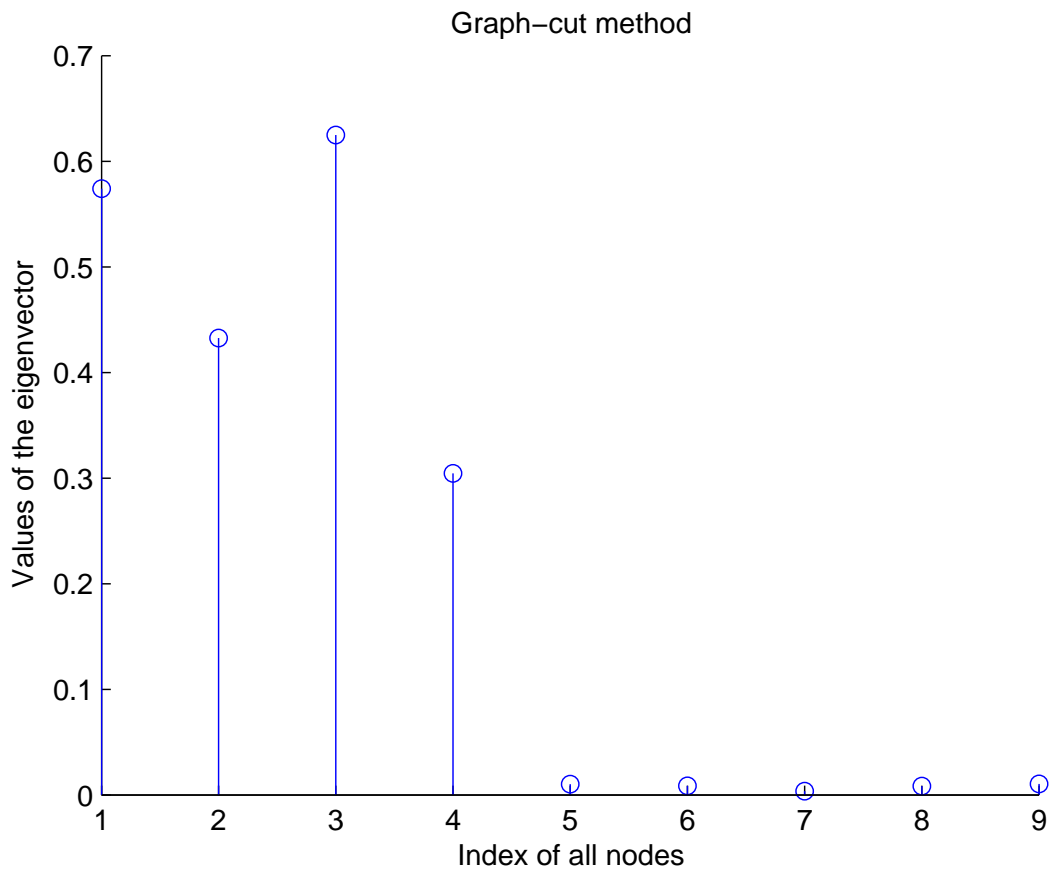


Figure 4-8. Graph-cut method to extract classification information from correlation matrix.

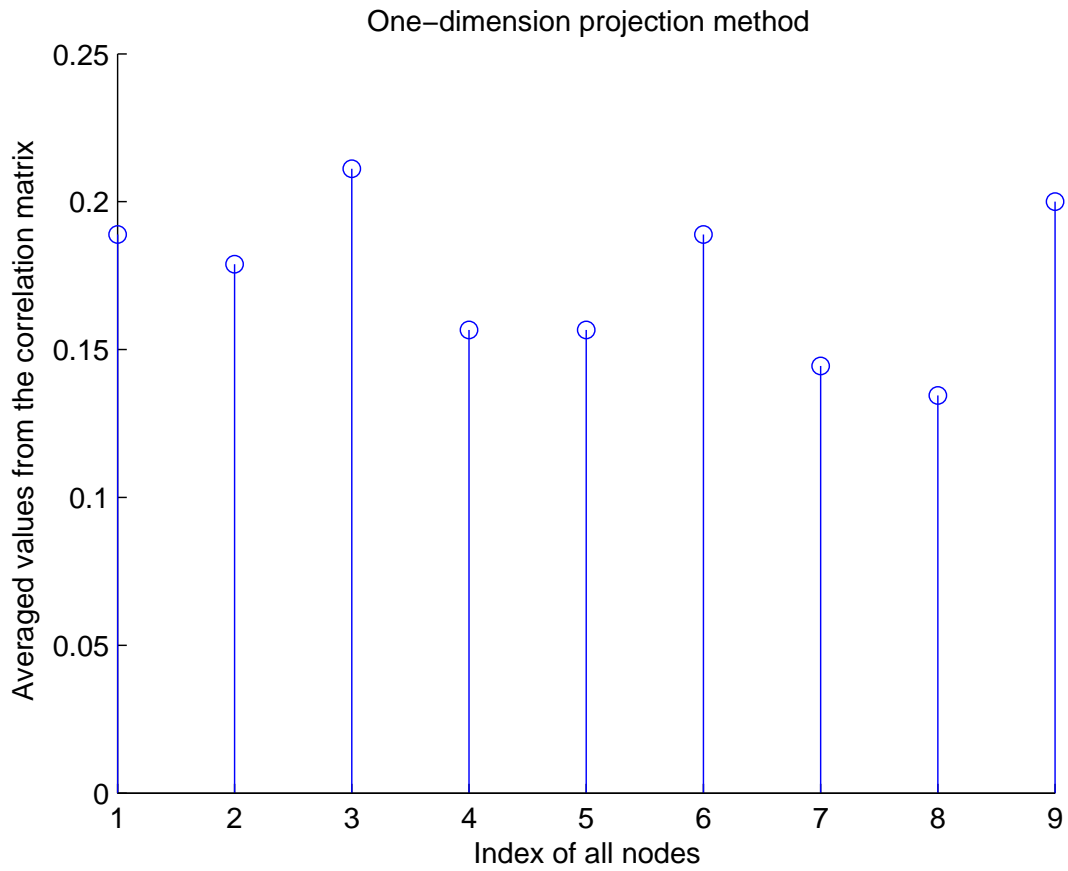


Figure 4-9. 1-D projection method to extract classification information from correlation matrix.

CHAPTER 5 GROUPING SCHEMES AND EXPERIMENTAL DESIGN

In the previous chapters we have discussed the estimation of instantaneous frequency, the application of cross-channel correlation and the utilization of graph-cut theory to identify frequency channels from the same speech source.

In this chapter, the solution of how to regroup frequency components identified from the same source will be discussed, which includes pitch detection and traditional speaker identification. In addition, a sieve function will be introduced to refine further the selected harmonic structure obtained from the cross-channel correlation function based on instantaneous frequency. A general discussion about the generation of binary masks will follow. Finally, experimental results will be presented that compare our proposed algorithm with several others, including baseline Mel-Frequency Cepstral Coefficients (MFCC), a multi-pitch tracking algorithm and an instantaneous-amplitude-based algorithm.

5.1 Grouping Schemes

As mentioned above, there are two major stages in speech separation, segregation and regrouping. Chapters 3 and 4 include a detailed discussion of how to use instantaneous-frequency-based cross-channel correlation to achieve segregation. In real experiments, this stage simply makes a decision about how many frequency channels are believed to have the same harmonic structure in each processed frame.

Nevertheless, this is not the end of the story. In order to reconstruct the entire utterance, we usually must determine whether the clustered frequency channels from the first stage in each individual frame are from the target speaker or from a competing speaker. This challenge introduces the second important stage in speech separation, regrouping.

In general, the evaluation of systems that separate two speakers is typically divided into two categories: the same-gender and different-gender cases. In this chapter we will describe two different schemes that address this problem, which are based on pitch detection for the different-gender case and speaker identification for the same-gender and the general cases.

5.1.1 Pitch Detection for Dominant Speakers for the Different-Gender Case

Pitch detection for grouping of speakers can be used for the different-gender case only, when it is known *a priori* that the target and masking speakers are of the opposite gender. The speech of speakers of different genders have fundamental frequencies that seldom overlap and that frequently are quite far from one another. The harmonic structures from the target speaker and interfering speaker are not very likely to overlap as well.

When the SNR is greater than zero, even though the interfering speaker might be the dominant speaker in some frames, the majority of the frames are likely to represent the pitch contour of the target speaker. After a simple pitch estimation, it is relatively easy to determine the pitch range of the target speaker, as a single pitch contour most likely represents the pitch from the dominant speaker from each individual frame. If the majority of the pitch contours is below approximately 160 Hz, there is a high chance that the dominant speaker of the entire utterance is a male speaker. Based on similar logic, a female dominant speaker is easy to detect if the majority of the pitch frames is above 160 Hz.

After applying the instantaneous-frequency-based cross-channel correlation for each individual frame, all frequency channels are classified into two groups, one associated with the dominant speaker and the other with the interfering speaker. Frames are sorted according to whether the dominant speaker is assumed to be the target or interfering speaker based on this pitch information.

Two comments are worth noting here. First, the pitch estimation described here is not the multi-pitch algorithm mentioned in previous chapters that provides separate pitch contours for the target and interfering speakers. This pitch extraction is nothing more than a very simple conventional pitch estimator that attempts to determine only the pitch of the dominant speaker in each frame, which may not be the target speaker. In addition, the resolution requirement for pitch estimation is very loose, as it is only necessary that the system be able to discriminate between the target and interfering speaker. The task

of determining which frequency channel belongs to target and interferor is handled by the instantaneous-frequency-based cross-channel correlation.

We remind the reader that the pitch-detection approach can work only for the different-gender scenario, as noted above. On the other hand, the pitch-detection method does not require any historical data or *a priori* information, which is needed for the speaker-identification method introduced below.

Figure 5-1 is a block diagram of a speech separation system that uses pitch detection to regroup cluster frequency components from each individual frame to reconstruct the speech. In the diagram, the simultaneous speech is first processed by two parallel processes. The upper panel implements the STFT, performs instantaneous frequency estimation, cross-channel correlation algorithm to cluster frequency components believed to be from the dominant speaker. In the lower panel, pitch estimation is performed in the time domain to obtain a rough estimate of whether the current processed frame is from the target or the interfering speaker. If a processed frame is believed from the target speaker, the clustered frequency components from that frame are selected to contribute to the final output speech. If a frame is from the interfering speaker, on the other hand, the frequency channels associated with it are suppressed instead.

5.1.2 Speaker Identification for the Same-Gender Case

Speaker identification is widely used as another way to detect the dominant speaker and use that information to accomplish further regrouping. The key idea here is each speaker has his or her own characteristics that can be identified using conventional speaker identification (SID) technology. These results are used as the basis to identify the dominant speakers associated with each input frame, assuming that the speakers to be separated are one of a number contained in the training data.

In a typical SID system, there is a certain amount of training data provided for each speaker. MFCC coefficients are typically used as the features and Gaussian mixture model

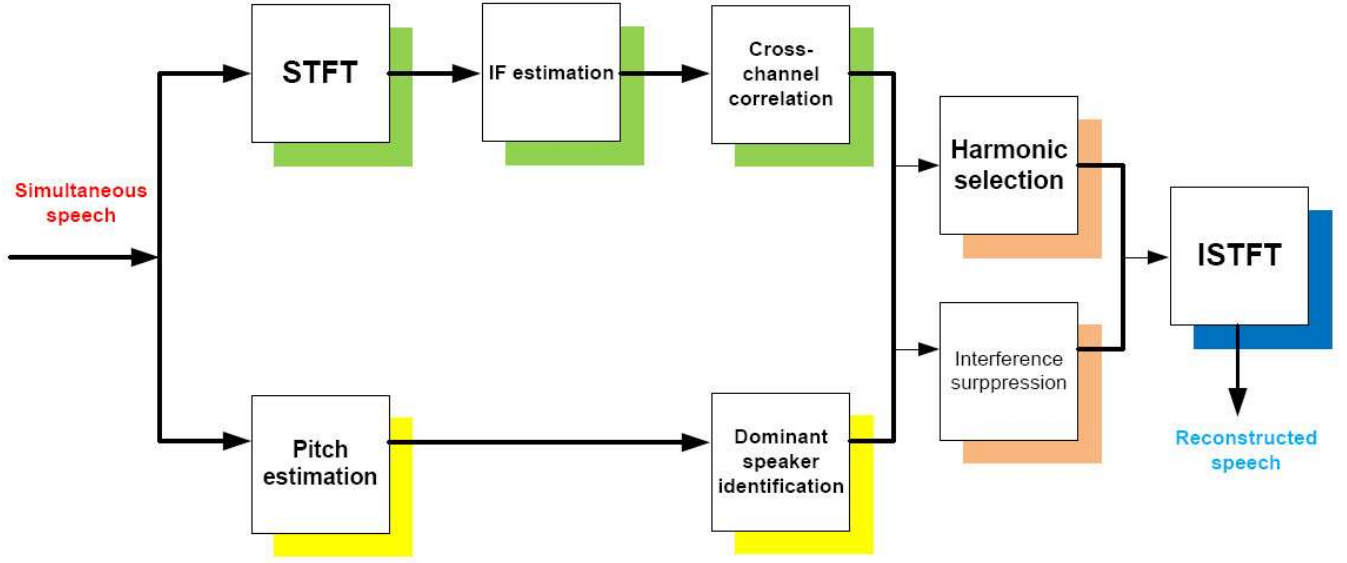


Figure 5-1. Block diagram of a system that uses pitch detection to determine the dominant speaker.

(GMMs) are used to characterize each speaker. A the parameter set λ that characterizes each speaker consists of p , $\vec{\mu}$ and Σ :

$$\lambda = \{p_i, \vec{\mu}_i, \Sigma_i\}, i = 1, 2, \dots, M \quad (5.1)$$

where p is the *a priori* probability of each Gaussian mixture, $\vec{\mu}$ is the MFCC mean vector, Σ is the covariance for each Gaussian component and M is the number of Gaussian components used. These three parameters can be estimated by maximum likelihood estimation [38].

The probability density for each component is a multi-variate Gaussian:

$$b_i(\vec{x}) = \frac{1}{(2\pi)^{D/2} |\Sigma_i|^{1/2}} \exp\left\{-\frac{1}{2}(\vec{x} - \vec{\mu}_i)^T \Sigma_i^{-1} (\vec{x} - \vec{\mu}_i)\right\} \quad (5.2)$$

The final Gaussian mixture density is easily obtained according to the equation:

$$p(\vec{x}|\lambda) = \sum_{i=1}^M p_i b_i(\vec{x}) \quad (5.3)$$

Using the formulation above, the SID system calculates *a posteriori* probability for each speaker according to the equation:

$$p(k|\vec{x}, \lambda_k) = \frac{g_k b_k(\vec{x})}{\sum_{k=1}^K g_k b_k(\vec{x})} \quad (5.4)$$

If there is a total K speakers and the *priori* for each speaker is g_k , the dominant speaker is determined to be the speaker with vector or observation sequence which contains the largest $p(k|\vec{x}, \lambda_k)$.

For simultaneously-presented speech, the dominant speaker is identified on a frame-by-frame basis, and either of the methods described in the previous chapter is used to determine which frequency bins in that frame belong to that speaker, as in the previous section.

While this method can be used for both same-gender and different-gender scenarios, it does require *a priori* information for each speaker. It will not work properly for speakers that are not known previously to the system.

Figure 5-2 is a block diagram of a system that use speakers identification to identify the dominant speaker and further regroup speech stream. The only difference between this figure and Figure 5-1 is the bottom branch, in which the identity of the dominant speaker for the current frame is determined based on previously-compiled statistical information.

5.2 Mask Generation

In Section 4, we discussed how to obtain a binary mask based on the spectrogram for every utterance processed. The general idea is to use cross-channel correlation classification based on instantaneous frequency to select frequency channels that are highly correlated with the same harmonic structure. While constructing the binary mask, those time-frequency cells that are believed to belong to the same harmonic structure as the dominant speaker are assigned a value of 1. All other cells are assigned a value of 0. The target speech is reconstructed using only those cells with a value of 1 are used, while the other cells with a mask value of 0 are suppressed.

In order to utilize the advantages of the short-time Fourier transform to track the changes in instantaneous frequency, while still analyzing features over a longer time period for separation purposes, each utterance is divided into multiple frames of duration 75 ms.

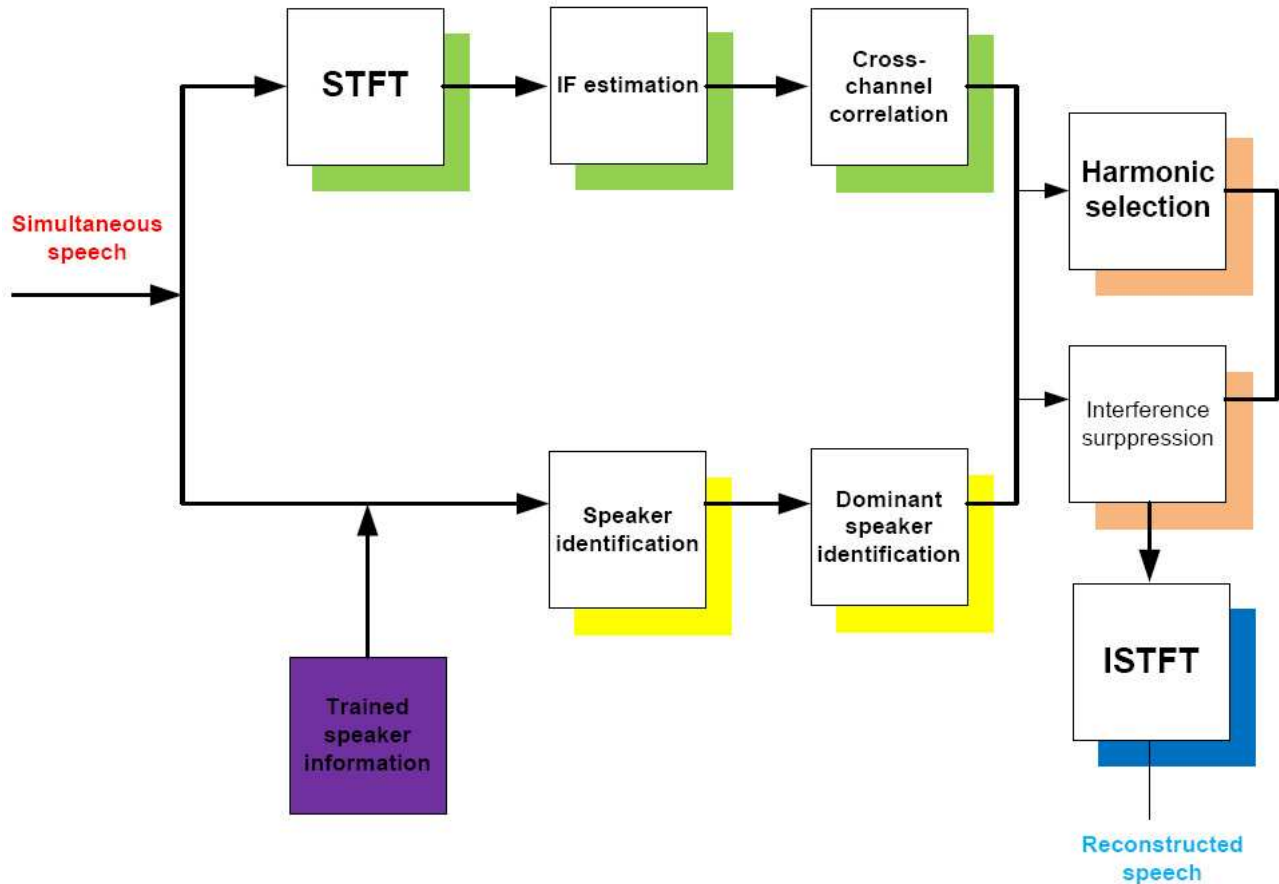


Figure 5-2. Block diagram of a speech separation system that uses speaker identification to determine the dominant speaker.

Each of these frames are overlapped by 25 or 50 percent of the frame length, depending on the application. The cross-channel correlation classification is applied within each frame to generate the binary mask.

One issue with this procedure is that multiple computations of the binary mask in each frame are obtained because of the overlap of analysis frames. This is addressed by averaging the values of the binary mask for a given frame over all of the analysis frames that include that frame. The components of this averaged mask are then compared to a pre-determined threshold:

$$M_1(n, k) = \frac{1}{n_1 - n_0 + 1} \sum_{n=n_0}^{n_1} M(n, k) \quad (5.5)$$

$$M_2(n, k) = \begin{cases} 1, & \text{if } M_1(n, k) \geq \textit{thresh}, \\ 0, & \text{otherwise} \end{cases} \quad (5.6)$$

where $M(n, k)$ is the original binary mask, n and k are the frame and frequency bin index, respectively. Alternatively, in many applications the averaged $M_1(n, k)$ can also be used directly and conversion into the binary mask $M_2(n, k)$ is not necessary.

5.3 Experimental Procedures and Databases

5.3.1 Sphinx-III Recognition Platform

We use the Sphinx open-source automatic speech recognizer developed at Carnegie Mellon University, one of the first systems to demonstrate speaker-independent, large vocabulary continuous speech recognition (LVCSR). The original Sphinx-I system was developed by Kai-Fu Lee in 1988, and Sphinx was extended by many individuals in later versions. Current versions of Sphinx are implemented in C and in Java, and there is also a version of the code that is optimized for embedded systems with a small footprint.

We make use of Sphinx-III in our work as it provides flexibility in modeling and feature development for speech recognition. As in the case of most other large vocabulary continuous speech recognition (LVCSR) systems, Sphinx-III is a phoneme-based system, with each phoneme modeled by an HMM. Word-level HMMs are obtained by concatenating associated phonemes together using triphone context-dependent acoustic models. HMMs states are modeled in the usual left-to-right fashion. Due to the large number of model parameters, the parameters of the Gaussian distribution characterizing each state can be shared by different states. In addition, states can be pruned or combined to reduce the number of parameters. Figure 5-3 [31] is a block diagram of the Sphinx-III recognition system.

5.3.2 The Resource Management and Grid Corpora

Two standard speech corpora were used to evaluate the various source separation algorithms considered: the Grid database which had been used in the Speech Separation Challenge of 2006 [11, 12] and the familiar DARPA Resource Management (RM) database [35]. The Grid

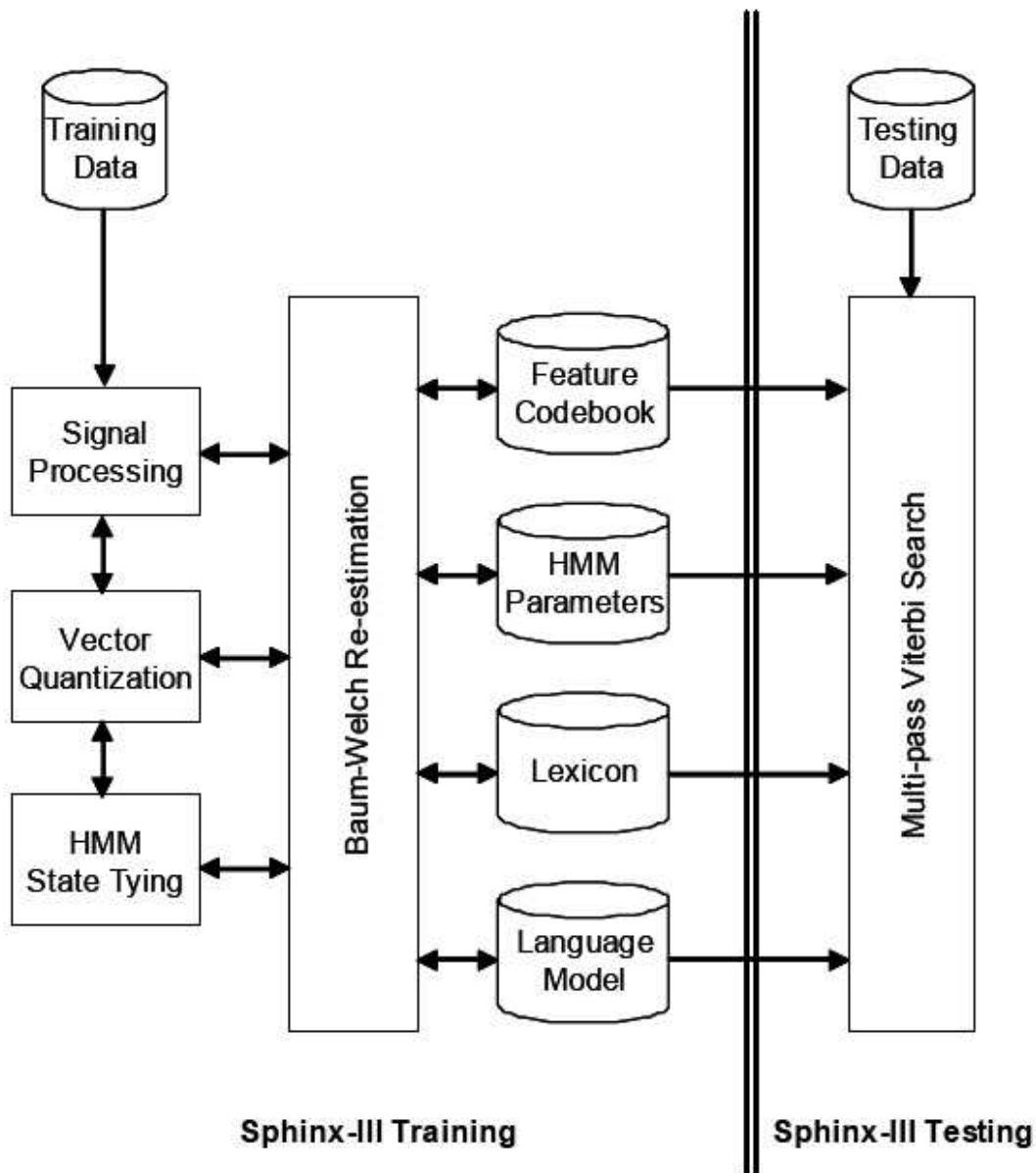


Figure 5-3. A block diagram of the Sphinx-III speech recognition system.

database is a large multitalker audiovisual sentence corpus to support behavioral studies in speech perception. In brief, the corpus consists of high-quality audio and video (facial) recordings of 1000 sentences spoken by each of 34 talkers (18 male, 16 female). All speech files are single-channel “wav” data sampled at 25 kHz and all material is endpointed. The corpus, together with transcriptions, is freely available for research use [11]. The Grid training corpus includes 34 speakers, each providing 500 clean utterances, for a total of

17,000 clean training utterances. The testing utterances are degraded at various SNRs, and each condition contains 600 sentences. All utterances in the Grid database have a fixed format as specified in Table 5-1. Specifically, each sentence contains six words, starting with a command, following by a color, a preposition, a letter, a number and finally an adverb. The database contains 4 command words, 4 colors, 4 prepositions, 25 letters, 10 numbers, and 4 adverbs [13]. For example, a typical sentence could be “Bin white at D 1 again”. We used only the speech with an SNR of +6 dB in the present work.

The DARPA Resource Management Continuous Speech Corpora (RM) [35] consists of digitized and transcribed speech for use in designing and evaluating continuous speech recognition systems. All RM material consists of read sentences modeled after a Naval resource management task. The complete corpus contains over 25,000 utterances from more than 160 speakers representing a variety of American dialects. The material was recorded at 16 kHz, with 16-bit resolution, using a Sennheiser HMD-414 headset microphone. Speaker-Independent training and testing data are used for this dissertation. This part of the DARPA RM database consists of 1600 training utterances and 600 testing utterances. The vocabulary size of RM database is nominally 1000 words and was purposefully made to be phonetically balanced.

VERB	COLOR	PREPOSITION	LETTER	DIGIT	ADVERB
bin	blue	at	A-Z	1-9	again
lay	green	by	(no ‘W’)	and zero	now
place	red	on			please
set	white	with			soon

Table 5-1. Structure of the sentences in the Grid database.

The evaluation methods used for the two corpora are quite different. As noted above, sentences in the Grid database all consist of a verb followed by a color, a preposition, a letter, a digit, and an adverb in precisely that sequence. The task is to recognize the digit and letter in the sentence which contains the color “white”. The only errors tabulated are substitutions for the digits and letters in the speech data due to their fixed positions. The task remains a difficult one, as digits and letters are frequently confused even by human

listeners when competing speakers are present. We used the scoring tool prepared by the University of Sheffield to score recognition results for the Grid database. As discussed in the previous section, speaker identification is used to regroup speech streams in the same-gender and general cases. In contrast, the task in Resource Management database is simply to recognize each testing sentence and the word error rate (WER) is tabulated. The WER is by definition the number of substitution, insertion, and deletion errors divided by the total number of words presented. Pitch detection is generally used to group the components of the final reconstructed speech stream.

5.4 Experimental Results and Discussion

This section describes various experimental results obtained for the algorithms described above using data from the RM and Grid databases.

In Chapter 4, we argued that the graph-cut approach is a good way to cluster the frequency components that are obtained from clustering information from the correlation matrix. Figure 5-4 below demonstrates that the graph-cut method is more effective in extracting correlation information than the 1-D projection method, and thus results in better recognition accuracy. These results were obtained using the RM database. We used the NIST tool `sc_stats` to test statistical significance between different algorithms. The differences between the two methods are all statistically significant at the level of $p < .05$ except for the clean case. The system shown in Figure 5-1 was used to extract features and reconstruct speech. The results are tested on the RM database for the different gender-case.

We also compared the performance of the cross-channel correlation algorithm based on instantaneous frequency that was developed in this thesis to other well known approaches. Figure 5-1 compares results using our approach to similar results obtained using baseline Mel-Frequency Cepstral Coefficients (MFCC), the multi-pitch tracking algorithm developed by de Cheveigné, and an algorithm based on instantaneous amplitude estimation.

The fundamental idea of the multi-pitch tracking algorithm is to estimate different fundamental frequencies one by one. The fundamental frequency from the dominant speaker

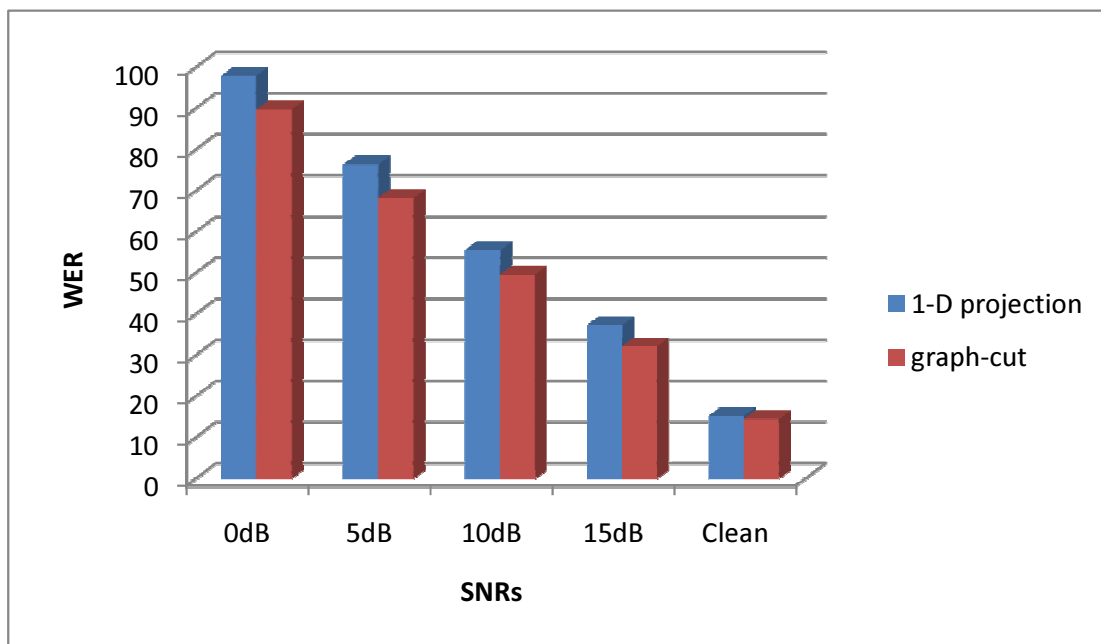


Figure 5-4. Experimental results using the RM database that compare the performance of the graph-cut and 1-D projection methods. The two speakers in these experiments were of different genders and presented at an SNR of +6 dB.

is estimated first. All harmonics related to this fundamental frequency will be removed used a comb filter. A second pitch estimate will then be obtained on the basis of the new signal after the first fundamental frequency is removed. Ideally, this procedure can continue without any constraint on the number of speakers. Nevertheless, in real cases, the algorithm becomes more and more difficult to implement with an increasing number of speakers.

The instantaneous amplitude algorithm exploits a common method to calculate instantaneous amplitude. We begin with the short-time Fourier transform (STFT):

$$X[n, k] = \sum_{m=-\infty}^{\infty} x[m]w[n - m]e^{-\frac{j2\pi mk}{N}} \quad (5.7)$$

where $x[n]$ is the time-domain speech signal, $w[n]$ is the window function, n is the frame index along the time axis, k is the frequency index and N is the total of frequency channels.

The square of the instantaneous amplitude is typically obtained from the sum of the squares of the real and imaginary parts of $X[n, k]$:

$$E[n, k] = (\Re X[n, k])^2 + (\Im X[n, k])^2 \quad (5.8)$$

where $\Re(X[n, k])$ is the real part of $X[n, k]$ and $\Im(X[n, k])$ is the imaginary part of $X[n, k]$.

Figure 5-5 compares the recognition accuracy obtained with the four procedures and demonstrates that the instantaneous-frequency-based algorithm provides the best performance of the four algorithms considered. Since the RM database tested here is for the different-gender case, the regrouping scheme used here is based on pitch detection, as described in Figure 5-1.

While the multi-pitch tracking algorithm is helpful in our experiment, it does not provide a large improvement in performance. The reason is that the final extraction and suppression of harmonic structure is highly dependent on the accuracy of pitch estimation. Any error made in pitch estimation will adversely affect the final results. In fact estimating simultaneous pitches of multiple signals is very challenging in and of itself.

Besides the instantaneous-frequency-based method, the instantaneous amplitude-based method also shows good improvement. In contrast to the instantaneous-frequency-based method, the change of instantaneous-amplitude movement is not very selective, which results in some frequency channels becoming mistakenly accepted due to false high correlation values. In addition to that, “coherent demodulation” is also very important for the instantaneous-amplitude-based method. Knowing exactly the carrier frequency of the test signal will greatly increase the accuracy of “coherent demodulation”. However, this is also a challenging topic by itself.

Compared to the multi-pitch and instantaneous-amplitude-based algorithms, our instantaneous-frequency-based algorithm does not require that the instantaneous frequency be estimated with high accuracy. Even with interfering components present, the cross-channel correlation is still able to pick up those frequency channels that are less affected by the interference. All these factors

enable the instantaneous-frequency-based algorithm to be more robust to the presence of interference.

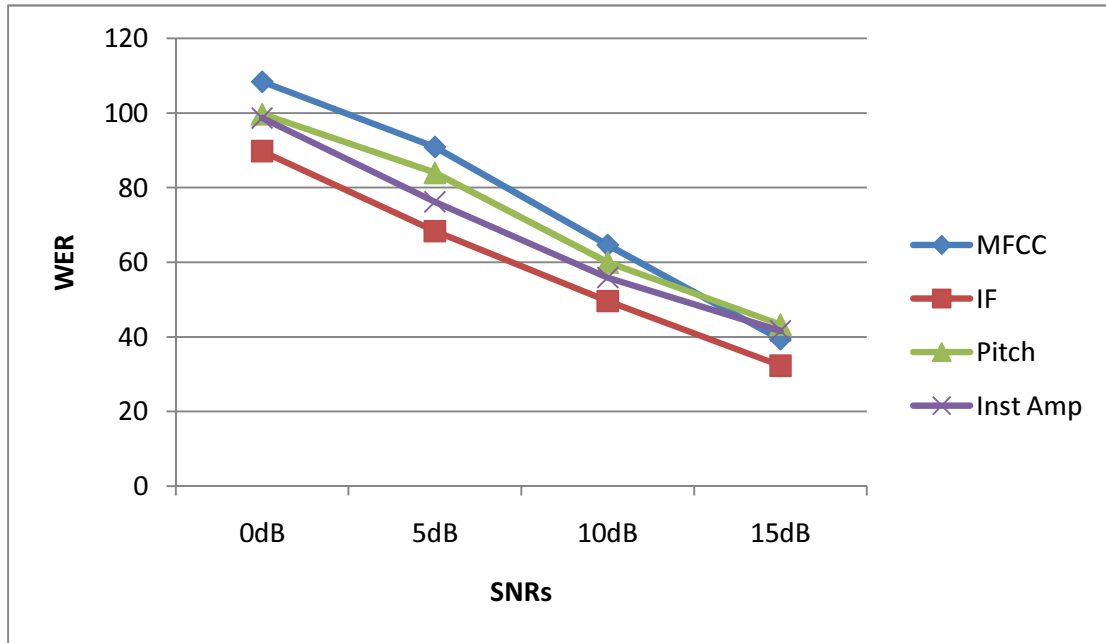


Figure 5-5. Performance comparison among instantaneous frequency, baseline MFCC, pitch tracking algorithm and instantaneous-amplitude-based algorithm obtained from the RM database.

Figure 5-5 compares the performance of the same four algorithms discussed above using the Grid database with an SNR of +6 dB. The figure shows accuracy (which is 100 percent minus the WER) rather than WER as the evaluation criterion. As in the case of the results in Figure 5-5, the instantaneous-frequency-based algorithm again provides the best performance. Because there was sufficient training data in the Grid database, the speaker identification regrouping scheme based on speaker identification was used. Although the performance for the same-gender case is worse than the different-gender case (as expected), the instantaneous-frequency-based algorithm still provides better performance than the other three algorithms at a level that is statistically significant.

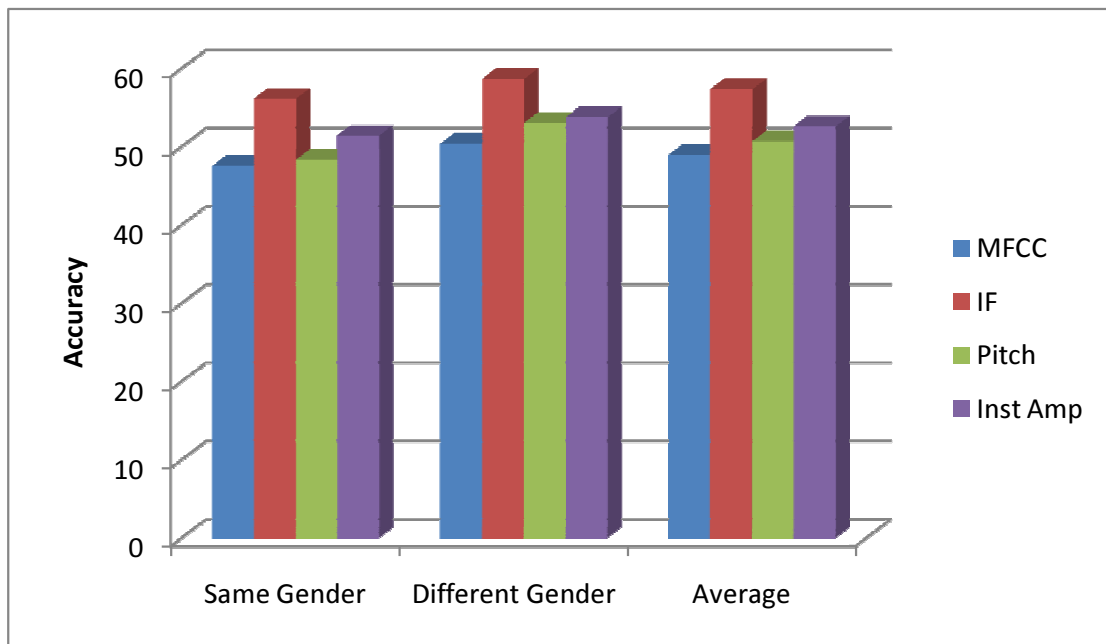


Figure 5-6. Comparison of performance of the instantaneous frequency, baseline MFCC, pitch tracking, and instantaneous-amplitude-based algorithm using data from the Grid database.

One advantage of using the instantaneous-frequency-based cross-channel correlation algorithm to separate speech is that it has the ability to filter out the parts of the harmonic structure from the target speech that are affected by the interfering speaker. For example, if the fundamental frequency of the target speaker is 150 Hz while the interfering speaker has a fundamental frequency of 200 Hz, the fourth harmonic of the target speaker is identical to the third harmonic of the interfering speaker, 600 Hz. In this case the instantaneous frequency estimated at 600 Hz would be severely affected by the interfering speaker, the instantaneous frequency estimated from this channel is unlikely to have a high correlation with other components of the target speaker that are less affected by the components of the interfering speaker. Thus this channel would be excluded from the final reconstruction.

Figure 5-7 shows the results of an experiment that was designed to illustrate this point on RM database. First, we estimated the fundamental frequency and all related harmonics for clean speech from a given speaker. Next we added interfering speech at various SNRs. The target speech was reconstructed in two ways using the instantaneous-frequency-based method: using a mask derived from the clean speech, which presumably contains all components of the signal, and using a mask that was obtained automatically from the noisy speech, which presumably excludes the components that were adversely affected by the presence of the masker. The results in Figure 5-7 clearly show that the reconstructed speech obtained from harmonics estimated from clean speech leads to worse recognition accuracy because of the inclusion of frequency channels that are degraded by the presence of the masker. In contrast, reconstructed speech from harmonics obtained directly from noisy speech yields substantially better WER.

5.5 A Sieve Function for Selecting Relevant Frequency Components from Partial Harmonic Structure

In previous chapters, frequency components believed to be from the same source were identified and grouped together based on the proposed temporal features of instantaneous frequency and the classification method used was that of cross-channel correlation. However, due to the presence of competing speech, there are inevitable estimation errors from both the procedure of estimating instantaneous frequency and of using the graph-cut algorithm to group similar frequency components. These estimation errors adversely impact on the final harmonic structure used to reconstruct speech, which eventually will limit the improvement of the final WER.

5.5.1 Harmonic Pattern Recognition

In this section, a sieve function scheme is proposed to compensate for this problem [44, 45]. This approach is based on the assumption that the components to be included are all harmonically related to one another. A harmonic “sieve” is applied with a fundamental frequency that is chosen to maximize the value of an objective cost function based on the

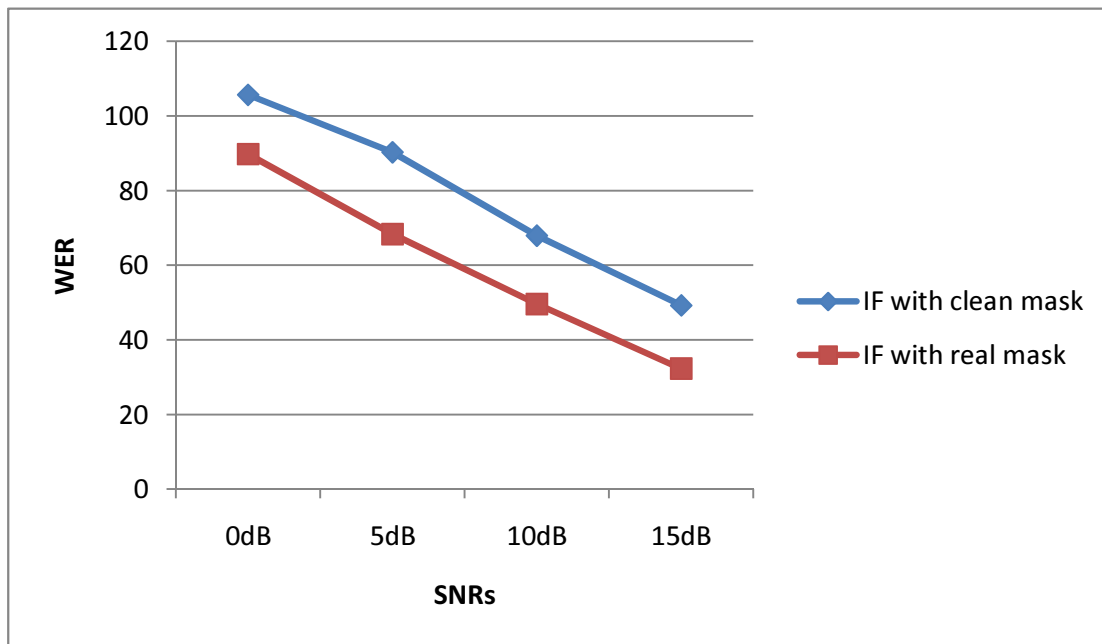


Figure 5-7. Comparison of WER obtained using a reconstruction of masked speech using all components of the dominant speaker (“clean mask”) with a similar reconstruction using only those components that are identified as undistorted by the instantaneous-frequency-based method (“real mask”).

input spectrum that is described below. Once the fundamental frequency is chosen in this fashion, the new estimated fundamental frequency and its associated harmonic structure will be used to further filter out those “noisy” frequency channels mistakenly selected in the original frequency-selection procedure used.

Assume that there is a superset F containing a set of fundamental frequencies f ranging from 80 Hz to 350 Hz. This frequency range includes most of the reasonable fundamental frequencies without regard to gender or age. Within this range we define a set of potential fundamental frequencies f that each have their own harmonic structure. These frequencies f are generally linearly spaced in F , although they do not need to be.

Given a specific fundamental frequency of f , all harmonic members related to this fundamental frequency can be represented as $f = [f_1 \pm \sigma, 2f_1 \pm \sigma, \dots, nf_1 \pm \sigma]$, where n is the total number of elements in the harmonic structure, σ is a small tolerance range around each harmonic in the set.

It is easy to see that the superset of F is fixed given a fixed number of fundamental frequencies f and small tolerance σ . If the fundamental frequency is time varying, the superset F is a function of f .

In this and the previous chapters we discussed a system that attempts to extract the important harmonic components of masked speech based on cross-channel correlation and graph-cut grouping. We refer to the harmonic structure estimated by the system described in this and the previous chapter as S , and this structure is estimated for real simultaneously presented speech. The set S can be given as $S = [s_1, s_2, \dots, s_m]$, where m is the total number of elements in the set S . It is worthwhile to point out that the length of each subset f inside F is not necessarily the same as the length of set S .

The harmonic pattern recognition goal is to compare each set of f belonging to the superset of F with the estimated harmonic structure set S . The final selection of f values that are assumed to be relevant is based on a pre-designed objective cost function to select the final winner f in the set of F based on the maximum or minimum in order to determine the final fundamental frequency.

5.5.2 The Harmonic Sieve

In the previous section, the basic idea of harmonic pattern recognition was discussed. In this section details about the harmonic sieve will be provided in order to complete the picture of how to filter out harmonic outliers.

Returning to the set F and S given above, set F is nothing but a superset dependent on each different fundamental frequency and its corresponding mesh. Every set of fundamental frequency and its mesh comprises one harmonic sieve. Let us consider a set of F harmonic sieves, in which the f^{th} sieve ($f = 0, 1, 2, \dots, F - 1$) has a fundamental frequency $S[y]$ and

L meshes at harmonic frequencies $f[y, h] = hS[y]$, $h = 1, 2, \dots, L$, where h is the number of harmonics. The range of $S[y]$ should be able to cover a reasonable range that contains most of the possible fundamental frequencies. In this dissertation, we use the range from 80 Hz to 350 Hz. For the meshes introduced above, instead of setting a fixed mesh for each harmonic frequency, we use a variable mesh, where each harmonic frequency $f[y, h]$ has a relative bandwidth of $2b$. For instance, for a given harmonic $f[y, h]$, the mesh begins from the most left of $(1 - b)f[y, h]$ and extends itself to the most right of $(1 + b)f[y, h]$. The value b is not necessarily a fixed value. In the experiments, we chose the value b from 10 to 15.

Now in reality, we have two different sets of frequencies. One is set F , which contains each mesh set $f[y, h]$ depending on the specific fundamental frequency y and order of harmonics h . The other is set S , which is obtained from the cross-channel correlation identification. Our goal is to use set F to further smooth set S and remove those outliers contained in set S . By shifting or changing the values of $f[y, h]$ while fixing the bandwidth b , only a certain number of elements in set S can remain. The others, which do not fall into any of the predesigned meshes, will be removed from the set.

5.5.3 Objective Function

An objective function is needed to compare among all possible sieve sets and determine the final optimal pitch and its harmonics.

The first step is to assign a proper value to a certain mesh if there is at least one value from set S falling into it. Let's assume each element in set S is represented as $s[i]$. The following equation shows how to label each mesh:

$$r[y, i] = \begin{cases} h, & \text{if } (1 - b)f[y, h] < x[i] < (1 + b)f[y, h], \\ 0, & \text{otherwise} \end{cases} \quad (5.9)$$

When moving all different harmonic sieves successively to compare with set S , in our experiments, we can obtain F sets of harmonic numbers $r[y_n, i]$, where $n = 0, 1, 2, \dots, F - 1$. Finally, we need to obtain an estimator to get the optimal $r[y_n, i]$.

In order to get the optimal pitch value, we design the error function in the equation below as follows. By minimizing function 5.10, the pitch value can be automatically achieved.

$$E = \sum_{i=1}^N (x[i] - p \times r[ym, i])^2 \quad (5.10)$$

By using maximum likelihood estimation, Equation 5.11 can be obtained.

$$\begin{aligned} \frac{\partial E}{\partial p} &= \frac{\partial}{\partial p} \sum_{i=1}^N ((x[i])^2 + p^2 \times (r[ym, i])^2 - 2p \times r[ym, i] \times x[i]) \\ &= \sum_{i=1}^N (2p \times (r[ym, i])^2 - 2x[i] \times r[ym, i]) \\ &= 0 \end{aligned} \quad (5.11)$$

Continuing from Equation 5.11, Equation 5.12 and 5.13 can be used to obtain the final optimal value p .

$$p \sum_{i=1}^N (r[ym, i])^2 = \sum_{i=1}^N x[i] \times r[ym, i] \quad (5.12)$$

$$p = \frac{\sum_{i=1}^N x[i] \times r[ym, i]}{\sum_{i=1}^N (r[ym, i])^2} \quad (5.13)$$

Consider the two examples below concerning the sieve function described above.

- Example 1: Incoming harmonic1 [110 220 330 390 550 610 660 880]
Filtered harmonic [110 220 330 550 660 880]
- Example 2: Incoming harmonic2 [105 215 330 390 540 610 675 880]
Filtered harmonic [110 215 330 540 675 880]

From the examples above, it is easy to see the harmonic sieve method can robustly remove many outliers while still leaving reasonable tolerance to those elements, which are not exactly multiple integers of the fundamental frequency but sufficiently close.

Figure 5-8 below shows the experimental results obtained from the RM database before and after applying the harmonic sieve function. Improvement is observed at high SNRs, but

recognition accuracy worsens for SNRs below 5 dB. The primary reason for this observation is that the mask information is needed to perform the sieve operation, and too many outliers are accepted at lower SNRs, contains too many outliers which deteriorate the final estimation of the right harmonic structure. Using the maximum likelihood estimation above, the correct pitch value will be very difficult to estimate.

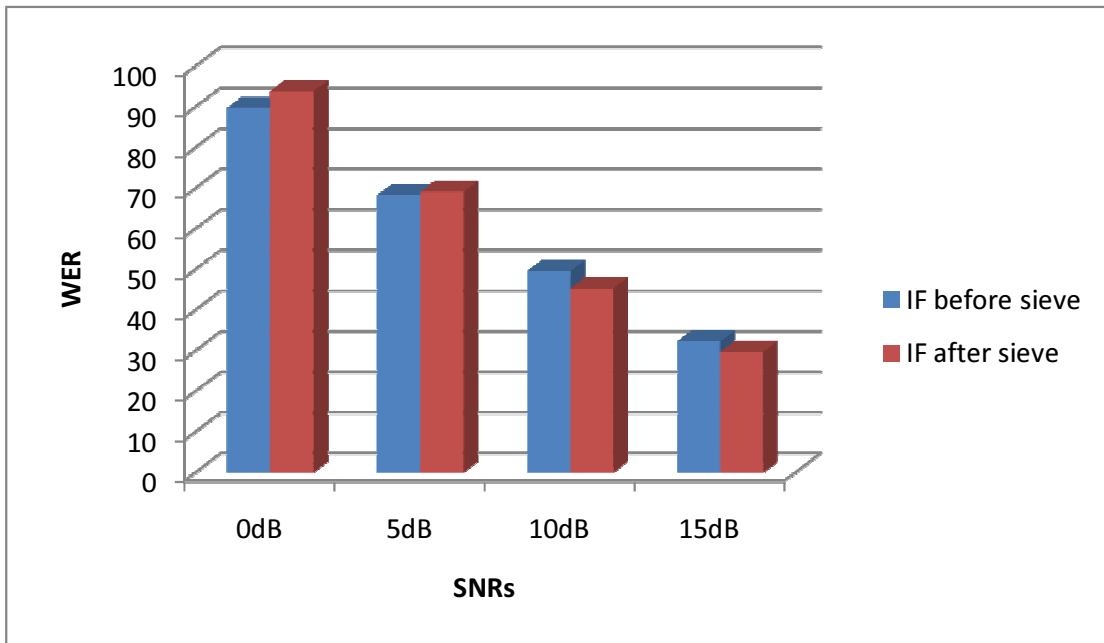


Figure 5-8. Comparison of WER obtained before and after applying the sieve function.

CHAPTER 6 INSTANTANEOUS-AMPLITUDE-BASED SEGREGATION FOR UNVOICED SEGMENTS

The results in the previous chapters have demonstrated that the use of instantaneous frequency to group correlated frequency components from the same source can improve speech recognition accuracy, as frequency components from the same speaker in a voiced segment tends to behave in a similar way with regard to modulation frequency. By applying the proposed method and testing on different databases, improvement on Word Error Rate (WER) is obtained. Unfortunately, the use of instantaneous frequency to group similar frequency components can only be exploited during voiced segments, and it is unclear how useful this method would be when there is no fundamental frequency present. When the processed segment is not voiced, the methods discussed previously cannot identify fundamental frequency and its harmonics.

Fortunately, even though there is no harmonic structure within unvoiced segments, the envelopes of energy associated with frequency channels that arise from the same source tend to increase or decrease in a similar fashion. If common energy that is increasing or decreasing from different frequency channels can be accurately identified, we can easily group these frequency channels together using the same means we had exploited for changes in frequency in the previous chapters.

A convenient way to locate common increases or decreases in energy is to take the first derivative of a given signal with respect to time. Next, a peak detection or valley detection is conducted to mark an energy burst if a peak is found, or an energy cessation if a valley is identified. However, the task of locating peaks and valleys itself is a very challenging problem. A certain number of peaks and valleys are not necessarily corresponding to dramatic energy change.

For our work on grouping in unvoiced segments we will apply cross-channel correlation just as we did in Chapter 4, with the only difference being that features used to calculate cross-channel correlation will be based on the first derivative of their instantaneous amplitudes

rather than instantaneous frequency. This method can tolerate a certain amount of false peaks or valleys because these false detections will lower the correlation value only if they occur simultaneously across different channels, which rarely happens. Hence, we will continue to use the cross-channel correlation and graph-cut based architecture that had been employed previously for voiced segments.

The final piece of the system is a module that searches for the boundaries between voiced and unvoiced segments. When a processed segment or frame is identified as voiced the instantaneous-frequency-based grouping scheme will be employed, or instantaneous-amplitude-based features will be used for the unvoiced segments.

The rest of this chapter will be organized as follows: we will begin with a description of the amplitude-based features. Next, we will discuss the formulation of the voiced/unvoiced segment detection system. Finally, we will describe and discuss our experimental results using the amplitude-based features in unvoiced-segments.

6.1 Feature Extraction Based on Instantaneous Amplitude

Figure 6-1 is a block diagram of the system that combines processing of instantaneous frequency for voiced segments with instantaneous amplitude for unvoiced segments. We note that V/UV discrimination is invoked after an initial frequency analysis, and the voiced and unvoiced frames are subsequently processed in parallel. Our focus in this section is on the processing for the unvoiced frames, as depicted in the lower branch of Fig. 6-1.

Equation 6.1 shows a discrete form of Short-Time Fourier Transform.

$$X[n, k] = \sum_{m=-\infty}^{\infty} x[m]w[n - m]e^{\frac{-j2\pi mk}{N}} \quad (6.1)$$

where $x[n]$ is the speech time domain signal, $w[n]$ is the window signal, n is the frame index in the time axis, k is the frequency index in the frequency axis and N is the total frequency channels in the transform. From Equation 6.1, it is that each time-frequency cell is deterministic with a given fixed time index and frequency bin index. The energy of each time frequency cell is determined by the following equation:

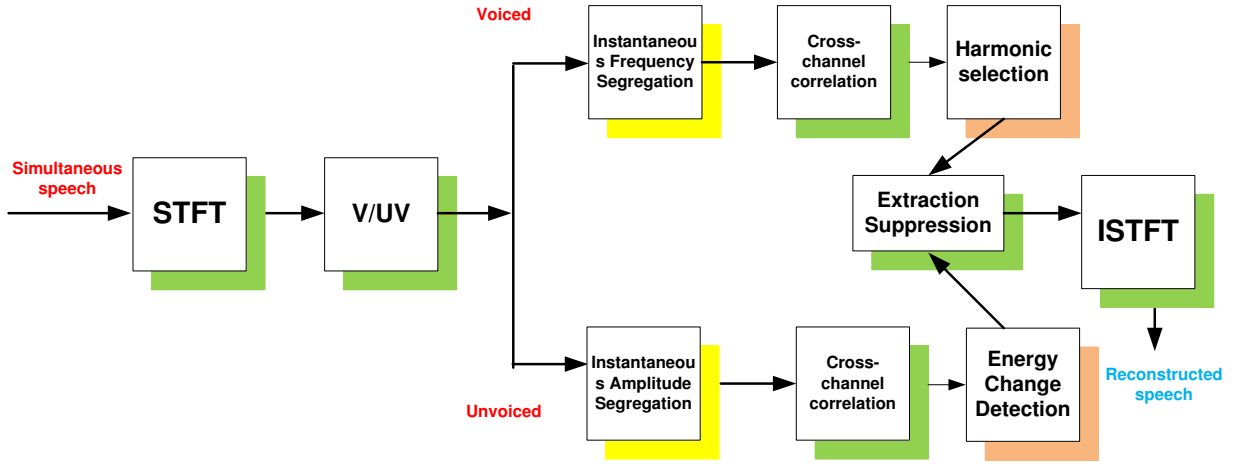


Figure 6-1. Block diagram of system that combines instantaneous frequency and instantaneous amplitude to separate simultaneously-presented speech.

$$E[n, k] = (\Re X[n, k])^2 + (\Im X[n, k])^2 \quad (6.2)$$

where $\Re(X[n, k])$ is the real part of $X[n, k]$ and $\Im(X[n, k])$ is the imaginary part of $X[n, k]$.

In our work in unvoiced segments, the instantaneous amplitude $E[n, k]$ is calculated from each frequency bin after the STFT based on Equation 6.2. Then a first-order difference is taken to highlight onsets and offsets of energy, as represented in Equation 6.3 below.

$$E_2[n, k] = E[n, k] - E[n - 1, k] \quad (6.3)$$

where k is the index of frequency channels while n is the index of frame in time.

After calculating the first-order difference, the similar cross-channel correlation is calculated based on the new feature of energy difference based on the following Equations 6.4 and 6.5.

$$R(k_0, k_1) = \frac{C(k_0, k_1)}{\sqrt{C(k_0, k_0)C(k_1, k_1)}} \quad (6.4)$$

where $C(k_0, k_1)$ is the covariance of the first-order difference between instantaneous amplitude for indices k_0 and k_1 :

$$C(k_0, k_1) = E[(E_2[n, k_0] - \overline{E_2[n, k_0]})(E_2[n, k_1] - \overline{E_2[n, k_1]})] \quad (6.5)$$

Following the cross-channel correlation, the graph-cut algorithm described in Chapter 4 can be directly utilized here to extract correlated information from the correlation matrix.

The entire system design is illustrated in Figure 6-1 above. To summarize, after applying voiced and unvoiced detection, the previously-developed structure of calculation of the cross-channel correlation and segregation using graph-cut analysis is used for both instantaneous frequency feature or instantaneous amplitude feature. Following these steps, harmonic selection is conducted for voiced segments based on frequency and for unvoiced segments based on energy change detection. Finally, the frequency components that are grouped are assigned to the target or interfering speaker based on the results of the speaker identification analysis.

6.2 Detection of Boundaries Between Voiced and Unvoiced Segments

The goal of detecting unvoiced segments and processing them in a different fashion is ultimately to improve recognition accuracy in those unvoiced segments by using instantaneous amplitude instead of instantaneous frequency. If some unvoiced segments are occasionally mis-identified as voiced segments, performance will not be greatly degraded, as previously all segments were processed as if they were voiced. In contrast, the mis-identification of a voiced frame as an unvoiced frame would be worse because the amplitude-based information is not as reliable as the frequency-based information. For these reasons, our goal is to develop an algorithm which can generate good accuracy and a minimum number of mis-identifications of voiced segments as unvoiced segments. For this reason the classifier will be somewhat biased to favor classification of ambiguous segments as voiced.

Figure 6-2 is a block diagram that describes the implementation of the voiced-unvoiced segregation for this work. While the features and the ways in which they are combined are somewhat *ad hoc* we will argue that they are effective for the present task. After windowing

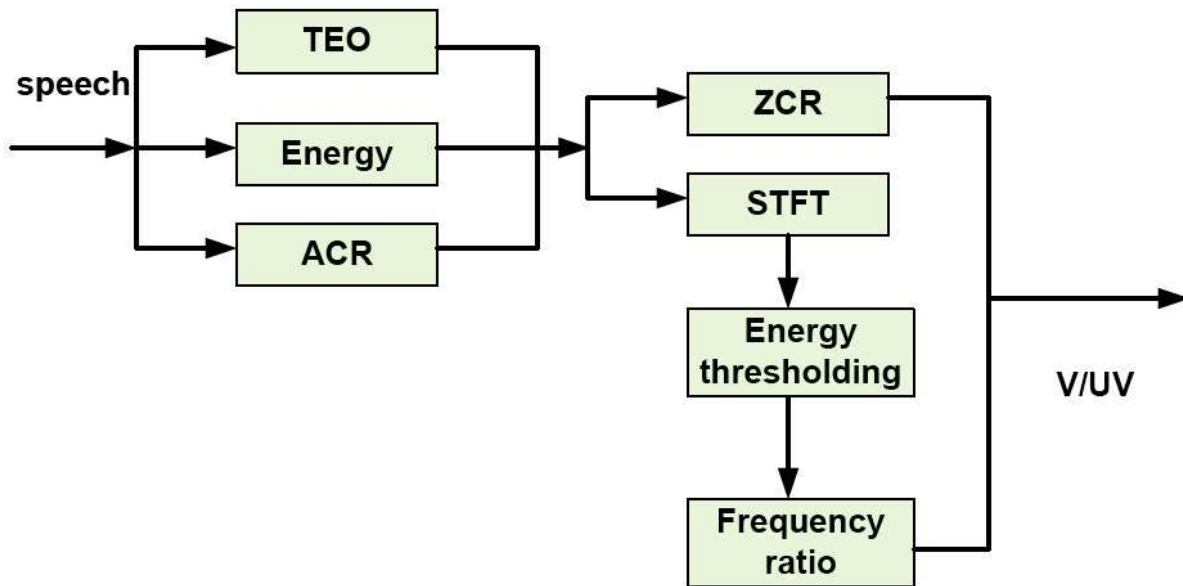


Figure 6-2. Block diagram of the system that detects boundaries between voiced and unvoiced segments.

the speech signal, a preliminary assessment of voicing is made based on analysis by the Teager Energy Operator (TEO), short-time energy, and the autocorrelation function of the short-time input. Frames are determined in a preliminary fashion to be unvoiced if the TEO output is high, the energy is low, or the autocorrelation is low. The number of putative unvoiced frames is reduced in a second assessment using zero crossings (ZCR), energy thresholding, and a comparison of the relative energy in high and low frequencies (“frequency ratio”). As we noted above, the disadvantage of claiming voiced as unvoiced is more severe than the other way around. Therefore, we only mark those frames both whose ZCR and frequency ratio are above certain thresholds in order to reduce the chance that voiced segments are classified as unvoiced.

We briefly summarize these features below.

6.2.1 The Teager Energy Operator

The Teager energy operator (TEO) is mainly used to compute the energy from a signal in a nonlinear manner. The TEO not only measures the energy itself, but also the frequency components the signal carries. This method has been proposed and used in various applications [22, 23, 29] to track the rough frequency changes from the signal. The TEO can be calculated in discrete time as

$$T[n] = x[n]^2 - x[n+1]x[n-1] \quad (6.6)$$

To illustrate the usage of the TEO, we design a signal which contains a pure sinusoid tone with frequency at 200 Hz from 0 to 1 s and another pure sinusoid with frequency at 1000 Hz from 1 to 2 s. The amplitude remains the same during the entire duration. Figure 6-3 shows that Teager energy can accurately identify where frequency starts to change, while a conventional energy operator fails to do the same job.

6.2.2 Autocorrelation

Autocorrelation is widely used in pitch-detection applications because the time lag representing the first major peak away from zero is at the reciprocal of the fundamental frequency. The height of that peak is a measure of the extent to which a signal is periodic. While voiced speech segments are not perfectly periodic, the autocorrelation value at this peak is usually much higher for voiced segments than for unvoiced segments. In this dissertation, the normalized autocorrelation is calculated for each frame. Only for those frames whose autocorrelation value of the peak is higher than a pre-determined threshold and for which that peak lies between 80 Hz to 350 Hz, will be considered to be voiced, and the others will be considered to be unvoiced. Figure 6.2.2 shows sample normalized autocorrelation pattern for voiced and unvoiced segments. It clearly shows that the autocorrelation pattern from the voiced segment look quasi-periodic and that they have high values at the first peak. In contrast, unvoiced segment contains very low autocorrelation values and the autocorrelation function looks more like a delta function.

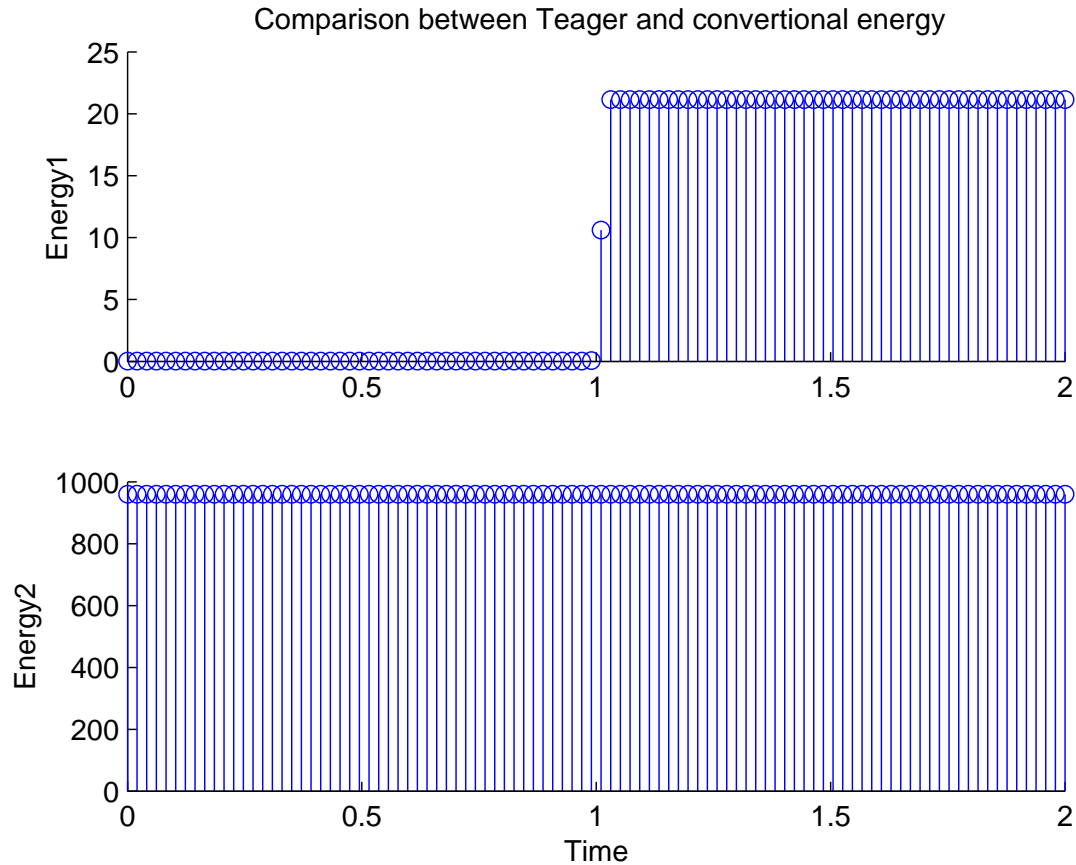


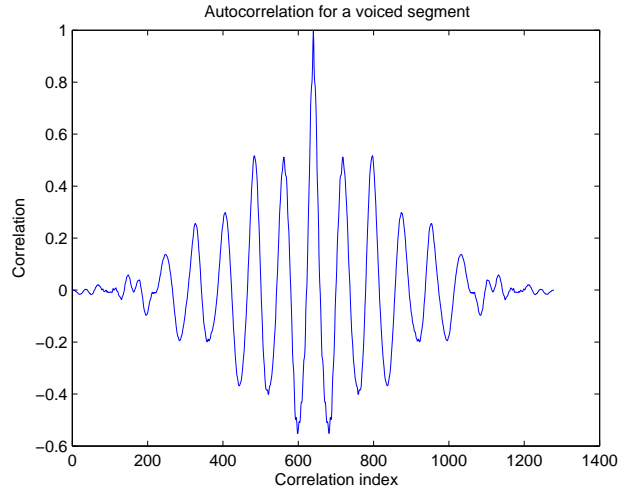
Figure 6-3. A comparison between Teager energy and conventional energy operator. In this case, the frequency is 200 Hz for the 1 s and changes to 1000 hz in the duration from 1 s to 2s, while the amplitude keeps the same.

6.2.3 Energy Detection

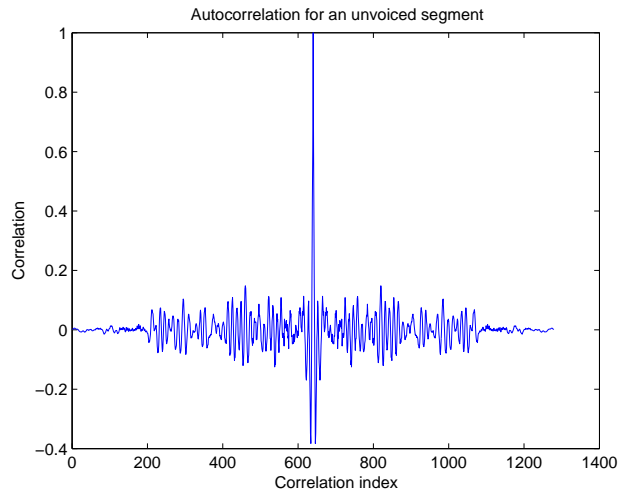
Besides the TEO and autocorrelation features mentioned above, a conventional energy operator is also applied in a frame-based manner. To search for unvoiced segments, we look for those frames containing either a high TEO value, low autocorrelation, or low frame energy. All other frames will be labeled as voiced segments in this stage. The final unvoiced segments will be a subset of the segments labeled as unvoiced after this screen process.

6.2.4 Zero Crossing Rate (ZCR)

The zero-crossing rate (ZCR) has been known for decades to be a robust feature with very low computation load. The ZCR is mainly obtained in the time domain according to the equation



A An autocorrelation for a typical voiced segment.

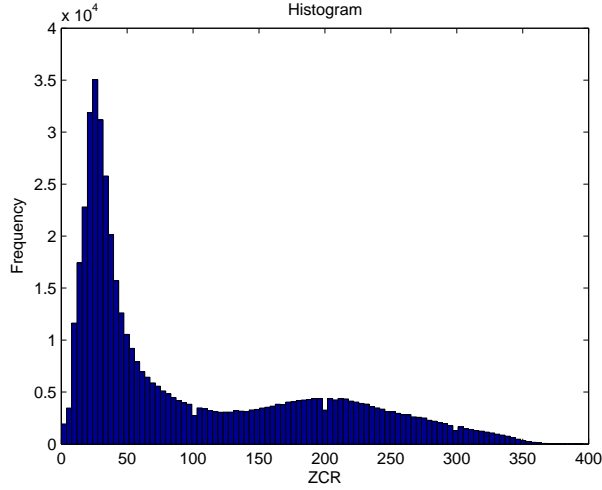


B An autocorrelation for a typical unvoiced segment.

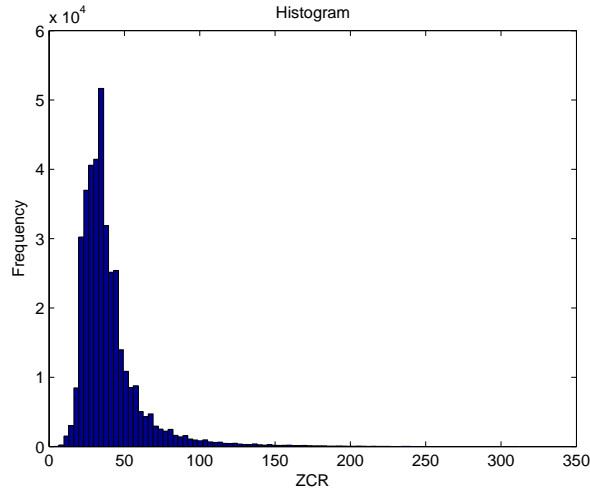
Figure 6-4. Autocorrelation comparison between voiced and unvoiced segments.

$$ZCR = \frac{1}{N} \sum_{n=1}^N \frac{|sgn(x[n]) - sgn(x[n + 1])|}{2} \quad (6.7)$$

where $x[n]$ is the speech sample in the time domain, N is the total number of speech samples in a given frame, and sgn is the signum function. As seen in Figure 6.2.4, the ZCR tends to have a higher valued during unvoiced segments, although there is a lot of overlap between the distributions.



A ZCR histogram for unvoiced segments.



B ZCR histogram for voiced segments.

Figure 6-5. ZCR histogram comparison between unvoiced and voiced segments

6.2.5 Ratio of Energy in High and Low Frequency Bands

Besides the ZCR, we also consider at this stage the ratio of the energy from high-frequency channels and from low frequency channels, calculated as in Equation 6.8. We use the threshold frequency of 4 kHz, half the Nyquist frequency, to distinguish between what are considered to be the high and low-frequency regions for the purpose of this feature.

$$Ratio1(n) = \frac{\sum_{k=\frac{K}{2}+1}^K E[n, k]}{\sum_{k=1}^{\frac{K}{2}} E[n, k]} \quad (6.8)$$

Figure 6.2.5 depicts histograms of the ratio-of-energy feature for typical voiced and unvoiced segments. We note that there is a clear separation of the densities. We typically use an amplitude threshold of that selects only 20 percent of the bins in the time-frequency display and discards the other.

Due to the high selective of the feature of high frequency energy derived from energy filtering, it can be considered as a robust feature to classify voiced and unvoiced segments. One good way to verify it is to observe the extent that histograms or distributions from voiced and unvoiced categories overlap. Figure 6.2.5 demonstrates the histograms' overlap is very limited.

6.3 Experimental Results using Instantaneous Amplitude-based Segregation

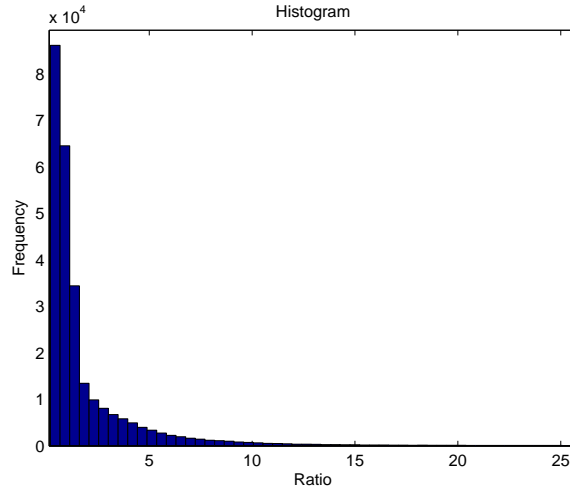
In this section we briefly describe two sets of experimental results. The first concerns the accuracy of classifying the voiced and unvoiced segments using the system shown in Fig. 6-2. The second concerns the improvement in WER that is provided through the use of amplitude-based features, using the entire system depicted in Fig. 6-1.

6.3.1 Evaluation of V/UV Decisions

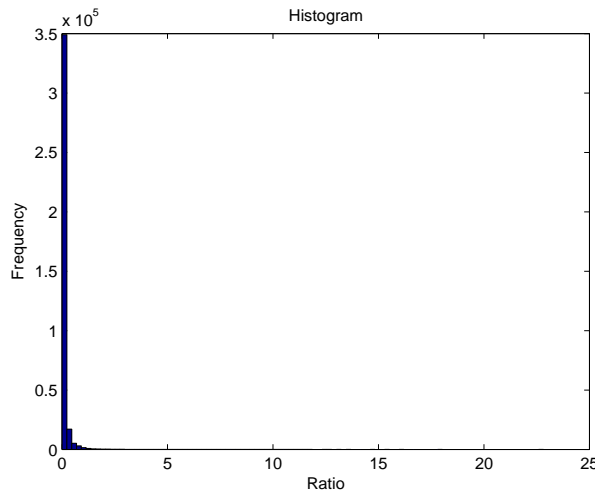
	UV(TESTED)	V(TESTED)
UV(TRUTH)	81%	19%
V(TRUTH)	17%	83%

Table 6-1. Confusion matrix of voiced and unvoiced detection using pitch detection developed by de Cheveigné.

Table 6-1 is obtained by running the pitch detection algorithm introduced in Chapter 5 developed by de Cheveigné [14, 15]. Those frames with reasonable pitch values are classified as voiced while all others are identified as unvoiced. Table 6-2 shows the results by using our algorithm introduced in this chapter. It is easily to see that the error rate of mis-identifying voiced segments as unvoiced segments has been significantly reduced, while the accuracy of identifying unvoiced segment remains similar with the method of de Cheveigné.



A Histogram of high frequency energy feature from unvoiced segments.



B Histogram of high frequency energy feature from voiced segments.

Figure 6-6. A comparison of histograms of high frequency energy feature from both unvoiced and voiced segments

6.3.2 Evaluation of WER Using Amplitude-Based Features

Figure 6-7 shows a comparison for the system described in this thesis with and without the formal classification of segments as voiced or unvoiced, followed by the use of amplitude-based features for the unvoiced segments. The relative improvement for both the same-gender and the different-gender group is about 7-8% relatively, and these improvements are statistically significant. From the results shown, it is clear that the use of instantaneous-amplitude-based

	UV(TESTED)	V(TESTED)
UV(TRUTH)	83%	17%
V(TRUTH)	9%	91%

Table 6-2. Confusion matrix of voiced and unvoiced detection using features developed in this thesis.

features for unvoiced segments does improve speech recognition accuracy in unvoiced segments where harmonic structures are not available to apply the instantaneous-frequency-based features. This observation combined with our results from provides evidence that although the speech signal may be modulated by amplitude and frequency simultaneously, it is reasonable to believe that the speech itself is more affected by frequency modulation when each harmonic is separately resolved in its own analysis channel. The most useful potential cue for grouping of unvoiced segments is amplitude if amplitude modulation is present in the signal.

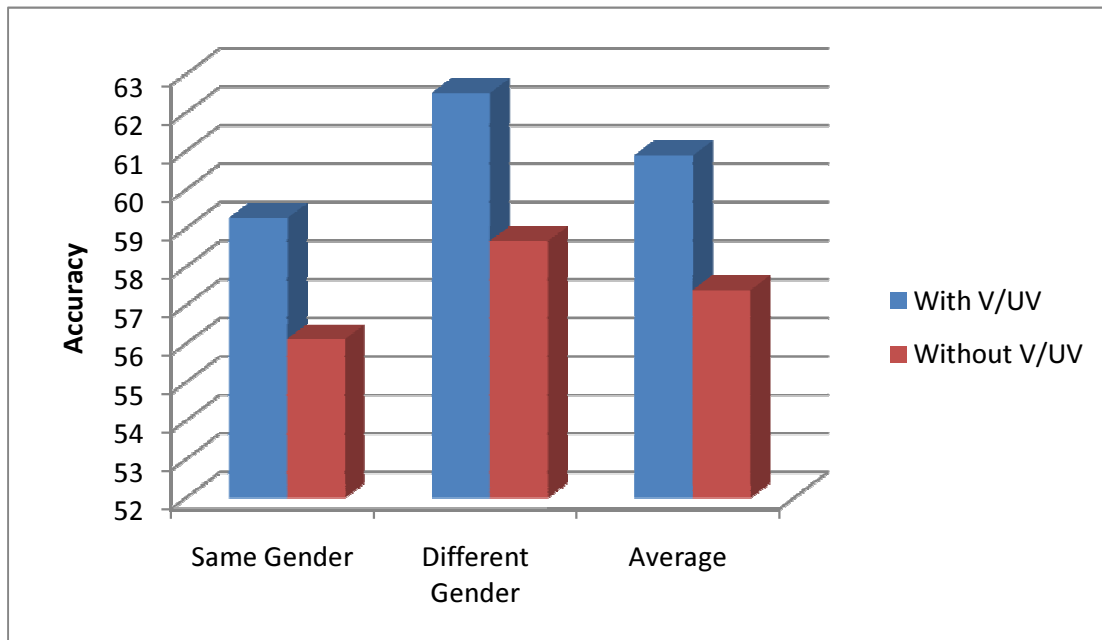


Figure 6-7. Recognition accuracy comparison between methods using voiced and unvoiced detection and without it on Grid database.

CHAPTER 7 SUMMARY AND CONCLUSIONS

In this dissertation, we have discussed an algorithm for instantaneous-frequency-based cross-channel correlation to deal with the very challenging task of speech separation when only one microphone is available.

Various instantaneous frequency estimation methods are covered in situations where the clean speech signal is not available and is mixed with an interfering speaker. Following the discussion about the estimation of instantaneous frequency, a discussion of how to use cross-channel correlation to select frequency channels from the same harmonic structure is presented, where simple averaging and the graph-cut method are discussed. In order to improve the separation results, the use of amplitude-based features is considered for the unvoiced segments, based on a detection of the voiced-unvoiced boundaries. Finally, the use of a sieve function and other techniques are also introduced to maximize the final performance of the separation system.

7.1 Major Findings and Contributions

The primary contribution of this dissertation is the development of a speech separation algorithm that uses instantaneous-frequency-based temporal features to reconstruct a desired speech signal that is presented in the presence of an interfering signal. The system is based on the CASA architecture. A detailed list of all contributions are given below.

- Introduction of a new approach to separate simultaneous speech using instantaneous frequency.
- Use of pair-wise correlation based on estimated instantaneous frequency to find harmonic structures and efficiently segregate frequency components.
- Use of the mean square difference, harmonic sieve and other methods as complementary tools to improve the noisy information contained in the correlation patterns.
- Utilization of graph cuts as an optimal solution to extract information from the pair-wise correlation results.
- Attainment of better performance in terms of WER by implementing a bottom-up instantaneous-frequency-based system.

7.2 Directions of Possible Future Research

Even with the performance improvements presented in this dissertation, single channel speech separation solutions are still far from perfect. Using instantaneous-frequency-based methods, there are several issues that could be improved in future research.

7.2.1 Combine long term and short term cross-channel correlation

Accurately estimating instantaneous frequency in noisy environments is remains challenging, and certainly more work in this area is possible. One possible approach would be to combine correlation estimates spanning very long durations with the present short-duration correlations. Long-duration correlations (*e.g.* across the entire utterance) could be used to identify several frequency channels which are highly correlated with each other globally. This information can give the system a rough idea how to limit the detailed local search to certain frequency regions, where short duration correlation would be applied to further refine the final correlation results.

7.2.2 Combine instantaneous frequency and amplitude

While instantaneous frequency is shown in this study to be useful for speech separation, other work in the literature has demonstrated the possibility of using instantaneous amplitude as another important cue. One possible solution is first to estimate the instantaneous amplitude and frequency as two independent features for each time-frequency cell and later combine these two features in the feature space to construct a two-dimensional distribution given certain amount of training data. With the known SNRs for the training data, a proper model have two distributions for reliable and unreliable time-frequency cells can be constructed. Finally, in evaluating simultaneous speech, the *a posteriori* probabilities can be computed to determine the extent to which a processed cell is reliable.

7.2.3 Introduce image processing algorithms for mask generation

Generating an accurate binary mask for unvoiced segments can greatly boost the final performance. In contrast to voiced segments, unvoiced segments lack of a clean and regular harmonic structure. In order to segregate time-frequency cells into proper regions, image

processing algorithms can be imported here, especially for some image erosion, fill, and edge detection algorithms. By using the eroding algorithms, many noisy time-frequency cells can be ignored and integrated into the final process without too much distraction. Fill and edge detection algorithms can also efficiently define where each time-frequency cell will be assigned for the purpose of regrouping procedure.

7.3 Summary and Conclusions

In this dissertation, a new single-channel speech-separation approach based on instantaneous frequency detection and cross-channel correlation is presented and evaluated. Using two different databases, we demonstrated that separation using instantaneous frequency provides better recognition accuracy than separation based on fundamental frequency alone, separation based on instantaneous amplitude information, and baseline processing using MFCC features.

REFERENCES

- [1] T. Abe, T. Kobayashi, and S. Imai, *Robust pitch estimation with harmonics enhancement in noisy environments based on instantaneous frequency*, Proceedings of ICSLP 1996, 1996, pp. 1292–1300.
- [2] L. Atlas and C. Janssen, *Coherent modulation spectral filtering for single-channel music source separation*, Proceedings of ICASSP 2005, 2005, pp. IV461–IV464.
- [3] F. Bach and M. Jordan, *Discriminative training of hidden markov models for multiple pitch tracking*, Proceedings of ICASSP 2005, 2005, pp. V489–V492.
- [4] S.P. Bacon and D.W. Grantham, *Modulation masking: Effects of modulation frequency, depth and phase*, Journal of Acoustic Society of America **85** (1989), 2575–2580.
- [5] J. Barker, A. Coy, N. Ma, and M. Cooke, *Recent advances in speech fragment decoding techniques*, Proceedings of Interspeech 2006, 2006, pp. 85–88.
- [6] C. Bey and S. McAdams, *Schema-based processing in auditory scene analysis*, vol. 64, 2002.
- [7] B. Boashash, *Estimating and interpreting the instantaneous frequency of a signal – part 1: fundamentals*, Proceedings of the IEEE **80** (1992), 520–538.
- [8] ———, *Estimating and interpreting the instantaneous frequency of a signal – part 2: algorithms and applications*, Proceedings of the IEEE **80** (1992), 540–568.
- [9] A.S. Bregman, *Auditory scene analysis*, MIT Press, Cambridge, MA, 1990.
- [10] F.J. Charpentier, *Pitch detection using the short-term phase spectrum*, Proceedings of ICASSP 1986, 1986, pp. 113–116.
- [11] M. Cooke, *Grid corpus*, Website, <http://www.dcs.shef.ac.uk/spandh/gridcorpus/>.
- [12] ———, *Interspeech 2006 speech separation challenge*, Website, 2006, <http://www.dcs.shef.ac.uk/~martin/SpeechSeparationChallenge.htm>.
- [13] M. Cooke, Jon Barker, Stuart Cunningham, and Xu Shao, *An audio-visual corpus for speech perception and automatic speech recognition*, The Journal of the Acoustical Society of America **120** (2006), 2421–2424.
- [14] A. de Cheveigné and H. Kawahara, *Multiple period estimation and pitch perception model*, speech communication **27** (1999), 175–185.
- [15] ———, *Yin, a fundamental frequency estimator for speech and music*, Journal of Acoustic Society of America **111** (2002), 1917–1930.
- [16] M. Dolson, *The phase vocoder: A tutorial*, Computer Music Journal **10** (1986), 14–27.

- [17] Richard Duda, Peter Hart, and David Stork, *Pattern classification*, Wiley, John and Sons, New York, 2000.
- [18] G. Edelman, W. Gall, and W. Cowan, *Auditory function: Neurobiological bases of hearing*, Wiley and Sons Press, New York, 1988.
- [19] J. L. Flanagan and R. M. Golden, *Phase vocoder*, Bell System Technical Journal (1966), 1493–1509.
- [20] D.J. Hermes, *Measurement of pitch by subharmonic summation*, The Journal of the Acoustical Society of America **83** (1988), 257–264.
- [21] G. Hu and D.L. Wang, *Monaural speech segregation based on pitch tracking and amplitude modulation*, IEEE Transactions on Neural Networks **15** (2004), 1135–1150.
- [22] J. F. Kaiser, *On a simple algorithm to calculate the energy of a signal*, Proceedings of ICASSP 1990, 1990, pp. 381–384.
- [23] ———, *On teager’s energy algorithm and its generalization to continuous signals*, Proceedings of 4th IEEE Digital Signal Processing Workshop, 1990, pp. 127–130.
- [24] E. Kandel, J. Schwartz, and T. Jessell, *Principles of neural science*, Elsevier, New York, 1991.
- [25] B.E.D. Kingsbury, N. Morgan, and S. Greenberg, *Robust speech recognition using the modulation spectrogram*, speech communication **25** (1998), 117–132.
- [26] A. Kusumoto, T. Arai, T. Kitamura, M. Takahashi, and Y. Murahara, *Modulation enhancement of speech as a preprocessing for reverberant chambers with the hearing-impaired*, Proceedings of ICASSP 2000, 2000, pp. 853–856.
- [27] M. Lagrange and S. Marchand, *Estimating the instantaneous frequency of sinusoidal components using phase-based methods*, Journal of the Audio Engineering Society **55** (2007), 385–399.
- [28] Q. Li and L.E. Atlas, *Coherent modulation filtering for speech*, Proceedings of ICASSP 2008, 2008, pp. 4481–4484.
- [29] P. Margos, J. F. Kaiser, and T. F. Quatieri, *Energy separation in signal modulations with applications to speech analysis*, IEEE Trans. Signal Processing **41** (1993), 3024–3051.
- [30] M. Weintraub, *A computational model for separating two simultaneous talkers*, Proceedings of ICASSP 1986, 1986, pp. 81–84.
- [31] Jon Nedel, *Duration normalization for robust recognition of spontaneous speech via missing feature methods*, Ph.D. thesis, Carnegie Mellon University, 2004.
- [32] S. Palmer, *Vision science*, MIT Press, Cambridge, MA, 1999.
- [33] J. Pickles, *An introduction to the physiology of hearing*, Academic Press, London, 1988.

- [34] M. R. Portnoff, *Implementation of the digital phase vocoder using the fast fourier transform*, IEEE Trans. Acoustic., Speech, Signal. Processing **24** (1976), 243–248.
- [35] P. J. Price, W. M. Fishe, J. Bernstein, and D. S. Pallett, *The darpa 1000-word resource management database for continuous speech recognition*, Proceedings of ICASSP 1988, 1988, pp. 651–654.
- [36] L. Rabiner, *A tutorial on hidden markov models and selected application in speech recognition*, Proceedings of the IEEE **77** (1989), 257–286.
- [37] L. R. Rabiner and R. W. Schafer, *Digital processing of speech signals*, Prentice-Hall, Englewood Cliffs, NJ, 1978.
- [38] D.A. Reynolds and R.C. Rose, *Robust text-independent speaker identification using gaussian mixture speaker models*, IEEE Transactions on Speech and Audio Processing **3** (1995), 72–83.
- [39] S.M. Schimmel and L.E. Atlas, *Coherent envelope detection for modulation filtering of speech*, Proceedings of ICASSP 2005, 2005, pp. I221–I224.
- [40] S.M. Schimmel, L.E. Atlas, and K. Nie, *Feasibility of single channel speaker separation based on modulation frequency analysis*, Proceedings of ICASSP 2007, 2007, pp. IV605–IV608.
- [41] Steven M. Schimmel, *Theory of modulation frequency analysis and modulation filtering, with application to hearing devices*, Ph.D. thesis, University of Washington, 2007.
- [42] F. Sha and L.K. Saul, *Real-time pitch determination of one or more voices by nonnegative matrix factorization*, Proceedings of Advances in Neural Information Processing System 17, 2005, pp. 1233–1240.
- [43] J. Shi and J. Malik, *Normalized cuts and image segmentation*, IEEE Transactions on Pattern Analysis and Machine Intelligence **22** (2000), 888–905.
- [44] R. Sluyter, H. Kotmans, and T. Claasen, *Improvements of the harmonic-sieve pitch extraction scheme and an appropriate method for voiced-unvoiced detection*, Proceedings of ICASSP 1982, 1982, pp. VII188–VII191.
- [45] R. Sluyter, H. Kotmans, and A. Leeuwaarden, *A novel method for pitch extraction from speech and a hardware model applicable to vocoder systems*, Proceedings of ICASSP 1980, 1980, pp. V45–V48.
- [46] A. Takayuki, T. Mahoro, K. Noboru, T. Yukiko, and M. Yuji, *On the important modulation frequency bands of speech for human speaker recognition*, Proceedings of Interspeech 2000, 2000, pp. III774–III777.
- [47] N. Viemeister, *Temporal modulation transfer functions for audition*, The Journal of the Acoustical Society of America **53** (1973), 312–312.

- [48] ———, *Modulation thresholds and temporal modulation transfer functions*, The Journal of the Acoustical Society of America **60** (1976), S117–S117.
- [49] ———, *Temporal modulation transfer functions based upon modulation thresholds*, The Journal of the Acoustical Society of America **66** (1979), 1364–1380.
- [50] D. Wang and G. Brown, *Computational auditory scene analysis: Principles, algorithms and applications*, Wiley-IEEE Press, New York, 2006.
- [51] M. Wu, D.L. Wang, and G.J. Brown, *A multipitch tracking algorithm for noisy speech*, IEEE Transactions on Speech and Audio Processing **11** (2003), 229–241.
- [52] W. Yost and S. Sheft, *Across-critical-band processing of amplitude-modulated tones*, The Journal of the Acoustical Society of America **85** (1989), 848–857.
- [53] ———, *A comparison among three measures of cross-spectral processing of amplitude modulation with tonal signal*, The Journal of the Acoustical Society of America **87** (1990), 897–900.
- [54] W. Yost, S. Sheft, and J. Opie, *Modulation interference in detection and discrimination of amplitude modulation*, The Journal of the Acoustical Society of America **86** (1989), 2138–2147.

BIOGRAPHICAL SKETCH

Lingyun Gu was born in Nanjing, Jiangsu, P.R. China. He received his B.S. in Electrical Engineering from University of Electronic Science and Technology of China, Chengdu, Sichuan, P.R. China in 1998 and M.S. in Electrical and Computer Engineering from Old Dominion University, Norfolk, VA in 2002, respectively. Now he is a PhD student in Language Technologies Institute, School of Computer Science at Carnegie Mellon University, Pittsburgh, PA.